Évaluation de potentiel d'immunité de renversement d'une configuration optimale de réservoir par la conception, la fabrication et l'essai d'un prototype

(Projet: 2004-SR-94173)

Rapport Final

Soumis à:
Fonds de Recherche de la Nature et Technologies du Québec

et
Le Ministère des Transport du Québec

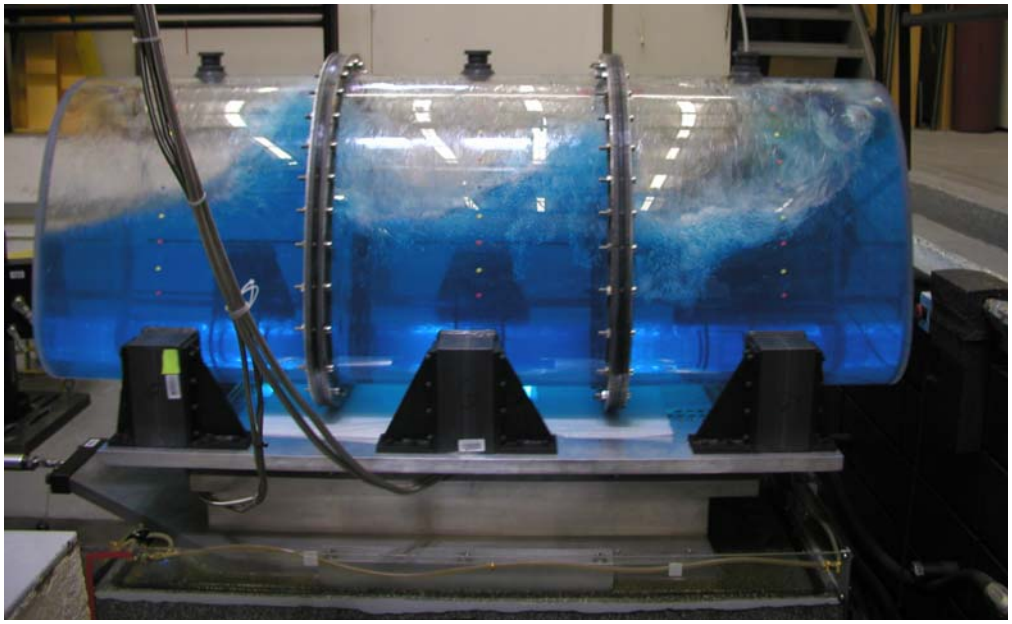

par:
S. Rakheja
Centre de recherche en CONCAVE
Université Concordia
1455 de Maisonneuve O.
Montréal (Québec) H3G 1M8

Novembre 2006

RESEARCH TEAM

Subhash Rakheja	Université Concordia
Marc J. Richard	Uinversité Laval
K. Siddiqui	Université Concordia
Ion G. Stiharu	Université Concordia
R.B. Bhat	Université Concordia
R. Sedaghati	Université Concordia
Z. Wang	Université Concordia
J. A. Romero	Mexico Institute of Transport
V. Mucino	University of West Virginia
G. Yan	étudiant, Université Concordia
B. Lin	étudiant, Université Concordia
Korang Modaressi	étudiant, Université Concordia
T. Ziriani	étudiant, Uinversité Laval
José Esteves	Technicien, Université Concordia

SUMMARY

This project was initiated in collaboration with MTQ with an overall objective to contribute towards attainment of improved roll and directional stability limits of tank trucks. The specific objectives involved fundamental studies in dynamic fluid slosh through development of a scale-model laboratory tank simulator, dynamic fluid slosh analyses through laboratory experiments and analytical methods, slosh model validations, studies on significance of transient fluid slosh and role of baffles, roll stability analysis of a vehicle in the presence of transient fluid slosh. The study was conducted in five systematic phases. In the initial phase of the study, a though review of published studies on dynamic fluid slosh analyses of moving tanks was conducted to identify proven analytical and experimental methods. From the review of literature, it was concluded that vast majority of studies on tank trucks consider only quasi-static fluid slosh within the partly-filled tank, while neglecting the forces and moments caused by dynamic fluid slosh. The studies of dynamic fluid slosh have mostly considered tanks of arbitrary cross-sections that may not be representative of highway truck tanks. Moreover, the vast majority of the studies focus on two-dimensional fluid flows, while a highway tank may encounter three-dimensional flows under applications of braking and steering maneuvers.

A few studies have also investigated slosh modes through laboratory experiments in order to predict fundamental slosh frequencies, to examine validity of analytical models and to explore potential benefits of alternate concepts in separating walls. The vast majority of experimental studies have utilized scaled tanks of different geometry that would not be applicable for highway tank trucks, namely rectangular, upright and horizontal cylindrical, and oblate spherical tanks. Moreover, the majority have employed very small size tanks that may produce boundary effects that are not representative of highway truck tanks. Only a few studies have investigated the role of baffles on the magnitudes of fluid slosh. These invariably suggest greater effectiveness of longitudinal baffles, which would impose excessive additional weight and cost. Both the analytical and experimental studies have clearly established that magnitudes of transient slosh forces and moments are significantly larger than those predicted using quasi-static formulations. The stability limits of partly-filled tank trucks may thus be even lower than those reported on the basis of quasi-static formulations. The review of literature further suggests that computational demands of dynamic fluid slosh models pose extreme challenges for analyses of coupled vehicle-tank-fluid system.

In the subsequent phase, the designs of two test tanks were conceived for fabrication. The primary purpose of this phase was to develop a laboratory tank simulator that could support current and future studies on dynamic fluid slosh, role of baffles and design of alternate anti-slosh mechanisms. The two test tanks included a circular cross-section tank and an optimal cross-section tank design that was realized by the team in its earlier study supported by NATEQ and MTQ. Owing to lack of knowledge and efforts on the role of baffles in controlling the fluid slosh, the designs emphasized modularity to facilitate studies with different types of baffles and separating walls. The results attained in collaboration with researchers at West Virginia University (WVU) and Mexico Transportation Institute (IMT) converged towards a relatively narrow tank, which revealed suppression of lateral motion of

fluid. The results thus showed insignificant lateral load shift and considerably higher slosh frequencies due to small dimensions. Relatively larger size tanks (cross-section area = 0.426 m^2; length =1.85 m) were thus realized at CONCAVE Research Centre to achieve appreciable slosh and load shifts in both the planes of the tanks. Each tank comprised three segments with flanges to adapt to different designs of baffles. The tanks were fabricated using 1.25 cm thick plexiglass sheets and 0.762 m diameter tubes to facilitate flow visualizations. Both the tanks provided identical cross-section area and volume.

The tank slosh simulator was realized by mounting each test tank on 3 three-axes quartz force plates (Kistler 9257BA dynamometers) through saddle supports. The tank with the dynamometers platform was fixed to the bed of a custom-designed horizontal slip table. This slip table coupled with a 0.45 m stroke servo-hydraulic actuator was permitted to glide on an oil-covered granite block along a specified constrained direction. The simulator was designed such that the tank may be installed either in the longitudinal or in lateral direction to simulate for longitudinal as well as lateral excitations. Moreover, the tank installation in a direction oblique to the excitation axis could result in simultaneous lateral and longitudinal excitations for simulation of combined braking and steering inputs. The forces arising from the liquid slosh were measured using the three dynamometers with built-in charge amplifiers. One of the dynamometer was located in the front and two in the rear. A linear variable differential transformer (LVDT) and a micro-accelerometer were also installed to measure the slip table displacement and acceleration, respectively, along the axis of excitation. A total of 11 channels were used for acquisition of force component signals from three dynamometers as well as the platform acceleration and displacement signals. The force signals were manipulated to derive slosh forces along the lateral, longitudinal and vertical directions, and roll, pitch and yaw moments.

Different baffles were further designed for both tanks, which could be easily inserted in the modular tank designs. These included a flexible separating wall, a single orifice baffle and a multiple orifice baffle. The experiments, however, were performed with single- and multiple-orifice baffles in conjunction with the optimal cross-section tank. A comprehensive test matrix was designed to measure slosh forces and moments caused by various fill levels within tanks with different baffles, while subject to different excitations. The test matrix included: three different configurations of the test tank (cleanbore, tank with single-orifice baffles, and tank with multiple orifice baffles); three fill volumes (30, 50 and 70%); two axes of excitations (lateral and longitudinal); and several transient and steady-state excitations. Transient excitations representing idealized path-change and braking maneuvers were synthesized in the laboratory with different magnitudes and rates. Harmonic excitations of varying frequencies and magnitudes were further applied to study the frequency response behaviour and natural frequencies of partly-filled tanks. The data acquired from the experiments were inertia corrected and analyzed to determine the nature of slosh forces and moments, and slosh frequencies under different fill volumes and excitations. These data were used in the subsequent phase for validating dynamic slosh models.

In the third phase of the study, a nonlinear three-dimensional model is developed for analysis of fluid slosh. The model was developed for both tanks and three configurations involving un-baffled and baffled tanks in order to characterize the nature of dynamic slosh forces and

moments under different excitations and to study the role of baffles. The nonlinear models were developed for both the scaled test tanks and full-size highway tanks. The models were solved under lateral, longitudinal and simultaneous lateral and longitudinal acceleration fields, using the FLUENT software. The pressure distributions at the submerged tank wall in the three-dimensional domain were analyzed to derive the resulting lateral and longitudinal forces, and roll, yaw and pitch moments imposed on the structure of the tank with and without baffles. The influences of magnitudes of acceleration and fill condition on the transient and steady-state forces and moments were further investigated for the cleanbore as well as baffled tank. The results obtained for the optimal cross-section test tank under various excitations and fill volumes were compared with the measured data to demonstrate the validity of the models. The model validity under different excitations was particularly emphasized due to nonlinear nature of slosh and lack of such results in published studies. The results were also analyzed to derive fundamental slosh frequencies, which were further compared with those estimated from an analytical method and experimental data. The model results in-general showed very good agreements with the measured data for all the fill conditions and excitations considered. Lateral or longitudinal excitations in the vicinity of fundamental slosh frequency resulted in whirling of free surface and considerable magnitudes of forces in direction other than the excitation axis. These results suggested strong coupling between the longitudinal and lateral slosh.

The validated model was subsequently applied to study the slosh forces and moments developed in a full size tank of circular cross-section and the significance of baffles. The model results were obtained under idealized ramp-step excitations along lateral, longitudinal, and combined lateral and longitudinal axes. The significance of dynamic fluid slosh was investigated by considering mean and peak slosh forces and moments, and variations in mass moments of inertia of the fluid cargo within cleanbore and baffled tank, for two different fill volumes and various magnitudes of excitations. The ratios of transient responses to the mean responses, termed as amplification factors, were further described to emphasize the significance of dynamic fluid slosh on the forces and moments induced on the vehicle. The results in general suggested that the mean responses attained from dynamic fluid slosh analyses correlate well with those attained from the quasi-static analyses for a cleanbore tank. The amplification ratios of the resulting forces and moments, however, could approach as high as 2. The results clearly show that the presence of baffles helps to suppress the peak as well as mean slosh forces and moments significantly. Moroever, the longitudinal baffles can also help limit the peak lateral slosh force and roll moment.

Owing to complexities associated with integration of computationally demanding dynamic fluid slosh model with the nonlinear vehicle model, a simplified roll moment equilibrium methodology was developed in the final phase of the study. This approach permitted for analyses of transient fluid slosh on roll stability limits of a partly filled tank vehicle. The transient forces and roll moment caused by fluid slosh within partly filled circular and optimal cross-section tanks, subject to a time-varying lateral acceleration field, were evaluated numerically and compared with those estimated from a quasi-static formulation. The variations in the center of mass coordinates, vertical and lateral forces, and roll moment were applied to the roll-moment model of a 6-axle tractor-semitrailer articulated tank vehicle for analysis of steady turning rollover threshold. The results showed that the magnitudes of

transient lateral force and roll moment approach significantly higher values, when compared to those estimated from the quasi-static formulations. The steady-turning rollover threshold accelerations of the vehicle combination with partly-filled tanks were thus considerably lower when transient slosh forces and moment were considered in the moment equilibrium, specifically for the intermediate fill volumes. The results further showed that the static roll stability limits of the combination with the optimal cross-section tank are considerably higher than those with a circular cross-section tank.

TABLE OF CONTENTS

1. INTRODUCTION

The dynamic stability and controllability limits of freight vehicles are known to be lower than those of other road vehicles, which have been attributed to the high center of gravity (*cg*), and relatively higher weights and dimensions of the freight vehicles [1]. Analyses of reported accidents suggest relatively higher frequency of accidents involving heavy trucks when compared with the passenger vehicles [2,3]. Furthermore, a large number of accidents have been attributed to maneuver induced instabilities, such as roll and yaw instabilities. Instabilities leading to vehicle rollover have been encountered more commonly that are associated with transient directional responses of vehicles under cornering, lane change, or braking-in-a-turn maneuvers. Analyses of accidents involving liquid cargo vehicles suggest that such vehicles exhibit even higher rollover risks [4,5], which may be attributed to two primary factors: (i) high *cg* design of the tanks; and (ii) the presence of high magnitude transient forces and moments caused by fluid slosh in the roll and pitch planes under partial fill conditions. Owing to the high safety risks associated with a potential rollover, extensive efforts have been made to enhance the roll stability of heavy vehicles [6]. These include developments in active roll control, rollover prevention and load transfer control systems. Enhancement of directional stability limits of tank trucks, however, involves additional special considerations related to tank design and anti-slosh mechanisms, namely, tank geometry, high and variable *cg* coordinates, cargo fill level, lateral and longitudinal load shifts during turning, braking and lane change type of highway maneuvers, as well as liquid-structure interactions.

Tank vehicles, employed in general purpose bulk transportation, are often partly-filled due to regulations governing maximum axle loads and variations in weight density of various products, while those employed in fuel transportation may encounter partial fill conditions during local delivery. Safe highway transportation of liquid products, that may be hazardous, requires highly skilled drivers and safer equipment. Moreover, the integrity of the tank structure to withstand stresses due to liquid surge, containability in the event of an accident, and stability and controllability limits of the vehicle influenced by mobility of the liquid cargo within the tank, need to be considered [7].

The fluid slosh within a partly-filled tank truck and its effects on the vehicle stability limits have been widely investigated by considering additional roll and pitch moments using kineto-static translation of the fluid cargo [8,9]. Such analyses are applicable for cleanbore tanks alone, and cannot simulate for the forces and moments caused by transient fluid slosh and anti-slosh property of the baffles. Alternatively, mechanical analogous models have also been proposed to account for the dynamic fluid slosh and its effects on directional responses of the vehicle [10,11]. These models pose considerable complexities in identification of model parameters and their validity for baffled containers has not been attempted. A number of dynamic liquid slosh models have been attempted using computational fluid dynamic methods to study the motion of free surface under idealized tank motions [12,13].

The above studies have shown that the dynamic fluid slosh is strongly influenced by the tank geometry apart from the magnitudes of body forces imposed by directional maneuvers. The earlier study conducted by the team revealed that circular cross-section tanks, often employed in general purpose transportation of chemicals and liquid food products, yield higher *cg* and partial

fill condition with heavier products [4]. Moreover, such tanks are often designed without baffles and compartments to facilitate cleaning, when an alternate product is transported in the same tank. Such a design causes considerable load shifts and thus significant destabilizing moments on the vehicle under directional maneuvers. The modified-oval cross-section tanks, designed with baffles and compartments, offer lower *cg* height and relatively wider cross-section. The partial-fill condition coupled with wider cross-section could cause excessive lateral load shift, specifically under low fill volumes. Furthermore, the thin aluminum shell of such tanks offers very little puncture resistance in the event of a highway accident. The study proposed optimal tank geometry to yield lower *cg* height with limited lateral fluid slosh [8,14,15]. The effectiveness of the proposed geometry in enhancing the roll stability limit was demonstrated for a tractor-tank-semitrailer vehicle using quasi-static fluid slosh within a cleanbore tank.

A few studies have also suggested that the magnitudes of forces and moments caused by transient fluid surge are significantly greater than those predicted by steady-state and quasi-static slosh models [16]. The quasi-static and steady-state slosh models may thus over-estimate the directional stability limits of partly-filled tank trucks. Moreover, a study of dynamic fluid slosh within a partly-filled tank truck and its effects on directional stability limits necessitates consideration of the coupled fluid-vehicle system in conjunction with the tank structure and the baffles. The reported studies on tank truck dynamics have mostly employed kineto-static fluid slosh models, which do not permit for consideration of the transient fluid slosh and the role of baffles. The complex formulations of the dynamic fluid slosh models and limited availability of reliable solution techniques, on the other hand, have limited their applications to comprehensive vehicle models. Additionally, the validity of the dynamic fluid slosh has been limited to very small rectangular tanks [16].

2. OBJECTIVES OF THE STUDY

This study was motivated by the outcome of the previous study [4], specifically to further explore the potential performance benefits of innovative optimal tank geometry. While the overall objective remained unchanged, to contribute towards attainment of improved roll and directional stability limits of tank trucks, the specific objectives involved comprehensive assessment of performance benefits in terms of rollover immunity potential of the optimal geometry through scale model design and fabrication, prototype testing, tank/vehicle model validations, and systematic analysis of different designs of baffles in terms of dynamic load shifts. The specific objectives of the study are summarized below:

- Conceive the design of two scale model tanks: (i) circular and (ii) optimal on the basis of geometry realized in the earlier study [4].
- Fabricate prototype tanks with sufficient flexibility to study the role of different designs of baffles in the medium-term with transparent materials, such as plexiglass, to facilitate visualizations of the fluid slosh.
- Develop a laboratory test bench design to study the fluid slosh within the tanks and effectiveness of baffles and partitions under varying synthesized excitations.
- Design an instrumented sub-frame for the tank installation in the laboratory to acquire longitudinal and lateral load-shifts, and slosh forces and moments under simulated braking and steering-induced accelerations.
- Perform prototype tests in the laboratory with the tanks with sub-frame assembly installed on a long-stroke slip-table driven by 40 cm stroke electro-hydraulic exciter.
- Develop different designs of baffles and perform experiments to assess their responses
- Develop dynamic fluid slosh models to derive responses of tanks in terms of dynamic load transfers, slosh forces and moments along the longitudinal and lateral axes.
- Analyze the acquired laboratory data to validate the computer models and conduct performance benefit analyses in terms of dynamic load shift and rollover immunity levels of a tank vehicle.
- Investigate the roll stability limits of a partly-filled tank truck in the presence of transient fluid slosh forces and moments, and assess the performance potential of the optimal tank geometry.

Apart from the above, the project resulted in a comprehensive laboratory simulation tool to study the impact of different concepts in baffles in the future. It is anticipated that the team will continue to conduct further experimental studies to evaluate potential benefits of different anti-slosh concepts, such as spiral baffles, inclined partition walls, and intermittent baffles. The education and training of young researchers in this essential discipline through graduate program supervision at Concordia and Laval also formed another objective of the project.

3. REVIEW OF RELEVANT LITERATURE

The directional response and stability characteristics of various conventional heavy vehicles carrying rigid cargoes have been extensively investigated in the past few decades. Limited efforts, however, have been made towards analysis and enhancement of vehicle stability and controllability under the influence of cargo movement. In view of the consistent increase in the volume of motor vehicles carrying liquid cargoes and relatively higher risks associated with accidents involving such vehicles, it is essential to explore alternate design and operational measures to enhance their maneuver stability and structural integrity, and to ensure that cargo tank vehicles possess safety performance characteristics that are either comparable to or better than those of the other highway vehicles. The studies on fluid slosh within moving containers have been mostly limited to tanks alone and require integration with the nonlinear vehicle dynamics models. The reported studies on dynamic fluid slosh within moving containers are briefly reviewed in order to develop appropriate analytical methods relevant to this study and to identify performance measures related to the effects of transient fluid slosh.

Mechanics of dynamic fluid slosh within partly-filled moving containers have been investigated for varying applications, involving aerospace, marine, rail and trucking transportation. Earlier studies were performed for analyses of fluid slosh in fuel tanks of space vehicles using linear slosh theory [11]. It was shown that the fundamental slosh frequency is a significant factor that may lead to instability of the vehicle. Budiansky [17] further investigated the transverse slosh in a horizontal open canal and derived slosh modes as a function of the fill level.

3.1 Analysis of Liquid Slosh and its Effects on Directional Dynamics of Road Vehicles

The above-stated earlier studies provided considerable insight into the slosh mechanics, particularly the fundamental slosh frequencies and deflection modes. Moreover, these studies served as the essential basis for investigating the effects of fluid slosh in aerospace, marine and road vehicles. The effects of liquid slosh on directional dynamics of vehicles have been investigated using two different methodologies. Quasi-static fluid slosh models have been invariably used to investigate the vehicle roll stability limits and braking performance. Dynamic slosh models of varying complexities have been developed and analyzed to study the transient as well as steady-state fluid motion within partly-filled tanks. The dynamic slosh models, however, have been mostly limited to the tank alone subject to idealized body forces. The reported studies have shown adverse effects of fluid slosh on the vehicle performance, irrespective of the modeling approach used.

3.1.1 Quasi-static fluid slosh

The effect of longitudinal fluid slosh within liquid tanks on the directional behavior of highway vehicles was investigated by Ervin et al. [18]. Strandberg [19] investigated the effect of tank shape and longitudinal baffles on the suppression of liquid slosh and its effect on road tanker stability. It was shown that both the tank shape and longitudinal baffles have significant effects on the lateral load shift, and thus the lateral stability of the vehicle. The longitudinal baffles, however, add considerable weight to the tank trailer. The effect of compliant suspension and tires on the liquid load shift was further accounted for using a roll-plane model of a circular tank

integrated to the steady turning roll model of an articulated tank vehicle to study the effects of fill level and on the rollover threshold of the vehicle under partial fill conditions [20]. The effect of tank geometry and the fill level on the overturning limit of a tractor-semi-trailer was further evaluated in an analytical study applying steady-state load shift induced by the lateral acceleration [4,15]. Using the quasi-static fluid slosh, it was illustrated that the destabilizing roll moment of a partly-filled vehicle subject to an idealized lane change excitation is considerably higher than that of an equivalent rigid cargo vehicle. The effect of liquid load shift on stopping distance performance of the tank vehicles was also investigated using the quasi-static liquid slosh solution under a straight-line braking input [21]. The effect of simultaneous application of lateral and longitudinal acceleration fields, idealizing braking-in-a-turn maneuver, on directional performance of a partly-filled tank vehicle with the optimized tank cross-section was investigated in the previous study [4].

The results attained from the above studies have invariably concluded that fluid movement within a partly-filled tank vehicle affects the vehicle stability limits in an adverse manner. The dynamic fluid slosh induces additional forces and moments on the vehicle, which may reduce its dynamic stability limits. The magnitudes of these forces and moments depend upon many design and operating factors, such as tank geometry, baffles, and fluid viscosity and fill level, and vehicle speed and maneuvers. A number of studies have demonstrated lower roll stability limits of partly-filled tank trucks through analyses of static as well as roll dynamic models of different vehicle configurations [4, 8, 15, 22, 23]. The vast majority of the studies based on quasi-static solution have considered destabilizing moments developed either in roll or in pitch plane. The effect of fluid slosh under simultaneous braking and steering has been investigated in a single study undertaken by the team through support from the NATEQ-MTQ-SAAQ program [4]. The team had applied the quasi-static methodologies to study the effects of tank geometry on the steering and braking performance of partly-filled tank trucks using comprehensive vehicle dynamics models, such as constant velocity yaw-roll and phase 4 models. Results attained from field measurements suggested that vehicle responses using quasi-static slosh model yield reasonably good agreements with the measured data in steady-state [24]. Such models, however, cannot predict the effects of transient fluid slosh and oscillations near the fundamental frequency, which may further reduce the directional stability limits of the vehicle [16].

3.1.2 Mechanical equivalent fluid slosh models

The sloshing of liquids and resulting fluid-structure interactions have been identified as important issues in the area of transportation engineering and many other fields since 1950's. These include the movement of liquid fuels within automobile tanks; movement of liquid products and chemicals in tank trucks, railroad cars and oceangoing vessels; fuel tanks of airplanes and space-crafts; liquid motions in containers of offshore structures, etc. Sloshing of liquid in a partially-filled container subjected to external excitations from the retaining structure may cause coupled dynamic interactions between the liquid and structure. The coupled problem associated with interactions of the sloshing liquid with the moving vehicle has been recognized as an important issue related to directional stability of various vehicles [25]. The dynamic interactions can adversely affect dynamics and stability of the vehicles as well as the structural integrity of the retaining structures. The vehicle and the retaining structure may be subjected to excessive forces and moments, when fundamental slosh frequency lies in the vicinity of the natural frequency of the vehicle structure or the control frequency. Owing to the complexities

associated with transient fluid slosh analysis, a number of mechanical equivalent models of fluid slosh have been proposed to study the influences of dynamic slosh forces and oscillation frequency on the vehicle responses. These models are based upon either a pendulum or damped spring-mass system analogies [11, 26-29], as shown in Figs. 3.1 and 3.2.

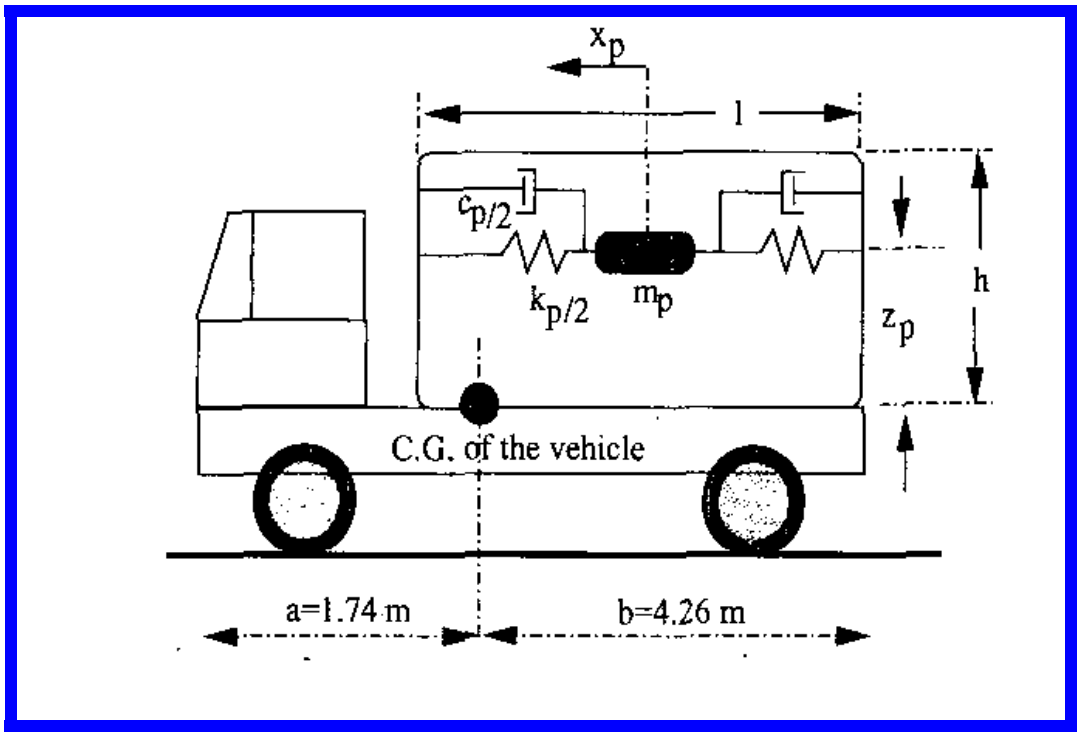

Fig. 3.1: A spring-mass analogous of the liquid tank.

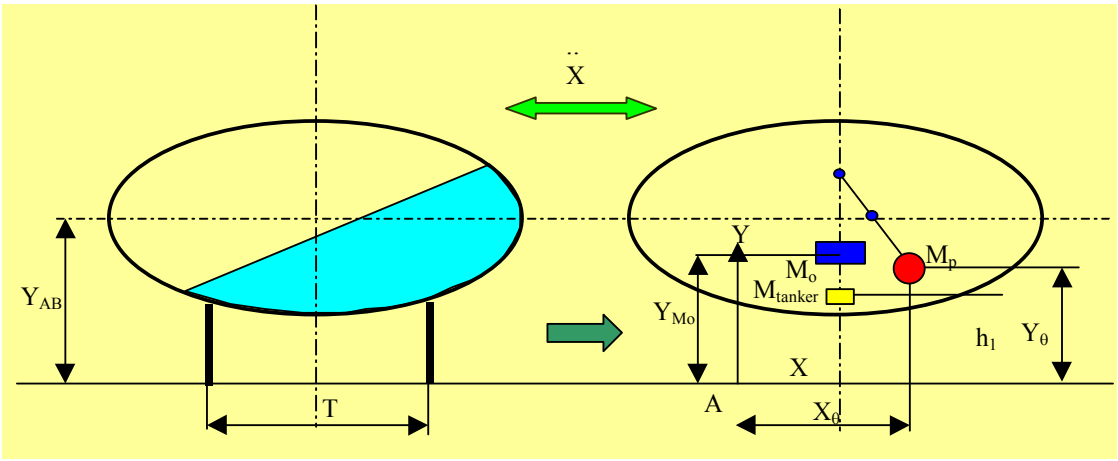

Fig. 3.2: A pendulum model of fluid motion within a partly-filled tank.

The mechanical analogies of fluid slosh have been applied to study, the effects of transient transverse liquid slosh on a road tanker dynamics in the roll plane under partial fill conditions.

The model parameters are derived from the experimental data assuming linear mechanical system models and small displacements. The identification of model parameters, however, is quite complex, while the model validity is questionable due to relatively large magnitudes of transient fluid slosh. Moreover, the model parameters and strongly depend on the tank geometry and the derivation of a mechanical analogy could be highly cumbersome, when complex tank boundaries are involved [21,22].

3.2 Dynamic Liquid Slosh Models

A number of dynamic fluid slosh models have been developed to study the liquid motion within moving containers, although majority of the studies have focused on the free surface motions [12,27,30]. Cooper [31] and Abramson [11] conducted comprehensive reviews on the topic of liquid sloshing problems. These preliminary works presented some important analytical solutions and experimental data for examining the validity of the linear theoretical models. Since the 1960's, a great number of investigations on liquid sloshing have been carried out in different applications involving space vehicles, cargo ships, large ground storage tanks, canals, etc. Majority of the existing theories on fluid sloshing are based on the assumptions of inviscid incompressible fluid, where a velocity potential exists, and small amplitudes of fluid motion compared with container dimensions, often the depth of the fluid. The complexities associated with the free-surface equation are overcome either by neglecting nonlinear terms assuming relatively small wave height and fluid velocities or by linearization [17, 32]. The majority of the reported theoretical and experimental works focus on liquid motions under harmonic disturbances, while the analyses under arbitrary excitations were reported in relatively few studies.

The experimental and analytical studies have shown that the liquid viscosity has insignificant effect on the fluid motion. The dynamic fluid slosh analyses are thus mostly performed assuming non-viscous flow. It was shown that the presence of lightly damped mode of liquid slosh in the vicinity of natural frequency of the navigational control system could cause rocket failure [11]. For road vehicles, the slosh mode in the vicinity of steering or lateral mode frequency could cause resonant fluid oscillation and thus affect the directional performance in a highly adverse manner. The potential theory has been widely used to formulate an inviscid flow inside a tank to derive the slosh frequencies and the distributed forces and moments imposed on the tank [25]. The potential flow has been further applied to study the slosh behavior in the presence of baffles within rectangular cross-section upright cylindrical tanks [11]. The results illustrate that frequency of fluid slosh in a baffled tank is significantly higher that that of slosh in a cleanbore tank. The potential flow theory, however, is limited to small displacement of the liquid and could only be applied to simple two-dimensional geometries.

In the past few decades, many numerical algorithms have also been developed to study the sloshing behavior of liquids in stationary and moving containers using finite difference, finite element, and boundary element methods [33-35]. Ortiz [36] presented a review on various solution procedures for fluid motion involving a free surface, and concluded that majority of past works on liquid sloshing are based upon prescribed motion of liquid retaining structure, where motions of the liquid and container are uncoupled, and that there is very little published information on true fluid-structure interactions including the nonlinear sloshing effects. In the context of a moving tank truck, the analysis of impact of fluid slosh requires three steps for

coupled motions of the fluid and the vehicle: (*i*) defining dynamics of the vehicle as functions of the liquid cargo pressure field; (*ii*) analysis of the pressure in the liquid domain as function of the accelerations of the moving frame attached to the tank trailer; and (*iii*) coupling these two sets of motions, which is quite complex due to nonlinearities associated with the vehicle and fluid motions.

The nonlinear liquid slosh in tank vehicles has been analyzed in a few studies through solution of Navier-Stokes equations for analysis of transient slosh forces exerted on the tank wall [16, 37-40]. Such models consider fluid viscosity and large amplitude of free surface deformation. Su [40] performed a thorough study on the dynamics of liquid slosh caused by roll, pitch or rectilinear motion of the tank through solution of the nonlinear incompressible fluid flow equations for distributed slosh forces. Popov [16] used finite difference technique to obtain transient solutions for incompressible viscous flows within a compartmented rectangular tank subject to horizontal acceleration fields. The Marker-and-cell (MAC) technique was applied to track the deformation of the free surface. It was shown that the peak forces and moments are functions of the fill level and the number of compartments. The study further investigated the role of baffle area on the attenuation of oscillating liquid slosh. The results revealed that the area of the baffle nozzle has significant effect on the alleviation of transient slosh force.

The dynamics of the liquid slosh within a partly filled tank with circular cross-section was analyzed using the same technique. It was shown that the peak forces and roll moments arising from fluid slosh are considerably larger than the corresponding mean values, which correlate well with those deduced from quasi-static solutions. The simulation results suggest that the magnitudes of transient forces and moments are significantly larger than the steady-state magnitudes, which may further deteriorate the dynamic stability limits of tank vehicles [16]. The effects of transient fluid slosh on the dynamics of the vehicle, however, have not yet been investigated due to complexity of the fluid slosh models. Moreover, only limited validations of the dynamic fluid slosh models have been presented. A few studies have performed laboratory measurements of the free surface using small scale model tanks, while the measurements of slosh forces and moments have not been attempted.

Owing to the complexities of the dynamic fluid slosh models, almost no efforts have been made towards integrating the dynamic fluid slosh models with the directional dynamics model of the vehicle. The analyses of effects of fluid slosh on the vehicle responses require effective and reliable dynamic fluid slosh models. The validity of such models in predicting the magnitudes of transient and steady-state slosh forces and moments thus needs to be established. Moreover, far more efforts are desirable to study the role of baffles in dynamic fluid slosh analyses.

3.3 Control of Liquid Slosh

Studies conducted on fluid slosh in a spacecraft have suggested various for slosh suppression techniques [12], which may also be applied for controlling slosh forces and moments in road vehicles. These techniques can be grouped under three categories, listed below:

- Through reduction of the proportion of the sloshing mass in relation to the total liquid mass.

- Tuning of slosh frequencies to ensure that these do not occur in the vicinity of the excitation and vehicle frequencies.

- Damping of slosh motion to reduce the peak magnitudes of transient slosh forces and moments.

The suppression of liquid slosh by means of reducing the sloshing mass is typically implemented by introducing of compartments within the tank. The magnitude of fluid slosh loads, however, depends upon the number of separating wall and their arrangement within the container [41]. An optimal order of unloading different compartments has also been proposed to ensure maximum roll stability of the partially-loaded road tanker [42]. Longitudinal separating walls are known to be most effective in enhancing the roll stability limits, while they impede the load carrying capacity [19]. Apart from the compartments, the transverse baffles tend to attenuate the dynamic forces considerably under partial fill conditions, particularly under braking [16].

Mucino [45] investigated dynamic slosh in elliptical tanks equipped with partial as well as full longitudinal baffles using FLUENT software. The analysis involved six different combinations of baffles, including a full partition wall, and single and partial longitudinal baffles, as shown in Fig. 3.3. The results revealed longest settling time for slosh in an un-baffled tank, while the dual baffle arrangement provided near critical damping under an acceleration excitation representative of a lane-change maneuver. These results confirm the findings of other studies based upon kineto-static analyses on the effectiveness of longitudinal baffles in suppressing slosh loads [19]. The implementation of such baffles, however, is very unlikely due to excessive weight and material costs of longitudinal baffles.

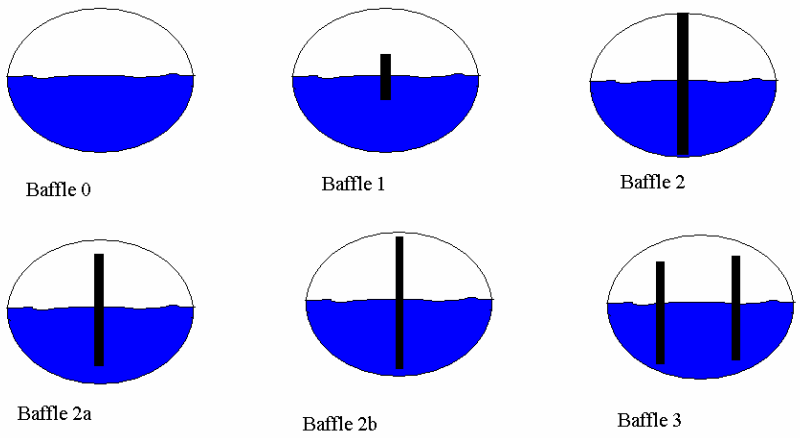

Fig. 3.3: Analysis of fluid slosh in an elliptical tank with different arrangements of full and partial longitudinal baffles [45].

The natural frequency of fluid slosh is directly linked to the ratio of sloshing mass to the total liquid mass, when the slosh frequency lies in the vicinity of the frequency of an excitation. The natural frequencies of slosh have been derived as a function of tank dimensions and fill level [17,43]. The addition of baffles or separating walls yields considerably higher slosh frequency

that may be well above the excitation frequencies. Typical steering frequencies may lie in the range of 0.1-0.5 Hz, while the fundamental slosh frequency of fluid within a partly-filled cleanbore tank has been reported to be near 0.6 Hz. It has also been shown that the peak slosh loads along the longitudinal and lateral directions may be two times higher than the corresponding steady-state magnitudes [44]. The addition of baffles can significantly reduce the transient peak magnitudes in the longitudinal direction. The laterally placed baffles also help to suppress the lateral fluid surge under simultaneous steering and braking inputs.

4. PROTOTYPE TANKS AND EXPERIMENT DESIGN

The dynamic fluid slosh within tanks of different geometry has been widely investigated using analytical techniques. A few studies have also investigated slosh modes through laboratory experiments in order to examine validity of analytical models and to explore the potential benefits of concepts in separating walls. The vast majority of experimental studies have utilized scaled tanks of different geometry that would not be applicable for highway tank trucks. For example, Lamb [46] proposed formulations for predicting frequency of fluid slosh in rectangular tanks, and Popov [16] experimentally investigated the transient fluid slosh for a very small size rectangular tank. Kobayashi et al. [47] reported that Lamb's formulation could be extended to predict slosh frequency response in horizontal circular cylindrical tanks subjected to a longitudinal excitation. Leonard and Walton [48] experimentally investigated the mode shapes and natural frequencies in an oblate spherical tank. The experimental and analytical studies by Abramson [11] and Bauer [7] focused on upright cylindrical containers. In a recent study, Romero *et al.* [43] proposed an analytical method for estimating slosh frequencies for various tank geometries including circular, elliptic and optimal tank proposed by this team [4]. The method was based on estimation of wavelength and speed at the free surface, while the validations were obtained through simple experiments with very small size model tanks.

The above studies have considered tank geometries that are not applicable to tank trucks. Furthermore, the vast majority of the studies have investigated planar slosh behaviour, while only limited efforts have been made on the effects of baffles. Although the results attained from experimental studies have proven to be most significant for validating analytical models, the experiments involved small size tanks. For instance, the cross-section areas of model tanks employed by Strandberg [19], Popov [16], Romero et al. [43] and Abramson [11] were no more than 0.03 m^2. The model tank used by Kobayashi et al. [46] had a cross-section area of 0.17 m^2. Owing to the nonlinear nature of fluid slosh and significant influences of tank geometry and boundary conditions, it is vital to undertake such experimental studies with tanks representative of the highway tanks. Furthermore, the most of the investigations have been limited to measure the hydrodynamic pressure at given points and mean surface wave height. The resultant slosh forces and moments have not been studied sufficiently, which are vital for study of the effects of slosh loads on vehicle stability limits. The design of experiments should also incorporate measurement of forces and moments, apart from the slosh frequencies and free surface motion. Such an experimental setup could serve as a vital tool for verifying the dynamic fluid slosh models and for study of different concepts in anti-slosh devices, particularly different types of baffles.

In this project, modular designs of two scale model tanks of circular and optimal cross-sections are realized, which permit for analyses with different types of baffles and compartments. The tank slosh simulator includes extensive measurement systems for acquisition of slosh forces and moments along the three translational axes. Moreover, the excitations along the lateral and longitudinal directions could be synthesized by appropriately orienting the tank to simulate for excitations arising from steering and braking maneuvers. Simultaneous applications of both excitations could also be realized by installing the tank in a direction oblique to the axis of excitation.

4.1 Design of Test Tanks and Laboratory Simulator

The project was initiated by realizing designs of two different prototype tanks of circular and optimal cross-sections. The optimal cross-section was taken as the OPT4 geometry that was identified in the earlier study conducted through support from NAREQT-MTQ [4]. Dynamic similarity analyses were performed to realize scale model tanks in consideration of the current weights and dimensional regulations, and fundamental slosh frequency. The results attained in collaboration with researchers at West Virginia University (WVU) and Mexico Transportation Institute (IMT) converged towards a relatively narrow tank, which was perceived to suppress the lateral motion of the fluid. These tanks were fabricated for experimental studies at IMT. The results showed insignificant lateral load shift and considerably higher slosh frequencies due to small dimensions. Alternate designs were realized at CONCAVE Research Centre to achieve appreciable slosh and load shifts in both the planes of the tanks. The tanks were designed with certain modularity to permit the use of different baffle designs in the study. Each tank comprised three segments with flanges to adapt to different designs of baffles.

The circular cross-section tank was realized from 76 cm outside diameter tubes of transparent 1.25 cm thick plexiglass material. The length of each section of the tank was 61 cm (24 in). The optimal cross-section tank, as identified in the previous study [4], also comprised three 61 cm long sections with flanges. Figure 4.1 shows assembly drawings of two tanks. Figure 4.2 illustrates dimensions of the optimal cross-section and molded tubular section used for fabrication of optimal cross-section tank. Each prototype tank was approximately 1.85 m long with flat end plates. Pictographs of assembled circular and optimal cross-section tanks are shown in Fig. 4.3.

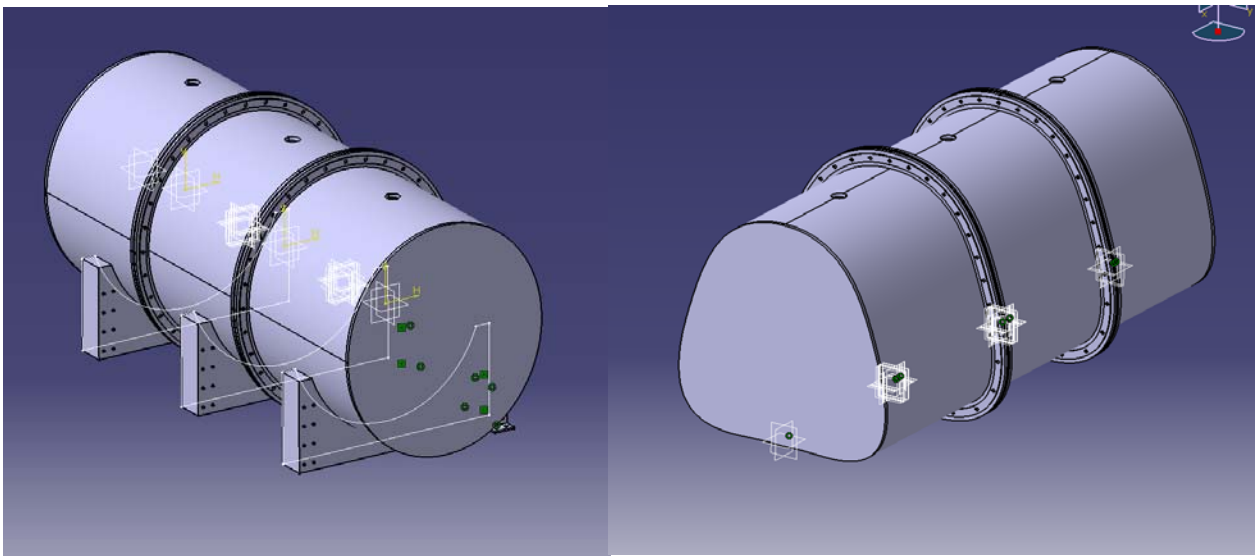

Fig. 4.1: Assembly drawings of two prototype tanks

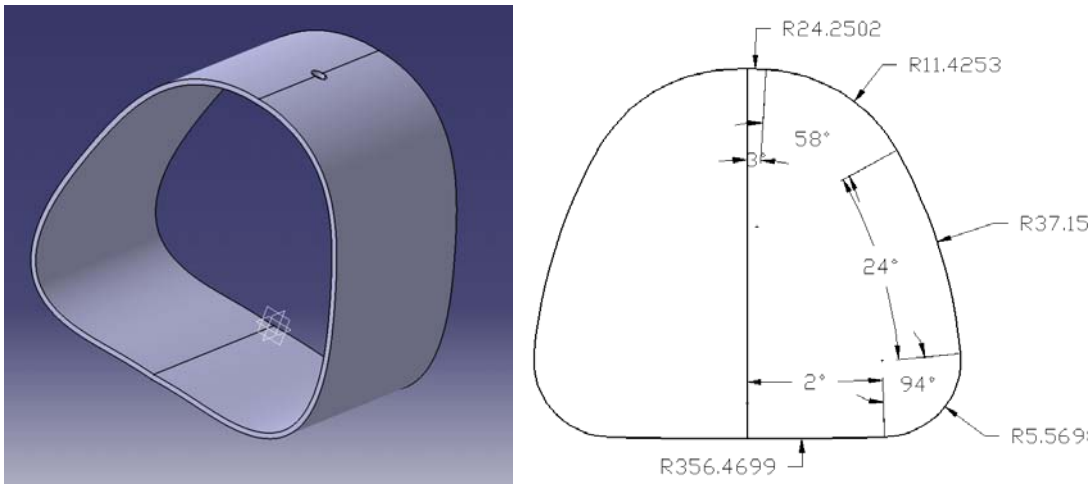

Fig. 4.2: Optimal tank cross-section geometry.

The designs were attempted to attain identical cross-section area and fluid volume for both tanks. Both the tanks provided a cross-section area of approximately 0.426 m^2. The cg heights and fluid volumes corresponding to for different fill levels were computed from the geometry. Table 4.1 summarizes cg and fill heights of fluid for 30, 50, 70 and 100% fill levels. The fill level is defined as ratio of the fluid volume to the total tank volume. The results clearly show that the cg height of fluid in the optimal tank is considerably smaller than that for the circular tank, which should yield direct benefits in terms of improved roll stability for the optimal cross-section tank.

Table 4.1: Fluid volume, fill heights and cg heights of fluid in two prototype tanks corresponding to different fill levels

Fill volume (%)	Optimal cross-section			Circular cross-section		
	Fill height (m)	cg height (m)	Volume (m^3)	Fill height (m)	cg height (m)	Volume (m^3)
30	0.18	0.095	0.236	0.251	0.147	0.236
50	0.294	0.151	0.394	0.368	0.212	0.394
70	0.418	0.210	0.552	0.486	0.274	0.552
100	0.682	0.305	0.788	0.737	0.368	0.788

Each test tank section was mounted on a saddle supports, as it is evident in Fig. 4.1. The tank with saddle supports was mounted on a aluminum plate. The tank with plate was installed on another force platform comprising 3 three-axis dynamometers for measuring slosh forces along all the three directions (x, y and z), as shown in Fig. 4.4. The figure also shows the support fixture of the tank, and dynamometers for measuring dynamic load shifts and slosh forces along the vertical, longitudinal and lateral axes. The test tank with its force platform was further mounted on another plate that was fixed to the bed of a custom-designed horizontal slip table. This slip table was permitted to glide on an oil-covered granite block along a specified constrained direction. The slip table was driven by a 45 cm stroke servo-hydraulic actuator. Figure 4.5 shows installation of a tank on the horizontal slip table, and the actuation system is

schematically shown in Fig. 4.6. The tank fixture was designed such that the tank may be installed either in the longitudinal or in lateral direction to simulate for longitudinal as well as lateral excitations. Figure 4.7 illustrates a schematic of the test system including the test tank oriented along a lateral (y) axis excitation. Moreover, the tank installation in a direction oblique to the excitation axis could result in simultaneous lateral and longitudinal excitation for simulation of combined braking and steering inputs

Figure 4.3: Pictographs of the circular and optimal cross-section test tanks

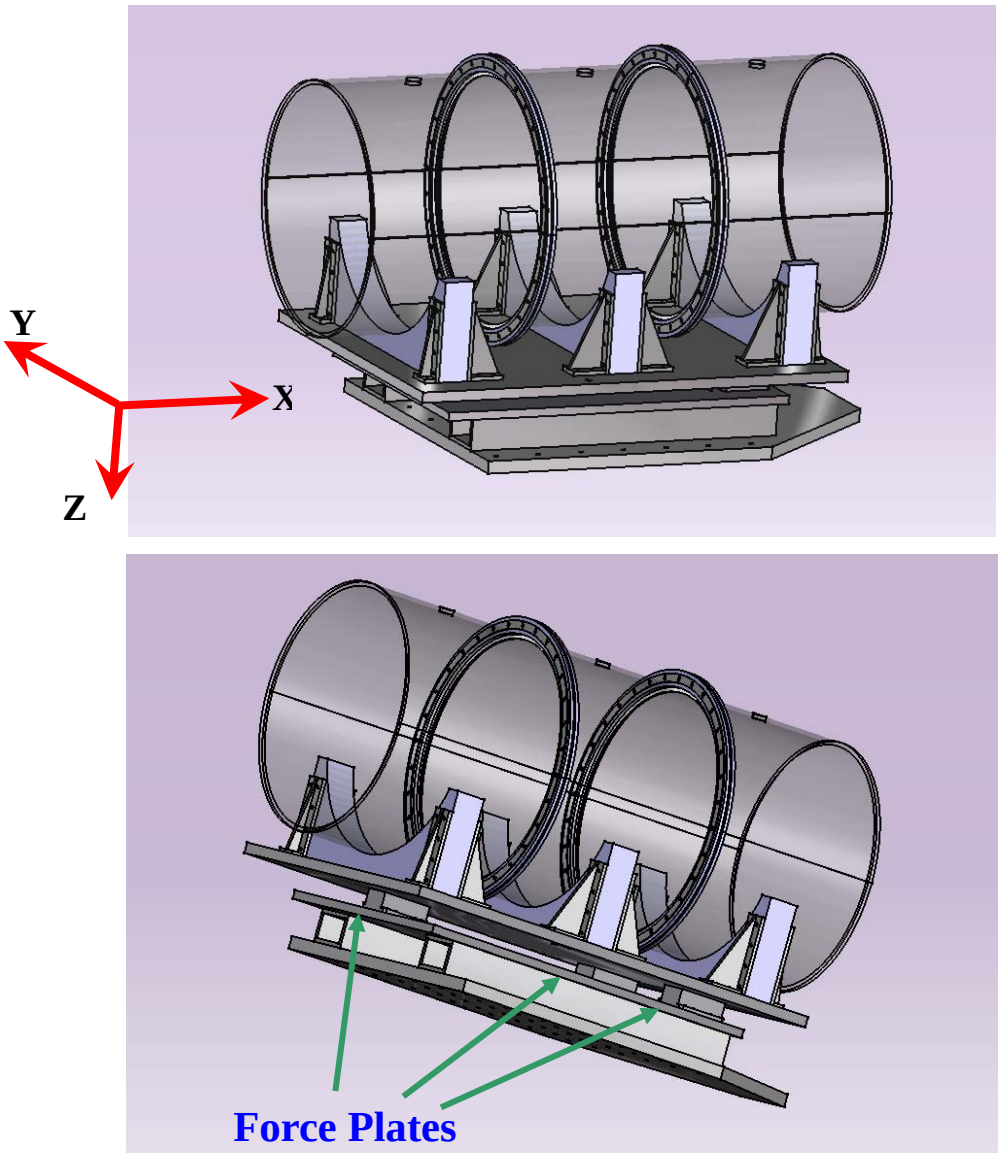

Figure 4.4: A schematic of the circular cross-section test tank together with its support structure and force plates

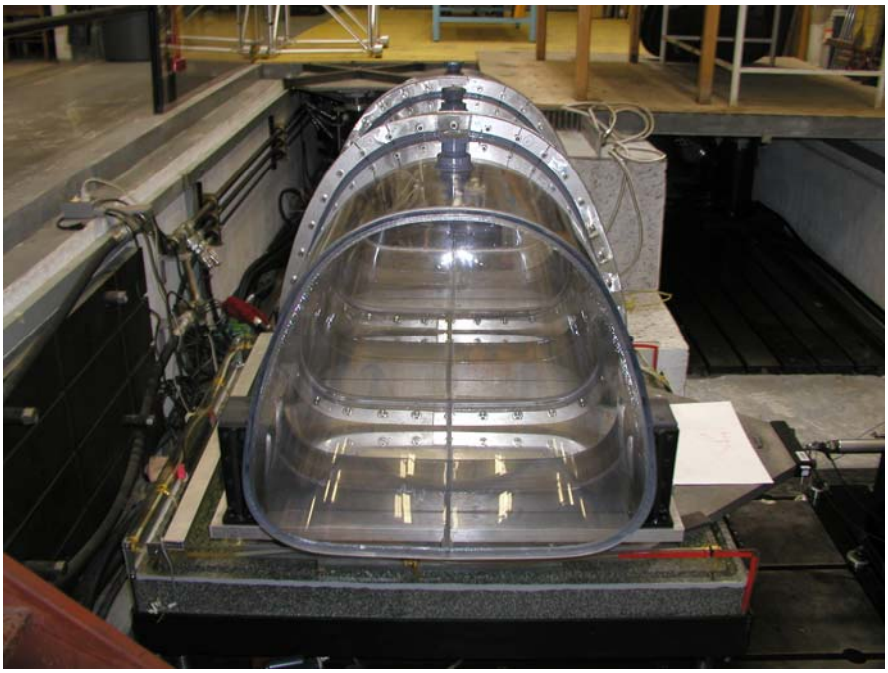

Figure 4.5: Pictographs of the optimal cross-section test tank and fixture positioned on a horizontal slip table and guided along the longitudinal (x) axis

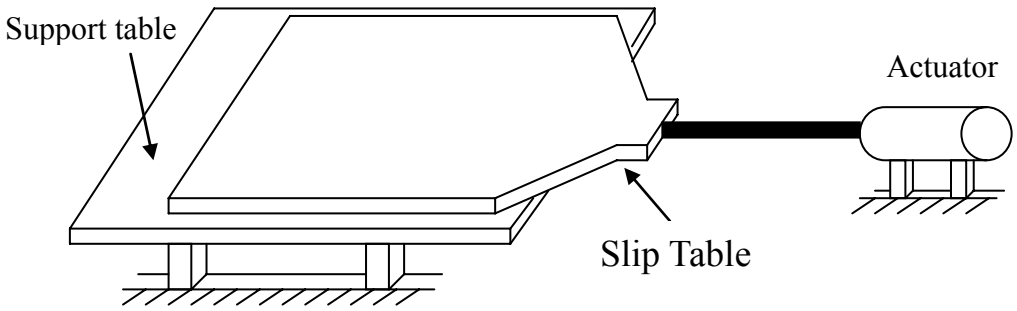

Figure 4.6: Slip table with a servo-hydraulic actuator

4.2 Instrumentation and Data Acquisition

The forces arising from the liquid slosh were measured using three quartz dynamometers Kistler 9257BA with built-in charge amplifiers. The three dynamometers were mounted beneath the tank mounting plate, one located in the front and two in the rear of the plate. Figure 4.8 shows the arrangement of dynamometers labeled as '1', '2' and '3'. Each dynamometer consists of four 3-component force sensors for measuring three force components along the orthogonal axis. The output range for each component is ± 5 V and an external amplifier is used with four options for the force range: ± 0.5, ± 1, ± 2, ± 5 kN in the x- and y-directions, and ± 1, ± 2.5, ± 5, ± 10 kN in the z-direction. The sensitivities for these four ranges are respectively 10, 5, 2.5, 1 mV/N in the x- and y-directions, and 5, 2.5, 1, 0.5 mV/N in the z-direction. In order to avoid any saturation due to large magnitude slosh forces, the largest output ranges were chosen in the

present experiment to obtain measurement system sensitivity of 1 mV/N for x- and y-components, and 0.5 mV/N for the z-component. The settings are summarized in table 4.2. The sensitivities for displacement and acceleration are 1 inch/V and 2g/V, respectively. A linear variable differential transformer (LVDT) and a micro-accelerometer were also installed to measure the slip table displacement and acceleration, respectively, along the axis of excitation. The operating range of the accelerometer was ± 4g with sensitivity of 500 mV/g, while that of LVDT was 254 mm (10 inch) with sensitivity of 39.4 mV/mm (1 V/inch).

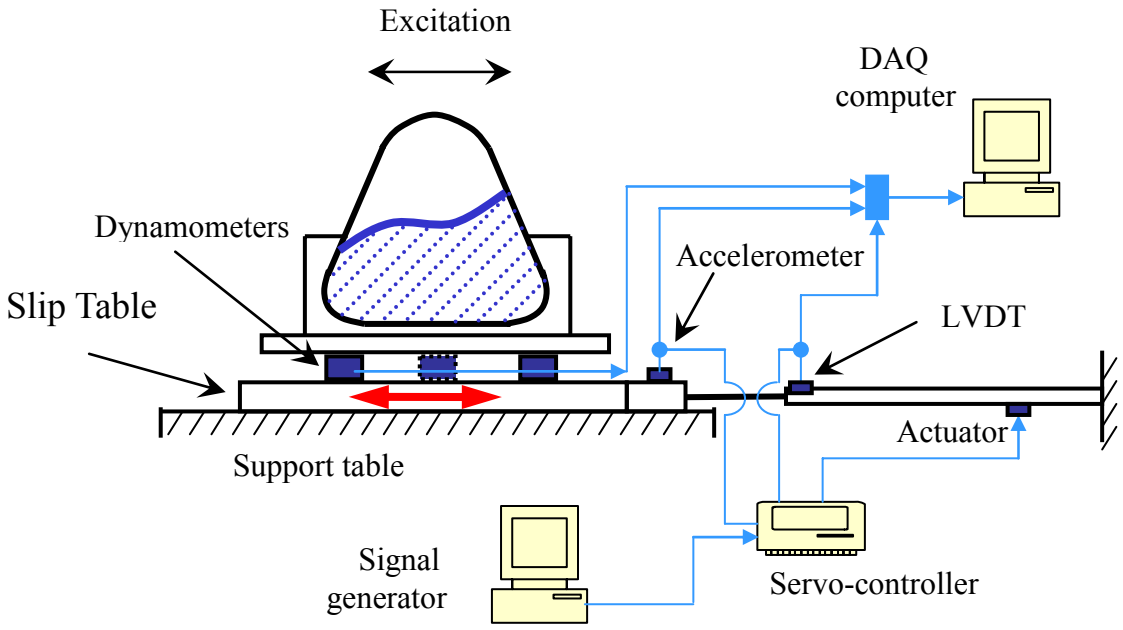

Figure 4.7: A schematic of the tank slosh laboratory simulator

Table 4.2: The sensitivity and ranges of measurement systems

Channel	Signal		Sensitivity	Range
1	Displacement		1 inch/V	254 mm
2	Acceleration		2g/V	$\pm$ 4g
3	Dynamometer (No.1)	F_{x1}	1 N/mV	$\pm$ 5 kN
4		F_{y1}	1 N/mV	$\pm$ 5 kN
5		F_{z1}	2 N/mV	$\pm$ 10 kN
6	Dynamometer (No.2)	F_{x2}	1 N/mV	$\pm$ 5 kN
7		F_{y2}	1 N/mV	$\pm$ 5 kN
8		F_{z2}	2 N/mV	$\pm$ 10 kN
9	Dynamometer (No.3)	F_{x3}	1 N/mV	$\pm$ 5 kN
10		F_{y3}	1 N/mV	$\pm$ 5 kN
11		F_{z3}	2 N/mV	$\pm$ 10 kN

The force, acceleration and displacement signals were acquired using a National Instrument PCI-6036E DAQ board. A total of 11 channels were used for acquisition of the force component signals from three dynamometers as well as the platform acceleration and displacement signals. Table 4.2 summarized the channel assignment and calibrations of the measurement systems. The data was sampled at a rate of 256 Hz and imported in the Labview 7.0 software for subsequent post-processing.

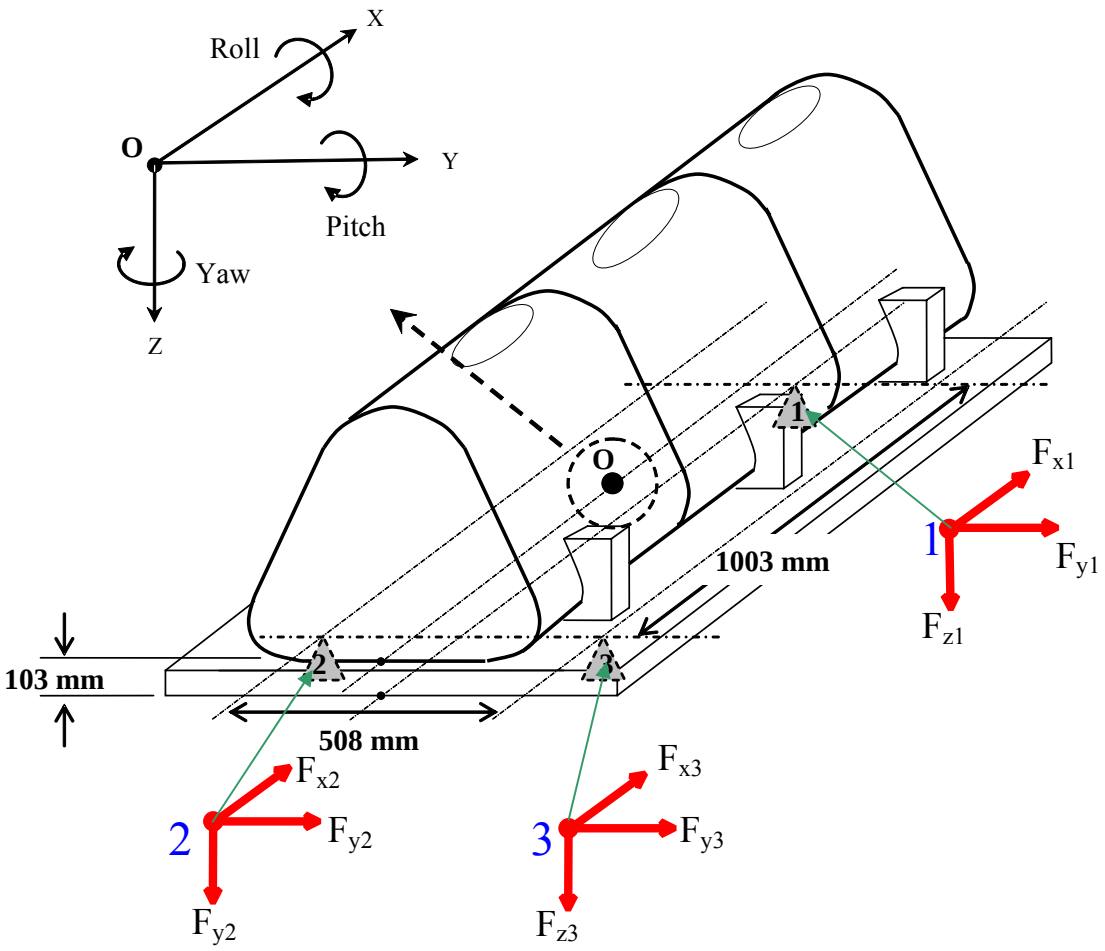

Figure 4.8: Location of dynamometers in the test setup

4.3 Experimental Method and Test Matrix

The primary goal of the experiments was to investigate slosh frequencies and magnitude of slosh forces and moments under given test conditions. The experiments were designed to measure three-components of slosh forces and moments under different tank configurations, fill volumes and acceleration excitations. A relatively large test matrix was designed in order to gain total fundamental understanding of the slosh forces and moments as functions of fill level, baffles geometry, and magnitude, frequency and direction of acceleration excitation. Owing to large size of the test matrix, the experiments for the present study were limited to the optimal cross-section

tank with total length of 1.85 m and cross-section area is 0.426 m^2. Two series of experiments were performed to study the slosh behavior under longitudinal and lateral acceleration, respectively. In the first series, the tank was positioned perpendicular to the actuator axis so as to subject the tank to a lateral acceleration. In the second series, the tank was oriented along the axis of the actuator to generate longitudinal acceleration excitation. Water was used as the test liquid and a coloring agent was added to visualize the flows.

The tank was designed to allow for installation of different types of baffles separating the three sections. Although different designs of baffles and separating walls were realized, the experiments in this study were limited to two different baffle designs. Each series thus involved three tank configurations: (i) cleanbore; (ii) tank with single-orifice (diameter 245.5 mm, located at centre) baffles; and (iii) tank with baffles with 38 small size (each of diameter 38.1 mm) orifices and a large centre orifice (diameter 101.6 mm). The opening area of the two baffles was approximately 11% of the total cross-section area. Figure 4.9 illustrates designs of baffles used in experiments. Experiments were conducted for 30%, 50% and 70% fill volumes. The fill volume is used to measure the fill condition due to the non-symmetrical tank geometry from the top to bottom. For the single-orifice baffle configuration, 30% fill volume was excluded from the test matrix due to lack of an equalizer. This fill condition caused the free surface to lie below the bottom edge of the orifice. Table 4.3 summarizes tank configurations and fill volumes considered in the study.

Table 4.3: Test matrix describing tank configurations, fill volumes and excitations

Tank Configuration	Fill volume (%) (fill height, cm)			Type and direction of excitation		
	30% (17.96	50% (29.39)	70% (41.79)	Harmonic	Step	Single-sinusoid
Cleanbore	√	√	√	Y, X	Y, X	Y
Single-orifice baffles	---	√	√	Y, X	Y, X	Y
Perforated baffles	√	√	√	Y, X	Y, X	Y

For each tank configuration and fill condition, the tank was subjected to harmonic as well as idealized step excitations in terms of acceleration in both lateral and longitudinal directions. The data obtained under harmonic excitations were used to study the dependence of fluid slosh on the frequency and magnitude of external disturbance. The responses to step excitations in the longitudinal and lateral directions were considered to simulate for idealized braking/acceleration and steady turning maneuvers, respectively. The magnitudes and frequencies of excitations were chosen with considerations of range of natural frequency of slosh, constraints imposed by the horizontal actuator stroke and safety of the experimental setup. The fundamental slosh frequencies for the cleanbore test tank were thus initially estimated for different fill ranges using the methodology developed by Romero [43]. Harmonic lateral acceleration excitations were generated at different peak magnitudes, ranging from 0.5 to 3 m/s^2 in the 0.5 to 3.0 Hz frequency range. The longitudinal harmonic excitations were generated at various frequencies in the 0.25 to 1.5 Hz range at three acceleration peak magnitudes: 0.25, 0.5 and 1 m/s^2. Tables 4.4 and 4.5 summarize the excitation magnitudes and frequencies considered along the lateral and

longitudinal axes, respectively. The harmonic acceleration excitations were converted to corresponding displacement signals in order to operate the servo-hydraulic actuators in a displacement feedback control mode.

Table 4.4: Magnitudes and frequencies of harmonic lateral acceleration excitations

Acceleration magnitude (m/s^2)	Frequency (Hz)												
	0.5	0.6	0.7	0.8	0.9	1	1.1	1.2	1.3	1.5	2	2.5	3
0.5	√	√	√	√	√	√	√	√	√	√	√	√	√
1	√	√	√	√	√	√	√	√	√	√	√	√	√
2			√	√	√	√	√	√	√	√	√	√	√
3					√	√	√	√	√	√	√	√	√

Table 4.5: Magnitudes and frequencies of harmonic longitudinal acceleration excitations

Acceleration magnitude (m/s^2)	Frequency (Hz)																	
	0.25	0.3	0.36	0.4	0.45	0.5	0.55	0.6	0.65	0.7	0.8	0.9	1	1.1	1.2	1.3	1.4	1.5
0.25	√	√	√	√	√	√	√	√	√	√	√	√	√	√	√	√	√	√
0.5			√	√	√	√	√	√	√	√	√	√	√	√	√	√	√	√
1						√	√	√	√	√	√	√	√	√	√	√	√	√

Apart from the harmonic and step excitations, a single-cycle sinusoidal acceleration excitation was synthesized in the laboratory to simulate for lateral acceleration encountered during a path-change type of maneuver. The synthesized signal, converted to displacement-time history, was fed to servo-controller as an external function via the Visual Designer software. The single-cycle sinusoidal acceleration function was constructed in a piecewise manner, such that:

$$a(t)=\begin{cases}\dfrac{A}{2}\left[1-\cos(4\pi f)\right] & t \le 0.25T \\ A\sin(2\pi f t) & 0.25T < t \le 0.75T \\ -\dfrac{A}{2}\left[1-\cos(4\pi f)\right] & 0.75T < t \le T \\ 0 & t > T\end{cases} \tag{4.1}$$

where T is period of one cycle; f is frequency in Hz; A is amplitude of sinusoidal function. The sinusoidal function is constructed in a piecewise manner instead of a continuous waveform in order to achieve smooth transition at the beginning and at end of the motion. In the default case, the constants f and A were set to values of 1 and 2, respectively, while the sampling rate was chosen as 1000 Hz. The sampling frequency, however, was varied to achieve different frequency of the waveform. Figure 4.10 shows the acceleration and the equivalent displacement histories corresponding to two different sampling rates of 1000 and 1500 Hz, which resulted in fundamental frequencies of 1 Hz and 1.5 Hz, and peak acceleration magnitudes of 1.93 and 4.35 m/s^2, respectively. The transient slosh behaviour under longitudinal excitations was also measured for various fill levels and tank configurations. For this purpose a periodic longitudinal

acceleration function comprising ramp-step like variations was synthesized as shown in Fig. 4.10(b).

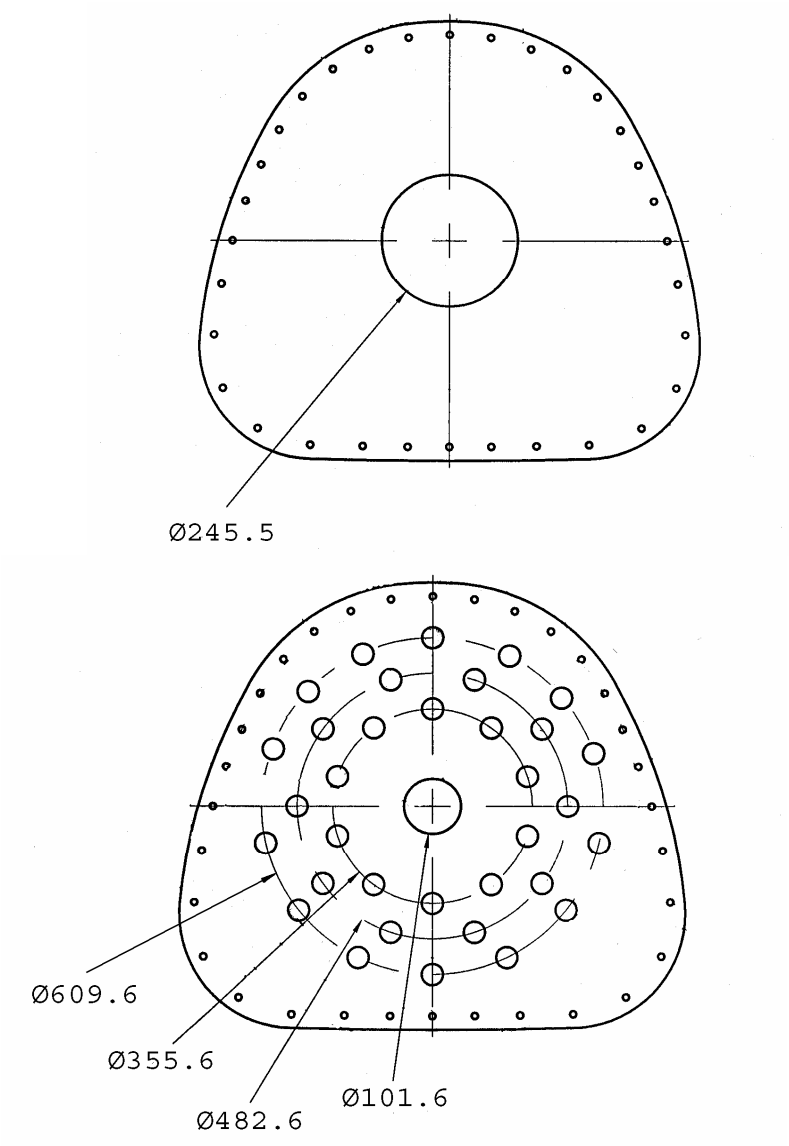

Figure 4.9: Designs of two different baffles used in experiments

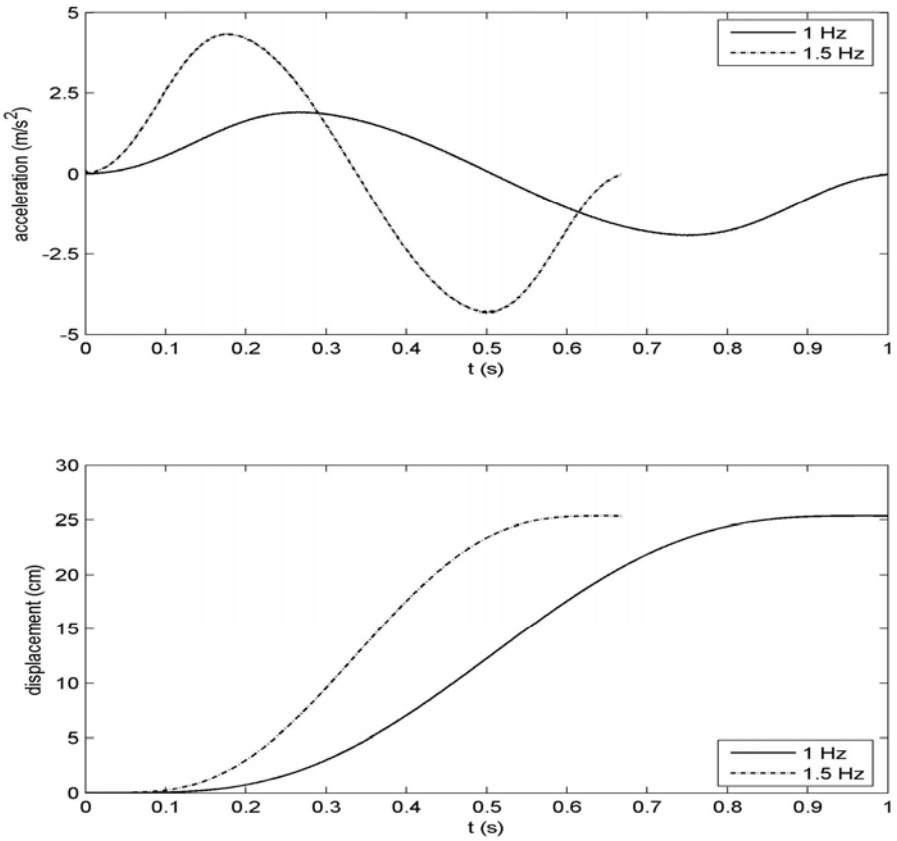

(a): Transient lateral excitation

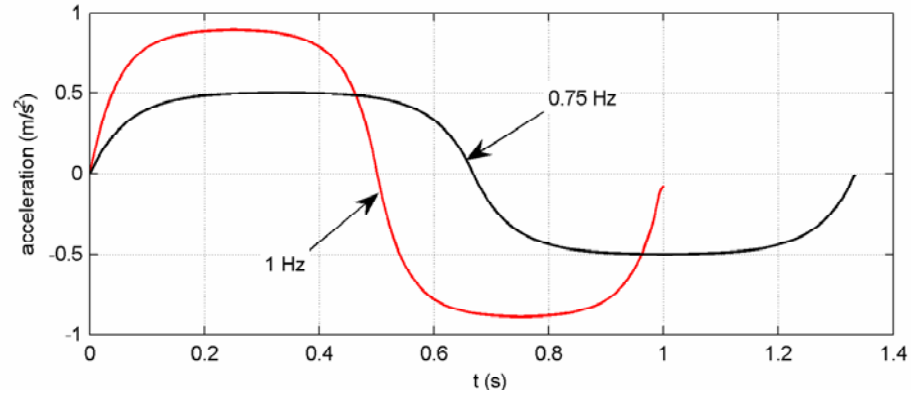

(b): Transient longitudinal excitation

Figure 4.10: (a) Acceleration and displacement time-histories derived from the synthesized single-cycle sinusoidal function to simulate for a path-change maneuver corresponding to two sampling rates; and (b) ramp-step type longitudinal excitation.

The excitation in each test was applied when the fluid was at rest. Owing to relatively shorter durations of step and single-cycle sinusoidal excitations, it was important to track the starting instant of tank motion. The data acquisition was thus initiated approximately 5 to 10 seconds

prior to the generation of the external excitation since the trigger was not used. The duration of data acquisition was set for 8 excitation cycles in the early experiments under harmonic lateral excitations for the cleanbore tank. It was later increased to 40 seconds, after the settling time was observed to be quite large. The data acquisition was also continued after the excitation signal was removed. These data were considered to represent free oscillation response of the free surface for computing fundamental slosh frequencies.

In order to ensure validity of the measured data, the mean values of the measured force data were verified against the gravity and quasi-static forces. For this purpose, the experiments were initially performed with an empty tank. The resulting forces were verified against the static structure weight and inertial forces along the longitudinal and lateral directions. Slight discrepancies between the measured data and expected values were observed, which were subsequently corrected through proper alignments of the dynamometers, slip table and the actuator. Subsequent measurements were performed under two different magnitudes (0.5 and 1 m/s^2) of longitudinal harmonic excitations and three magnitudes of lateral (0.5, 1 and 2 m/s^2) excitation at various frequencies. The data were analyzed to derive the apparent mass of the empty tank with support plate. The results revealed nearly constant mass values close to static mass of the tank structure and the support plate in the two respective axes, as it is evident in Fig. 4.11. The peak deviations between the measured static masses and dynamic apparent masses were observed to be in the order of 5.8% and 7.25% for the longitudinal and lateral acceleration excitations. It can be further seen the measured dynamic mass is not dependent upon the acceleration magnitude. This deviation was attributed to the contributions due to screws and upper plates of the dynamometers that effectively attach to the support plate but could not included in static mass measurements. It should be noted that the mass of each dynamometer was 7.3 kg. The data acquired with the empty tank were stored for performing inertial correction of the forces measured with partly-filled tank configurations.

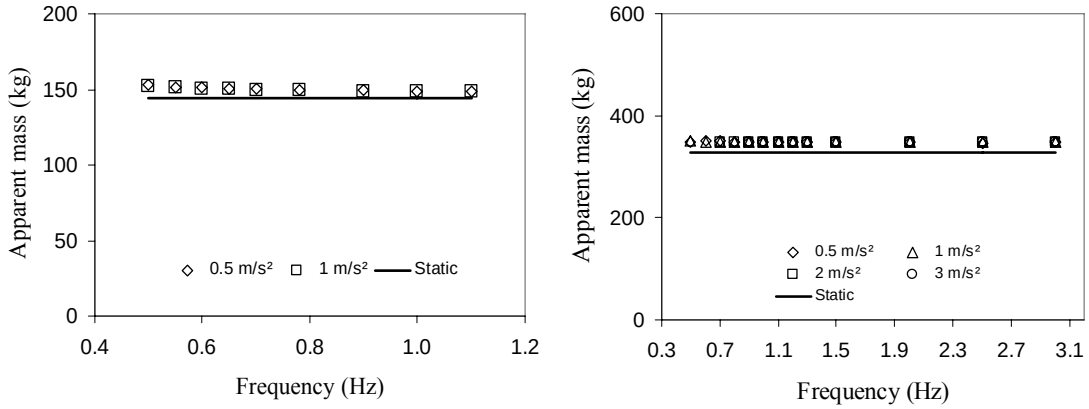

Figure 4.11: Comparisons of measured dynamic masses with static masses of tank and support structure. (a) Longitudinal excitation; and (b) Lateral excitation.

4.4 Data Analysis

The acquired signals revealed presence of a high frequency component (near 13 Hz) that may arise from the guides, flexible coupling between actuator and slip table, and slight misalignment of the slip table. Each data were thus post-processed using a low-pass filter. An 8th order Butterworth digital low-pass filter was used with cutoff frequency of 6 Hz for data acquired under lateral excitation and 3 Hz for data acquired under longitudinal excitation. The force signals acquired by three dynamometers were manipulated to derive moments due to fluid slosh. From Figure 4.8, it can be seen that z-components of forces measured by dynamometers '2' and '3' can be applied for deriving roll moment due to fluid slosh. In a similar manner, the vertical, longitudinal and lateral force components measured from three dynamometers would yield pitch and yaw moments due to fluid slosh. The moments were initially evaluated for empty tank structure to compute the coordinates of the cg of empty tank structure. This cg value was verified using the results attained from the CATIA software. The comparisons revealed reasonably good agreements between the measured and analytical estimation.

The measured data generally revealed large variabilities in the measured force signals, which was mostly attributed to slight misalignments in the slip table and the tank. The free surface generally showed a whirling motion even under single-axis excitation. The peak magnitudes of forces and moments were thus calculated on the basis of 96% confidence level. The measured data were also analyzed to derive the slosh natural frequencies, which are known to depend upon fill level, tank geometry and excitation magnitude [11,17,47]. Fast Fourier transforms of force signals acquired under free oscillation of the surface after removing the excitation were obtained for identifying the slosh frequencies.

4.4.1 Analyses of slosh forces and moments – Lateral excitation

The experiments involved measurements of a total of 9 force components, three at each of the dynamometer location. Under application of a lateral acceleration, the total slosh forces are computed by summing the respective force components with appropriate inertial correction along the lateral axis, such that:

$$F_X(t) = \sum_{i=1}^{3} F_{xi}^{f}(t);$$

$$F_Y(t) = \sum_{i=1}^{3} F_{yi}^{f}(t) - m_e \cdot a_Y(t); \text{and} \qquad (i=1,2,3) \qquad (4.2)$$

$$F_Z(t) = \sum_{i=1}^{3} F_{zi}^{f}(t)$$

where F_X, F_Y and F_Z are total slosh forces developed along X, Y and Z axes, respectively, under the lateral acceleration excitation a_Y. F_{xi}, F_{yi} and F_{zi} are the three force components (Fig. 4.8) measured by dynamometer i ($i = 1$, 2 and 3). The superscript f represents the cases involving liquid filled tank and m_e is the equivalent mass of rigid structure including empty tank and its mounting plate. The subscript X, Y and Z refer to the global coordinate system, while the lower case letters denote the local coordinate systems of dynamometers. The lateral slosh force is corrected by subtracting for contribution of inertial force of the rigid structure, including the platform and empty tank. Such corrections were not performed for the longitudinal and vertical

components due to negligible inertial force along these axes. The force components, however were zeroed prior to data acquition so as to acquire the dynamic force components alone. The vertical slosh force thus revealed variations about zero mean rather than fluid and tank weight.

The roll (M_X), pitch (M_Y) and yaw (M_Z) moments due to fluid slosh were computed from the measured force componets in the following manner:

$$\begin{cases} M_X(t) = \left(\frac{W}{2} N_Y\right) C_{corr} - hF_Y \\ M_Y(t) = \frac{L}{2} N_X + h \cdot \left(\sum_{i=1}^{3} F_{yi}^f\right) \\ M_Z(t) = \frac{L}{2}\left[F_{y1} - \left(F_{y2} + F_{y3}\right)\right] + \frac{W}{2}\left(F_{x2}^f - F_{x3}^f\right) \end{cases} \tag{4.3}$$

where L is longitudinal distance between center of the front dynamometer ('1') and a lateral line connecting the centers of rear left and the rear right dynamometers ('2' and '3'). W is lateral distance between centers of rear left ('2') and rear right ('3') dynamometers, and h is height of the lowest point of tank bottom from top surface of the dynamometers. C_{corr} is a correction factor introduced for computing the roll moment on the basis of only two force components measured at the rear. N_Y is lateral slosh load shift from left side to right, while N_X is longitudinal load shift from front to rear.

The load shifts are computed from the force components in the following manner:

$$\begin{cases} N_Y(t) = \left(F_{z3}^f - F_{z2}^f\right) - N_Y^e \\ N_X(t) = \left(F_{z2}^f + F_{z3}^f\right) - F_{z1}^f \end{cases} \tag{4.4}$$

where N_Y^e is attributed to inertial correction and represents lateral load shift arising from the structure alone, which is linearly dependent on lateral excitation acceleration a_Y.

4.4.2 Analyses of slosh forces and moments – Longitudinal excitation

Under application of a longitudinal acceleration a_X, the total slosh forces are computed by summing the respective force components with appropriate inertial correction along the longitudinal axis, as in the case of lateral acceleration excitation, such that:

$$\begin{cases} F_X(t) = \sum_{i=1}^{3} F_{xi}^f(t) - m_e \cdot a_X(t) \\ F_Y(t) = \sum_{i=1}^{3} F_{yi}^f(t) \qquad ; (i = 1,2,3) \\ F_Z(t) = \sum_{i=1}^{3} F_{zi}^f(t) \end{cases} \tag{4.5}$$

The moments due to slosh forces are also computed in a similar manner, such that:

$$\begin{cases} M_X(t) = \left(\frac{W}{2} N_Y\right) C_{corr} - h \cdot F_Y \\ M_Y(t) = \frac{L}{2} N_X + h \cdot F_X \\ M_Z(t) = \frac{L}{2}\left[F_{y1}^f - \left(F_{y2}^f + F_{y3}^f\right)\right] + \frac{W}{2}\left(F_{x2}^f - F_{x3}^f\right) \end{cases} \tag{4.6}$$

where the lateral and longitudinal load shifts, N_Y and N_X, are computed from:

$$\begin{cases} N_Y(t) = F_{z3}^f - F_{z2}^f \\ N_X(t) = (F_{z2}^f + F_{z3}^f - F_{z1}^f) - N_X^e \end{cases} \tag{4.7}$$

Several experiments were performed in accordance with the test matrices. The measured data were analyzed to compute the amplitudes of transient as well as steady-state slosh forces and moments. A number of studies have suggested that the magnitudes of steady-state forces and moments are greater than those derived from kineto-static analyses. The measured forces and moments were expressed in terms of dimensionless ratios by normalizing the lateral force by the inertial force generated by the "frozen" liquid (rigid equivalent of the liquid) under the same test condition, while the longitudinal and vertical force components are normalized by the liquid weight. All the three moments were normalized by the moment yielded by the "frozen" liquid. Apart from the measurements, the flows are examined to study the contributions of baffles. Pictographs of some of the flows observed during experiments are presented in Annexe B.

5. MODELING AND ANALYSIS OF DYNAMIC FLUID SLOSH

The magnitudes of forces and moments caused by oscillatory fluid slosh are known to be considerably larger than those estimated from the kineto-static analyses. The simplified kineto-static analyses of the fluid motion, however, could yield a good estimate of mean values of dynamic slosh forces. Reported studies on dynamic fluid slosh analyses of cargo tanks are limited to either lateral or longitudinal acceleration excitations. Applications of simultaneous braking accelerations and steering maneuvers could cause dynamic motions of fluid in both the pitch and roll planes. A three-dimensional kineto-static fluid flow model of a partly-filled cleanbore tank subject to lateral and longitudinal acceleration fields was developed by the team in a recent study [4]. The study demonstrated significant influence of simultaneously applied acceleration fields on the steady-state free surface gradient, and variations in the center of mass (cg) coordinates, mass moments of inertia of liquid cargo, and thus the directional dynamics characteristics of a vehicle combination.

Lateral baffles are frequently employed to enhance the structural integrity, which tend to limit the longitudinal fluid slosh under braking and acceleration maneuvers. The effects of separating walls (compartments) on the dynamic load shifts in either the roll or the pitch planes have also been investigated using the kineto-static analyses [21,41]. A few studies have explored the role of baffles and separating walls via experimental means, only a few studies have attempted to develop and analyze analytical models and demonstrated the effectiveness of lateral baffles in rectangular horizontal and vertical cylindrical tanks. Two-dimensional slosh models were developed to illustrate the influence of baffles on attenuation of slosh in rectangular tanks [12,16]. Sheu [12] and Abramson [11] assumed harmonic acceleration fields to derive the results, although free vibration of liquid was also considered in their studies. The directional stability limits of a partly-filled tank truck are strongly influenced by the dynamic forces and moments arising from the fluid movement within tank under the influence of both the longitudinal and lateral accelerations. A three-dimensional analysis of the fluid slosh is thus essential to characterize the nature of dynamic slosh forces and moments. Such analyses could also yield significant insight into the slosh resistance offered by different designs of transverse baffles. The results could then be applied to study the coupled directional dynamics of the tank-vehicle system, using a methodology similar to that employed in [49]. In this study, a nonlinear model of the fluid flow is formulated in the three-dimensional domain and solved under lateral, longitudinal and simultaneous lateral and longitudinal acceleration fields, using the FLUENT software. The pressure distributions at the submerged tank wall in the three-dimensional domain are analyzed to derive the resulting lateral and longitudinal forces, and roll and pitch moments imposed on the structure of the tank with and without baffles. The influences of magnitudes of acceleration and fill condition on the transient and steady-state forces and moments are further investigated for the cleanbore as well as baffled tank.

5.1 Three Dimensional Liquid Slosh Model

On the basis of the quasi static model of liquid slosh in the roll plane, it has been shown that the lateral load shift in a partly-filled tank vehicle poses additional roll moment that contributes to

reduction in the overturning threshold acceleration of the vehicle. A three dimensional kineto-static model has also been formulated to compute the liquid load shifts in both the roll and pitch planes under simultaneous applications of lateral and longitudinal acceleration fields [4]. These studies focus on computation of free surface gradient, which is directly related to magnitude of acceleration and coordinates of instantaneous mass center of moving cargo through moment integrations over the liquid domain. The resulting roll, pitch and yaw moments imposed on the vehicle, and the mass moments of inertia are subsequently applied within comprehensive nonlinear vehicle models to predict directional behaviours of the vehicle as functions of the fill level, and magnitudes of the steering and braking inputs. While the kineto-static analyses can provide reasonably good estimates of the mean forces and moments, the analyses of oscillatory slosh forces and moments, particularly within baffled tanks, require dynamic fluid slosh analyses.

The motion of an incompressible liquid inside a tank as a function of time may be represented by the momentum (the Navier-Stokes) and mass conservation equations. Assuming laminar flow with constant viscosity, equations for the three-dimensional fluid flow with respect to an inertial Cartesian coordinate system (x,y,z) can be expressed as:

$$\frac{\partial u}{\partial t} + u\frac{\partial u}{\partial x} + \upsilon\frac{\partial u}{\partial y} + w\frac{\partial u}{\partial z} = a_x - \frac{1}{\rho}\frac{\partial P}{\partial x} + \nu\left(\frac{\partial^2 u}{\partial x^2} + \frac{\partial^2 u}{\partial y^2} + \frac{\partial^2 u}{\partial z^2}\right) \tag{5.1}$$

$$\frac{\partial \upsilon}{\partial t} + u\frac{\partial \upsilon}{\partial x} + \upsilon\frac{\partial \upsilon}{\partial y} + w\frac{\partial \upsilon}{\partial z} = a_y - \frac{1}{\rho}\frac{\partial P}{\partial y} + \nu\left(\frac{\partial^2 \upsilon}{\partial x^2} + \frac{\partial^2 \upsilon}{\partial y^2} + \frac{\partial^2 \upsilon}{\partial z^2}\right) \tag{5.2}$$

$$\frac{\partial w}{\partial t} + u\frac{\partial w}{\partial x} + \upsilon\frac{\partial w}{\partial y} + w\frac{\partial w}{\partial z} = g_z - \frac{1}{\rho}\frac{\partial P}{\partial z} + \nu\left(\frac{\partial^2 w}{\partial x^2} + \frac{\partial^2 w}{\partial y^2} + \frac{\partial^2 w}{\partial z^2}\right) \tag{5.3}$$

$$\frac{\partial u}{\partial x} + \frac{\partial \upsilon}{\partial y} + \frac{\partial w}{\partial z} = 0 \tag{5.4}$$

where u, υ and w are the liquid velocity components in the x, y and z directions, respectively, P is fluid pressure, ν is kinematic viscosity of fluid, and a_x, a_y and a_z are unit body forces acting along x, y and z directions, respectively.

In the above formulation, a two-phase fluid flow (air and liquid) is considered for analysis of slosh in a partly-filled tank. A homogeneous field of body force has been assumed in the formulations, and momentum and mass conservation equations are solved in conjunction with appropriate boundary conditions to compute the velocity components and pressure distribution in the flow domain as a function of time and space. It would be reasonable to assume that the tank is bounded by a rigid wall, which yields that the velocity component normal to the wall is zero at the boundary, such that:

$$\frac{\partial U_T}{\partial n} = 0 \qquad (5.5)$$

where U_T is the total velocity of the liquid and n is the normal direction to the boundary. It has been also assumed that the fluid flow is with constant viscosity and the component of velocity of the fluid tangent to the boundary (wall) is zero, implying no-slip boundary condition, such that $U_{Tan} = 0$ at the boundary.

A number of reported studies have considered laminar flow model in solutions of the Navier-Stokes equations, which provided reasonably good correlations with the experiment data [12,16]. It has been suggested that magnitude of viscous forces exerted on the tank wall is negligible even for a fluid with a high dynamic viscosity (μ=0.98 kg/ms) [50]. The laminar flow assumption would thus be valid in the formulation of the slosh inside a moving tank. Bauer [7] showed that only small portion of the liquid bulk inside the container is involved in the acceleration-induced oscillatory motion.

5.2 Geometry Discretization and Solution Methodology

The fluid flow equations are formulated for the circular as well as optimal cross-section tanks with three lateral baffles. Both the single as well as multiple orifice baffles are considered for analysis. Figure 5.1, as an example, illustrates the circular cross-section tank model and geometry with three single-orifice baffles with nozzle diameter equal to 30% of the tank diameter. The total volume of the tank considered in the study is 23.6 m^3. The baffles and end caps are modeled with curved shapes in accordance with the ASME standard. The tank and baffle structure together with the fluid domains are discretized using GAMBIT available within the FLUENT software [51].

Equations (5.1) to (5.4) were solved in the vector form assuming rigid wall and zero-velocity boundary conditions using the FLUENT software version 6.1.18. Instead of linear kinematic restriction, defining the free surface as another boundary condition, the *volume of fluid* (VOF) method is selected for the solution, since it permits for simulation of large amplitude slosh, including the separation of the free surface [52]. The VOF method, available within the FLUENT environment [51], is applied to solve for the transient flows involving free surface separating the liquid phase from the air phase within the non-filled cross-section of the tank. Fuel oil (ρ = 850 kg/m^3) is considered as the baseline fluid for the analyses, while the analyses are performed for both the cleanbore and baffled tanks. Moreover, the segregated method of solution is applied to solve for linearized discrete equations, assuming laminar flow with two phases and primitive variables i.e. pressure at the center of each cell and velocity components at the cell faces. First-order upwind and the body-force-weighted schemes are applied for the momentum and, pressure correction equations, and spatial components of the governing equations are descritized using a fixed time step and the first order time advancing scheme. The FLUENT environment also employs PISO algorithm for pressure-velocity coupling. The convergence criteria is based on the residual values of computed variables, namely, velocity components, pressure and volume fractions within the cells, derived using unity value of under-relaxation. The convergence criterion based on the residual values was chosen as 0.0001.

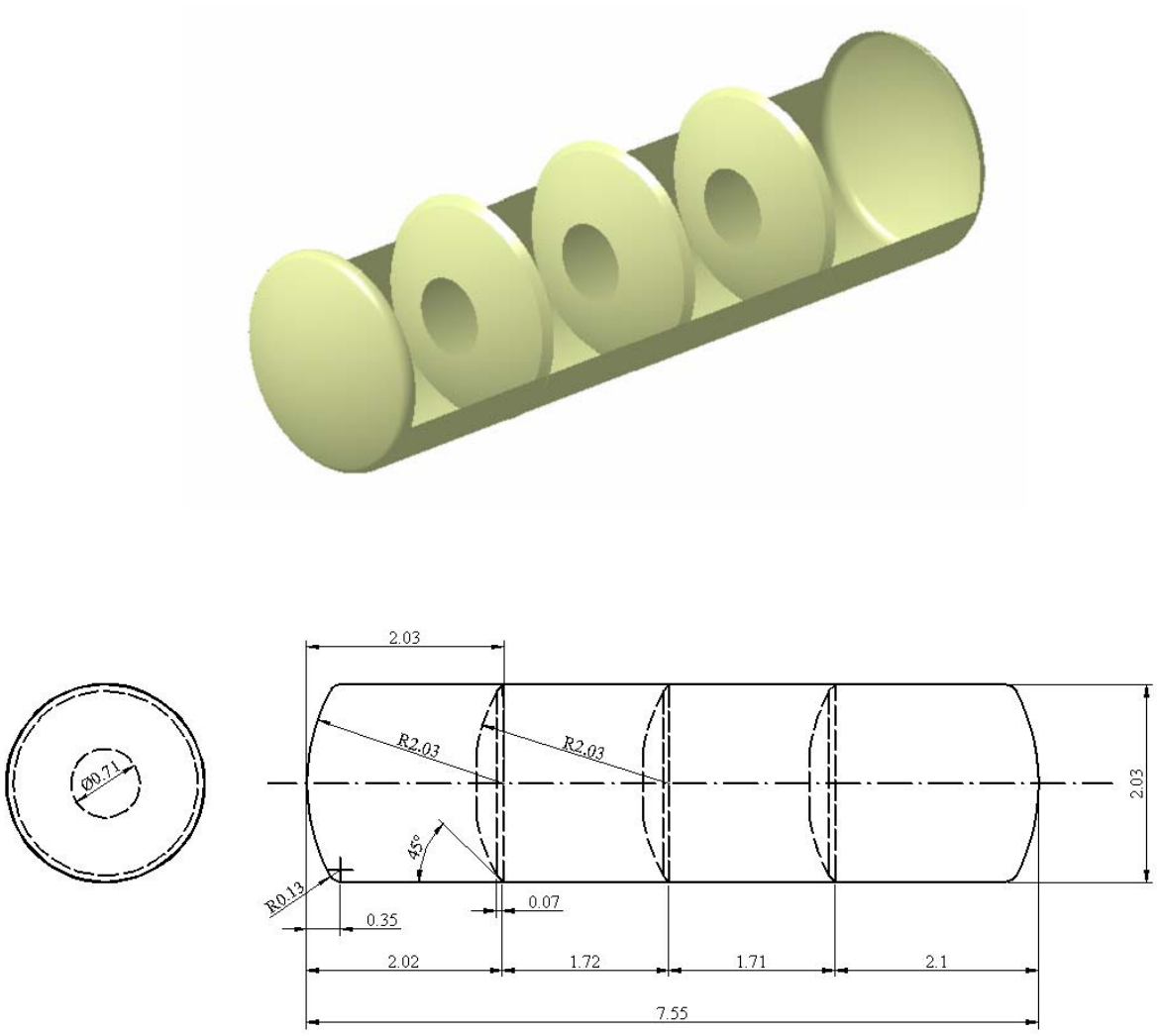

Fig. 5.1: Circular cross-section tank model and geometry

The magnitudes of forces and moments in the transient as well as steady-states are derived from the pressure distributions over the wetted boundaries of the baffled as well as the cleanbore tanks, such that:

$$F_x = \sum_{c}^{wet\ area} P_c \vec{A}_c \cdot \vec{i}\ ,\ F_y = \sum_{c}^{wet\ area} P_c \vec{A}_c \cdot \vec{j}\ ,\ F_z = \sum_{c}^{wet\ area} P_c \vec{A}_c \cdot \vec{k} \qquad (5.6)$$

where F_x, F_y and F_z are the resultant slosh forces acting on the tank wall along the fixed x, y and z axes due to pressure P_c acting on cell "c" with area vector $\vec{A}_c$, as shown in Fig. 5.2, and $\vec{i}$, $\vec{j}$ and $\vec{k}$ are unit vectors in the x, y and z directions, respectively.

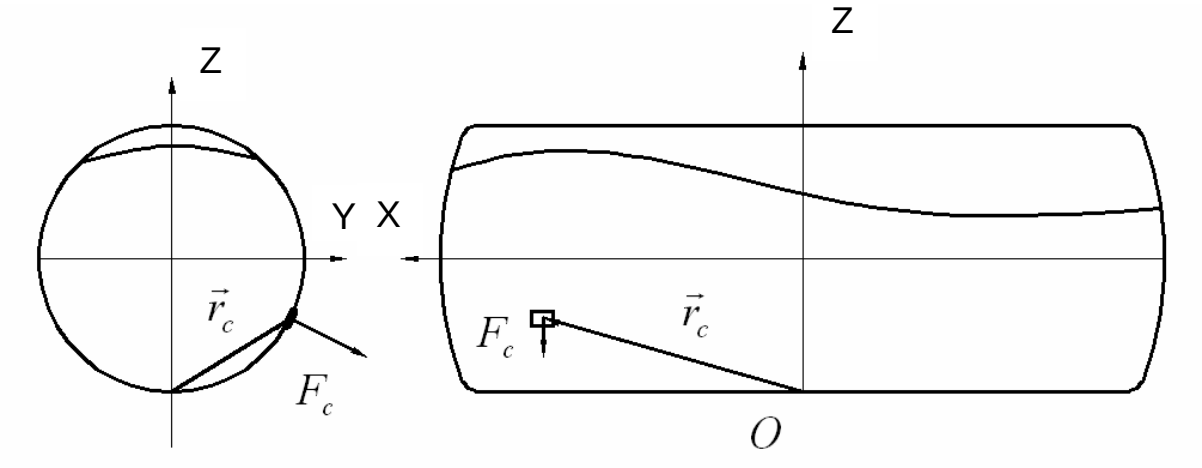

Fig. 5.2: Computation of pitch and roll moments from distributed pressure on tank wall.

Apart from the dynamic slosh forces, the pitch, yaw and roll moments about point '*O*' located at the bottom of the tank directly beneath the origin (center of the tank) are obtained upon integrating the moments corresponding to each cell over the wetted area:

$$\vec{M} = \sum_{c}^{wet\,area} \vec{r}_c \times \vec{F}_c \qquad (5.7)$$

where $\vec{F}_c$ is the force vector caused by a cell '*c*' on the boundary, $\vec{r}_c$ is position vector of cell 'c' with respect to 'O' and $\vec{M}$ is moment vector about point 'O'. The coordinates of this point 'O' are (*0*,-*R*,*0*), where *R* is the tank radius.

The instantaneous pitch, yaw and roll mass moments of inertia of fluid about the geometric center of the tank are obtained through integrations over the liquid volume, using coordinates of the liquid cells centroids, such that:

$$I_{XX} = \rho \sum_{c}^{liquid} \left(y_c^2 + z_c^2\right) V_c \,, \quad I_{YY} = \rho \sum_{c}^{liquid} \left(x_c^2 + z_c^2\right) V_c \,, \quad I_{ZZ} = \rho \sum_{c}^{liquid} \left(x_c^2 + y_c^2\right) V_c \qquad (5.8)$$

where V_c is the volume of the cell 'c', I_{xx}, I_{yy} and I_{zz} are the roll, pitch and yaw mass moments of inertia of the liquid, and x_c, y_c and z_c define the coordinates of the centroid of cell 'c'.

Owing to the strong dependence of the solutions on the grid size, the fluid slosh analyses for the discretized tank geometry were initially attained using different grid sizes. Figure 5.3 illustrates the geometry and the flow domain for the circular cross-section tank comprising 31205 hexahedral cells, and geometry of baffles considered for both tanks. The relative deviations in the solutions for different mesh sizes were evaluated in terms of resulting peak lateral and longitudinal forces derived using Eq (5.6). The mesh sizes considered in the analyses revealed deviations in the order of 1 and 2%, respectively, in the respective peak lateral and longitudinal force responses. The detailed results of this study are presented in [54]. The preliminary analyses were also attempted using different time steps under identical excitation and fill conditions. The results revealed comparable magnitudes of peak forces (F_x and F_z) and moments (M_x, M_y and M_z), which gradually approached their respective steady-state values. A relatively larger time

step (0.025) was thus chosen for enhancing the simulation efficiency. As an example, Fig. 5.4(a) illustrates the free surface profile of liquid within the 40%-filled circular cross-section baffled tank, attained using selected mesh and step size under simultaneous application of longitudinal (a_y=*0.25g*) and lateral (a_x=*0.3g*) accelerations. Figures 5.4(b) and 5.4(c) show the free surface of fluid within the scaled optimal cross-section tank with single- and multiple-orifice baffles (configurations 'T2' and 'T3'). These results are presented for 50% and 30% fill volumes, and lateral and longitudinal harmonic excitations, respectively.

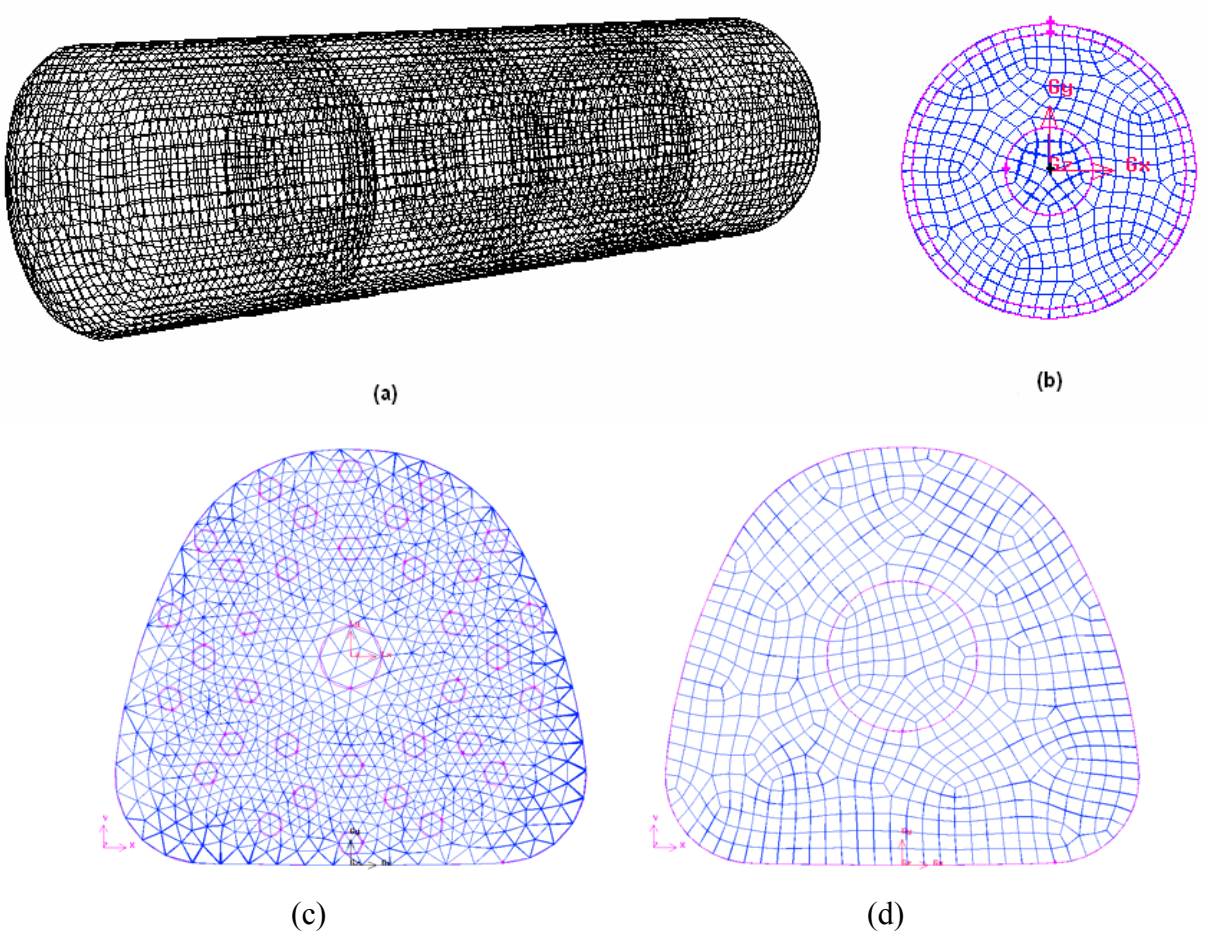

Fig. 5.3: Discretized tank and baffles structures, and flow domain (a) perspective of circular tank (b) single-orifice circular tank baffle; (c) single-orifice optimal tank baffle; and (d) multiple-orifice optimal tank baffle.

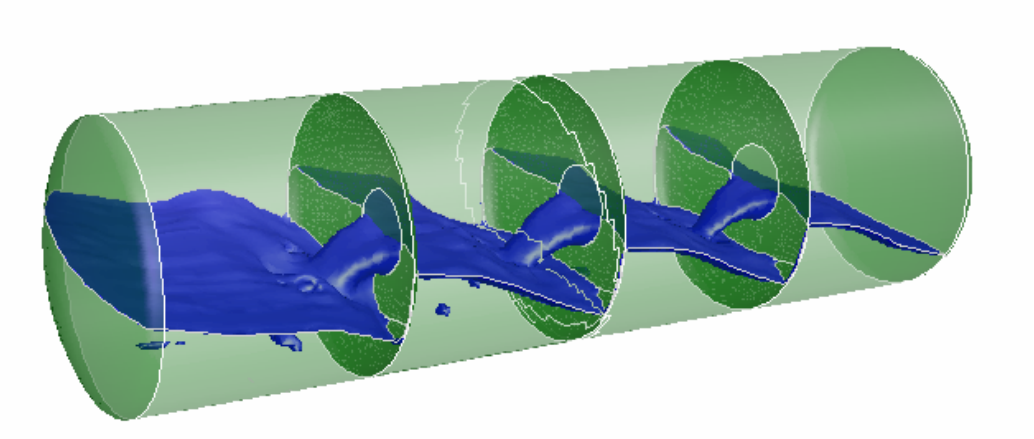

(a): Full-size circular cross-section (Fill: 40%; ramp-step lateral and longitudinal accelerations)

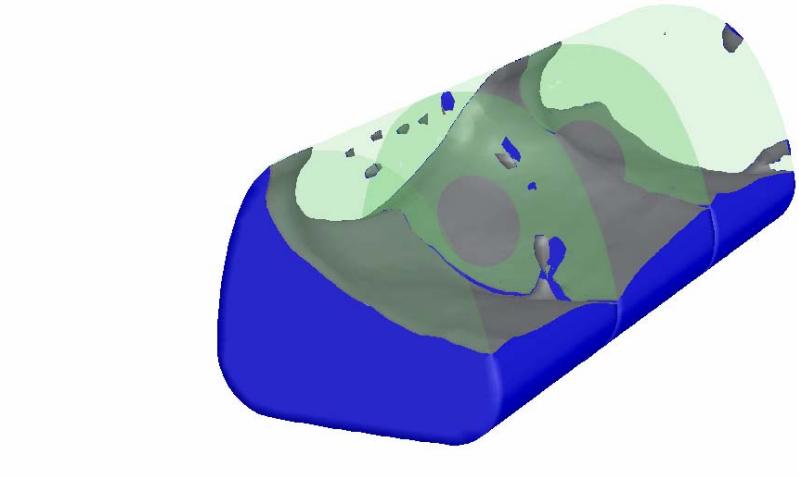

(b): Optimal cross-section test tank (Fill: 30%; Configuration: 'T2'; 1 m/s^2 lateral excitation at 1 Hz)

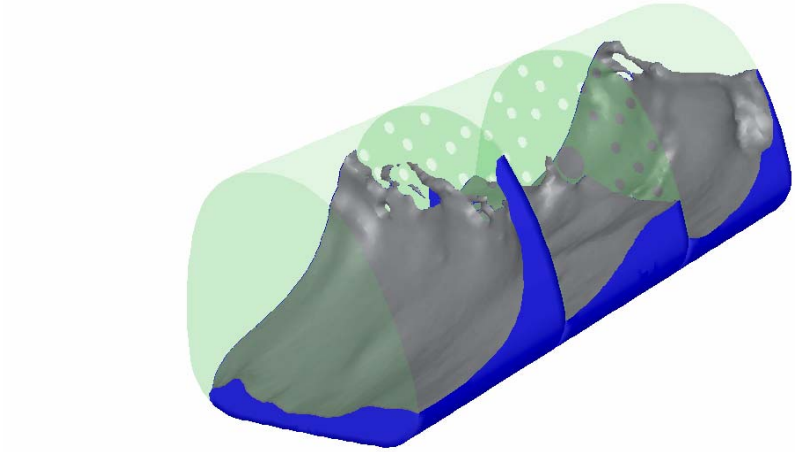

(c): Optimal cross-section test tank (Fill: 50%; Configuration: 'T2'; 1 m/s^2 longitudinal excitation at 0.9 Hz)

Fig. 5.4: Liquid free surface within partly-filled tanks

5.3 Excitations and Simulation Matrix

The dynamic slosh analyses were performed under different types of excitations along the lateral and longitudinal directions. These included single sinusoid motions described in the previous section, idealized ramp-step changes in accelerations and harmonic accelerations. The first two were used for verification of transient forces and moments, while the last one was used for validation of the flow in steady state. The optimal tank model size was scaled to the test tank used in the study, and the simulation results were compared with experimental results in order to demonstrate the validity of the model. The simulations for the full-size tank were also performed under ramp-step types of inputs, and the model validity was further examined using the results obtained from quasi-static analysis. For this purpose, rounded ramp-step functions were employed to realize linearly varying acceleration for t<0.5 s and a constant magnitude at t≥0.5 s, as shown in Fig. 5.5. The discontinuity associated with the ramp-step function is eliminated by smoothing the interface of the ramp and the step parts using an arc function, which is tangent to both linear and constant parts. The rounded ramp-step function is an analytic function comprising a linear, an arc and a constant function in time, expressed as:

$$\begin{aligned} g(t) &= at && 0 \langle t \langle T_a \\ g(t) &= G - 0.2 + \sqrt{0.2^2 - (t-0.5)^2} && T_a \le t \langle 0.5 \\ g(t) &= G && t \ge 0.5 \end{aligned} \tag{5.9}$$

where *g(t)* is instantaneous acceleration input, *G* is steady state acceleration magnitude and *a* is slope of linear part of the acceleration function. The analyses were performed for two different magnitudes of a_x representing idealized braking, a_y representing turning, and combinations of a_x and a_y representing turning and braking. The model validity was examined in terms of natural frequencies, and slosh forces and moments for different tank configurations, and various fill and excitation conditions. Three configurations of the tank, scaled to geometry of the test tank, including cleanbore tank, tank with single-orifice baffles and tank with perforated or multi-orifice baffles, were considered. These configurations are referred to as 'T1', 'T2' and 'T3', respectively, in this report. The total length of tank is 1.85 m and the cross-section area is 0.426 m^2. The transverse width of the tank is approximately 1/3 of the real tank of road tank vehicles. In the baffled case, the tank was divided into three sections of equal length by the baffles. The opening area of the two baffles used in optimal cross-section tank is approximately 11%.

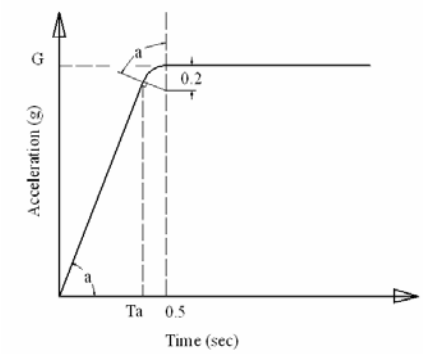

Fig. 5.5: Rounded ramp-step function with the constant value of G for t≥0.5 s

Tables 5.1 and 5.2 summarize the excitations and simulation conditions used for validation purposes. The single-cycle sinusoidal excitations were applied in the lateral direction alone, as described in previous chapter (Fig. 4.10a). The configuration 'T3' was excluded from this analysis, since the experiment results showed negligible effect of the transverse baffles under lateral excitations. The idealized ramp-step excitations (Fig. 4.10b) were applied in the longitudinal direction for validation of transient slosh in baffled and un-baffled test tanks. The simulations under lateral harmonic excitations were performed under various excitation frequencies ranging from 0.6 Hz to 1.5 Hz at two different magnitudes (A = 1 and 2 m/s^2). Since a significantly finer mesh is required for perforated baffles used in configuration 'T3', the simulations for this configuration were carried out only near the resonant frequency to reduce the computational time. The slosh force responses under a harmonic longitudinal excitation were obtained for various excitation frequencies, as evident in Table 5.3. The 30% fill case for configuration 'T2' however was not attempted for reasons stipulated in previous chapter.

Apart from the above-stated excitation, the slosh analyses were also performed under swept harmonic excitations. The resulting responses provided the natural frequencies, and frequency response characteristics as functions of fill volume. For all tank configurations, lateral acceleration excitation was swept at a constant rate of 0.025 Hz/s, while the amplitude was held as 0.5 m/s^2. Considering the notable differences in longitudinal mode natural frequencies of the baffled and un-baffled tank configurations, the longitudinal excitation was swept in the 0.001 to 2 Hz rate at a constant rate of 0.025 Hz/s.

Table 5.1: Simulation matrix – Single cycle sinusoid (lateral) and ramp-step (lateral and longitudinal) excitations

Excitation direction	*A* (m/s^2)	*f* (Hz)	Tank configuration & fill volume
lateral	1.93	1	Configuration 'T1' (30%)
	4.34	1.5	Configuration 'T2' (50%, 70%)
longitudinal	0.5	0.75	All configurations* (30%,50%, 70%)
	0.89	1	All configurations* (30%,50%, 70%)

* Configuration 'T2' under 30% fill volume was excluded

Table 5.2: Simulation matrix – Lateral harmonic excitation

	f (Hz)					*Configuration*	*Fill volume*
A (m/s^2)	0.6	0.8	1	1.2	1.5		
1	√	√	√	√	√	T1, T2	50%
2	--	√	√	√	√	T1, T2	50%, 70%

Table 5.3: Simulation matrix – Longitudinal harmonic excitation

Configuration	Fill volume	A (m/s^2)	f (Hz)
T1	30%	1	0.36
	50%		0.5
	70%		0.5
T2, T3	30%*		0.9
	50%		1
	70%		1.1

* Configuration 'T2' under 30% fill volume was excluded

5.4 Model Validations

The dynamic fluid slosh model for the partly filled tank was scaled down to the optimal cross-section test tank and the simulations were performed according to the simulation matrices defined above. The validity of the simulation model, and the chosen grid and step size was initially examined for configuration 'T2' (optimal cross-section tank with single orifice baffles) by comparing steady-state slosh forces and slosh moment responses to various harmonic excitations. The slosh forces and moments responses of the simulation model were evaluated from the distributed pressures at the wetted boundary using Eqs (5.6) and (5.7). The measured slosh forces and moments were derived upon inertial correction using Eqs (4.2) and (4.3). Although ths simulations were performed for various fill levels and excitation magnitudes and frequencies, the model validity, as an example, is illustrated for 50% fill condition and 1 m/s^2 lateral harmonic excitation at the resonant frequency near 1 Hz. Figures 5.6 and 5.7 illustrate comparisons of slosh forces and moments derived from the simulation and measured results, respectively.

Reasonably good agreement could be observed between the simulation and experimental results, particularly for the lateral force and roll moment responses that are expected to be most significant under a lateral acceleration excitation. Some deviations between the simulation and experimental results, however, are also evident, particularly in longitudinal force (F_X), and yaw (M_Z) and pitch (M_Y) moments, which are of relatively smaller magnitudes. Such deviations were mostly attributed to differences in initial conditions. While the simulations were performed assuming that the fluid is initially at rest, while each experiment was initiated with slight residual fluid motion from the previous experiment. The results tend to show better agreements at durations exceeding 25 s, when the residual effects diminish. The results also show oscillations at a frequency of 1 Hz, with the exception of vertical force that oscillates at twice the excitation frequency (2 Hz). This is attributed to the wave effect and is evident in both the simulation and experimental results. Both the simulation and experimental results also show presence of a low frequency component, which is more clearly evident in the vertical force response. This is attributed to swirling of fluid within the tank. Similar degrees of agreements were also observed for other fill volume and excitation conditions considered. The results suggest that the model could effectively predict the steady-state dynamic fluid slosh behaviour of the partly-filled tank.

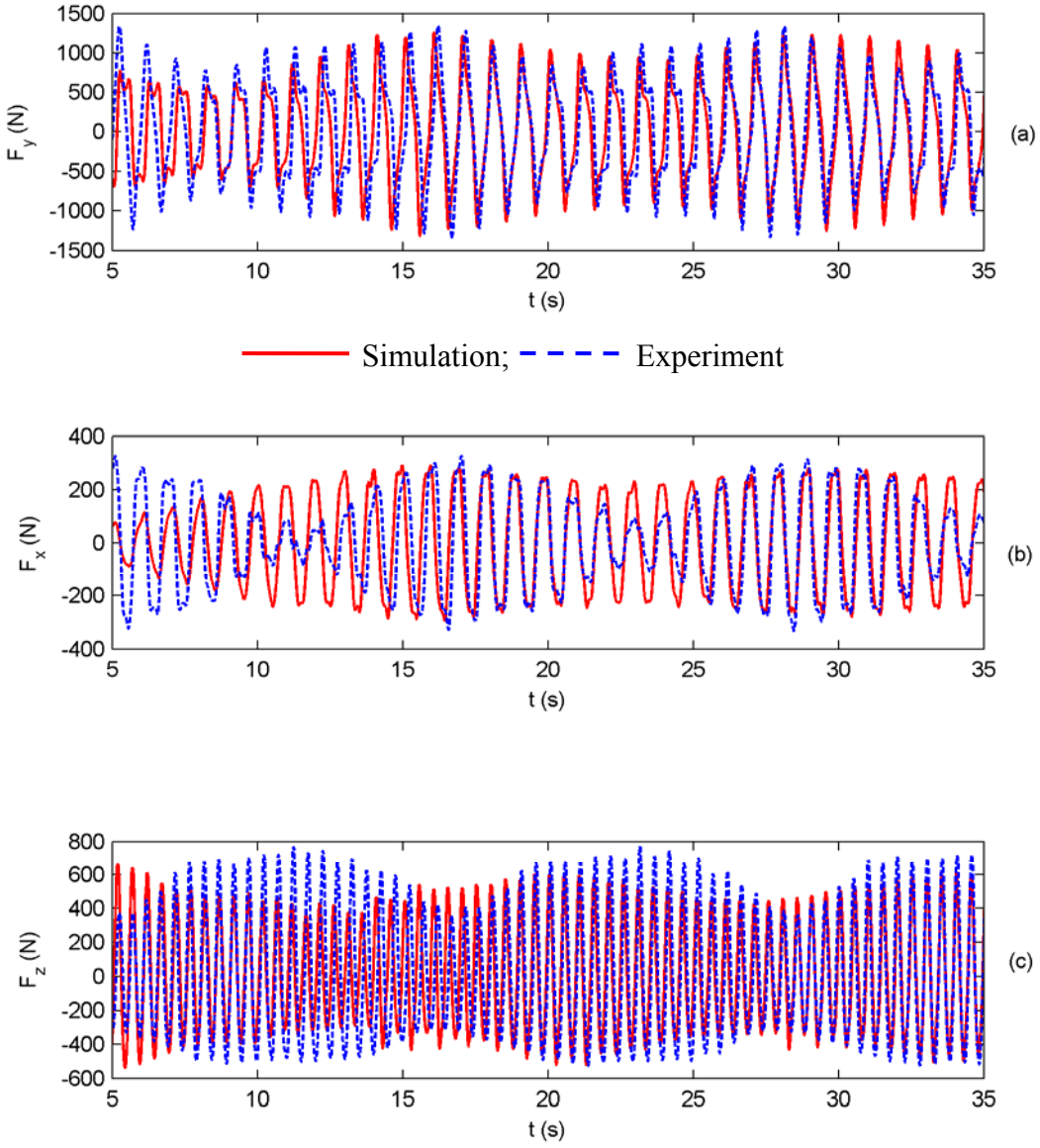

Fig. 5.6: Comparisons of steady-state slosh forces responses of simulation model with measured results (a) lateral force; (b) longitudinal force; (c) vertical force. (Tank – 'T2"; Fill volume – 50%; Excitation - 1 m/s^2 lateral acceleration at 1 Hz)

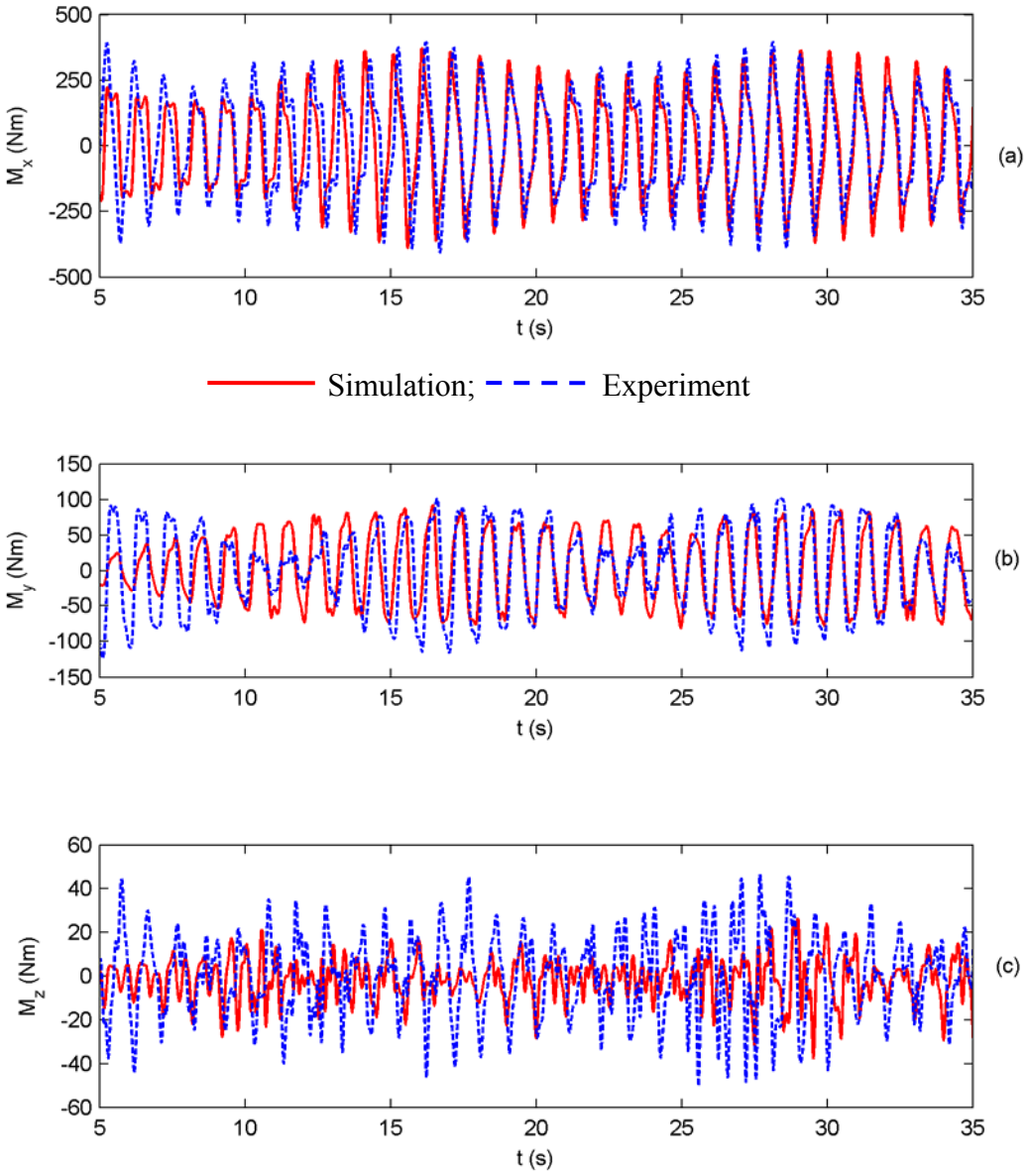

Fig. 5.7: Comparisons of steady-state slosh moment responses of simulation model with measured results (a) roll moment; (b) pitch moment; (c) yaw moment. (Tank – 'T2"; Fill volume – 50%; Excitation - 1 m/s^2 lateral acceleration at 1 Hz)

5.4.1 Natural frequencies

The model validity was further examined in view of its ability to predict fundamental slosh frequency. For this purpose, the slosh frequencies were estimated from three different methods. The natural frequencies were initially estimated from the analytical method proposed by Romero et al. [43] on the basis of their limited experiments performed on a very small size tank. The validity of this method for a baffled tank, however, has not been established. These estimated frequencies were applied for identifying frequency ranges of excitations in the experiment design. Secondly, the natural frequencies were estimated from the simulation results attained

under swept harmonic excitations. The spectra of slosh force responses were evaluated using FFT technique and the fundamental slosh frequency was identified as the frequency corresponding to peak spectral magnitude. Finally, the fundamental frequencies were identified from the measured data through spectrum analysis of measured force responses under ramp-step excitations, as described in previous chapter. The model validity was examined by comparing the frequencies derived from simulation results with those from analytical and experimental methods under various fill conditions and tank configurations. As an example, Fig. 5.8 illustrates comparisons of lateral and longitudinal mode fundamental slosh frequencies derived from the three methods for a cleanbore tank.

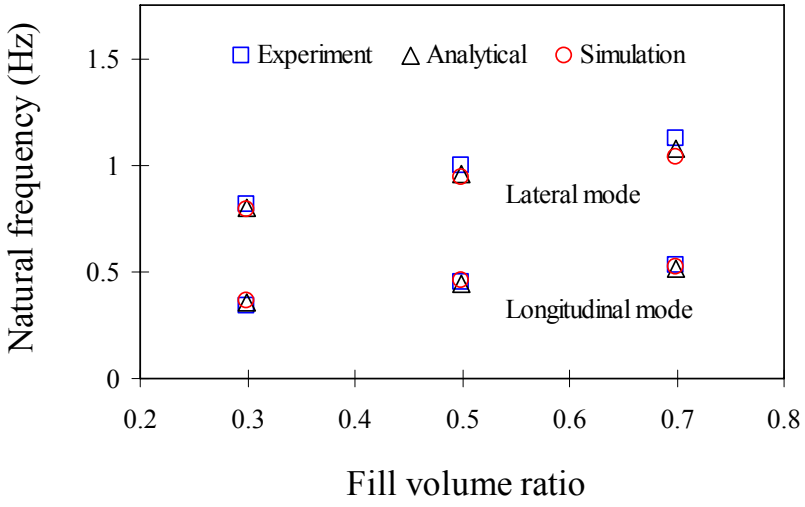

Fig. 5.8: Comparisons of fundamental slosh frequencies derived from simulation model results, analytical method and experimental data for various fill volumes of the cleanbore tank ('T1').

The results show very good agreements between the model and experimental results, and also with analytical frequencies. For both lateral and longitudinal modes, the maximum deviation between the model and measured results is in the order of 8%, while the deviations with respect to analytical results are below 4%. Similar trends were also observed for configuration 'T2' (optimal cross-section tank with orifice baffles). Table 5.4 presents a comparison of fundamental slosh frequencies estimated from the simulation model and experimental data. The results clearly show very good agreements in the natural frequencies derived from simulation model and measured data. The maximum difference between the simulation and experiment results is less than 8% for 50% and 70% fill volumes in the lateral mode, but not larger than 4% in the longitudinal mode. Since the analytical method is not suited for baffled tanks, comparisons with analytical results could not be performed.

Table 5.4: Comparisons of fundamental slosh frequencies derived from model and experimental results under in the lateral and longitudinal modes (tank – 'T2')

Mode Direction	Method	Fill volume 50%	70%
Y	Model	0.946	1.038
	Experiment	1.000	1.125
Percent Difference		5.4	7.7
X	Model	1.038	1.099
	Experiment	1.078	1.141
Percent Difference		3.9	3.7

5.4.2 Transient slosh forces and moments – Lateral acceleration excitation

The magnitudes of slosh forces and moments developed during transient oscillations may be considerably larger than those of the steady-state force responses. The directional stability limits of a partly-filled vehicle may thus be lower in the presence of transient fluid slosh. The model validity is thus further explored in view of transient responses under single sinusoid lateral acceleration excitation (synthesized path-change) and ramp-step longitudinal excitation for different fill volumes. The model validity is demonstrated by comparing slosh forces and moments derived from model results and measured data corresponding to various fill volumes and excitations.

Figures 5.9 and 5.10 compare slosh forces and moments, respectively, derived from the model and experimental data for the 30% filled cleanbore tank (configuration 'T1') subject to lateral single-cycle sinusoidal excitation of magnitude 1.93 m/s^2 at 1 Hz. Good agreements are observed for lateral and vertical forces, and roll moment, while the magnitudes of longitudinal force, and yaw and pitch moments are quite small. The model tends to predict the transient slosh behaviour in reasonably fine details, including the clipping effect of the wave. The results, however, show a slight phase difference between the simulation and experimental results, which is attributed to slight differences in the slosh frequency. Although large differences are evident in the longitudinal force, and pitch moment and yaw moment responses, their magnitudes are very small suggesting dominantly 2-dimenisonal slosh. Similar trends were also observed for different fill volumes and inputs. Figure 5.11, as an example illustrates comparisons under a more intense single sinusoid excitation (4.34 m/s^2 at 1.5 Hz). The results, presented for lateral and vertical forces and roll moment, show similar degree of agreements.

Figures 5.12 and 5.13 show comparisons of transient responses of the model with measured data for baffled tank configuration 'T2' under 50% and 70% fill volumes, respectively. These results were obtained under single sinusoid lateral acceleration excitation of magnitude 4.34 m/s^2 at 1.5 Hz. The simulation results show very good agreements with the experimental results, as in the case of cleanbore tank.

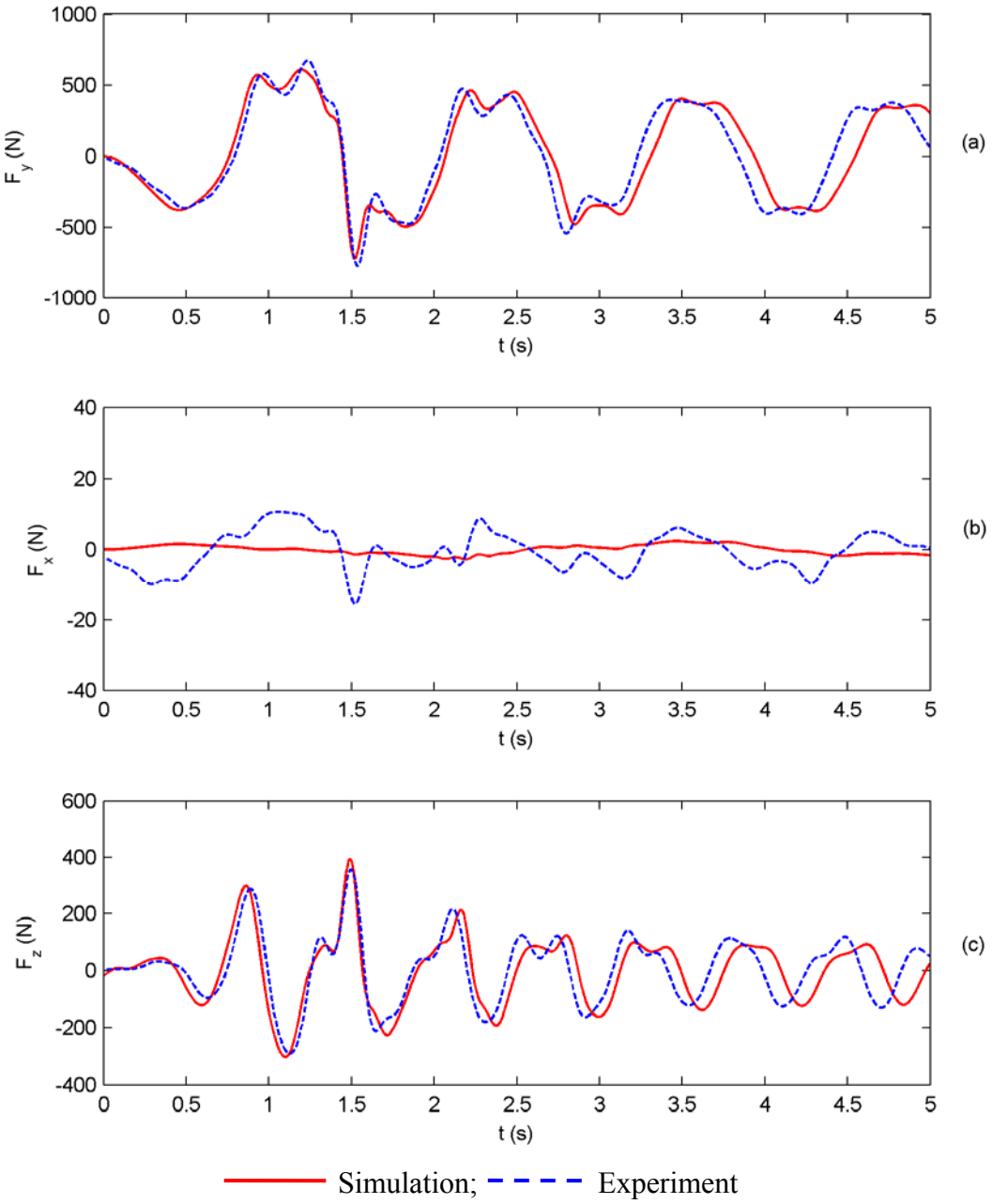

Fig. 5.9: Comparisons of transient slosh force responses of simulation model with measured results (a) lateral force; (b) longitudinal force; (c) vertical force. (Tank – 'T1"; Fill volume – 30%; Excitation – single cycle sinusoid lateral acceleration of magnitude 1.93 m/s^2 at 1 Hz)

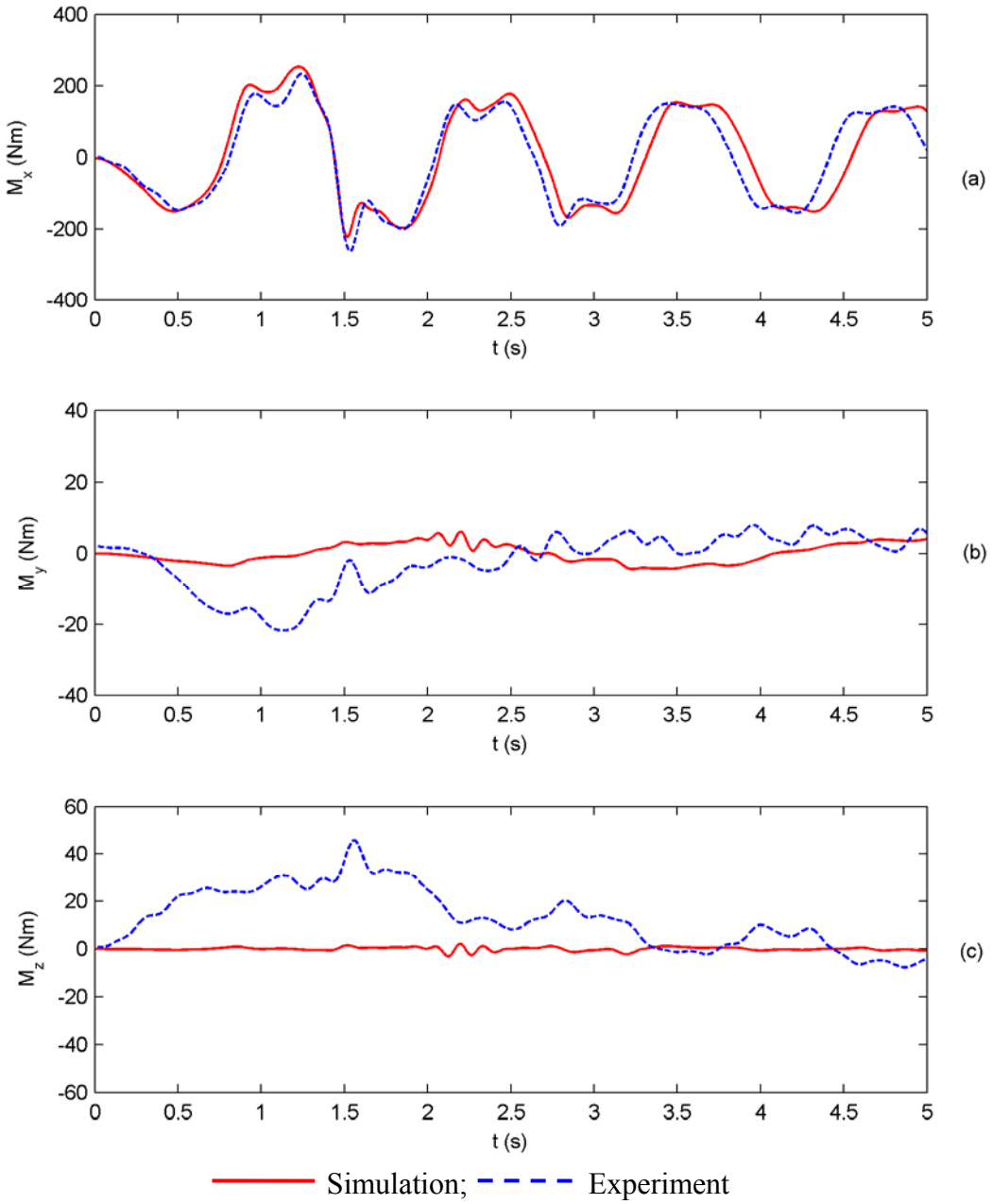

Fig. 5.10: Comparisons of transient slosh moment responses of simulation model with measured results (a) roll; (b) pitch; (c) yaw. (Tank – 'T1"; Fill volume – 30%; Excitation – single cycle sinusoid lateral acceleration of magnitude 1.93 m/s^2 at 1 Hz)

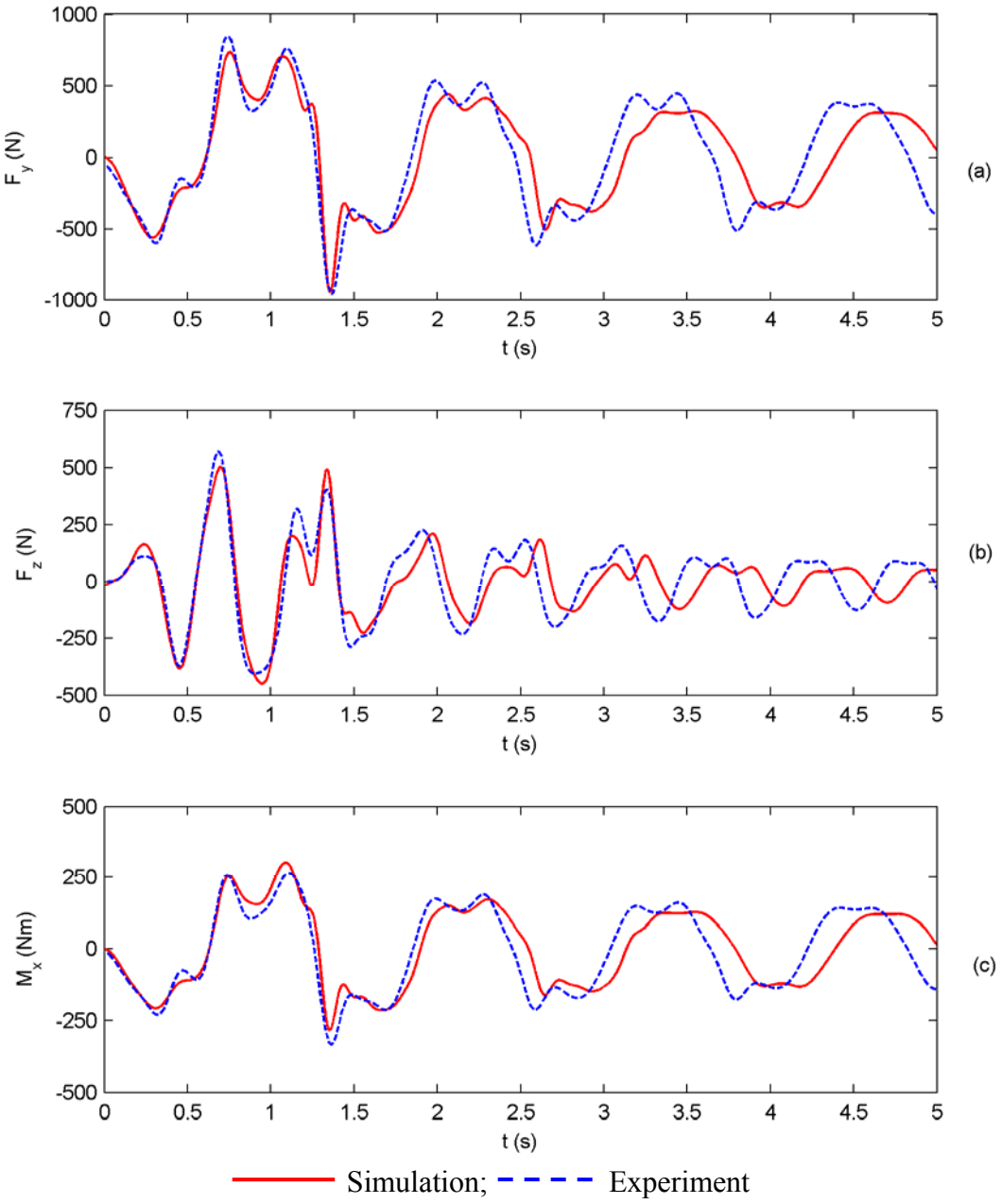

Fig. 5.11: Comparisons of transient slosh force and moment responses of simulation model with measured results (a) lateral force; (b) vertical force; (c) roll moment. (Tank – 'T1"; Fill volume – 30%; Excitation – single cycle sinusoid lateral acceleration of magnitude 4.34 m/s^2 at 1.5 Hz)

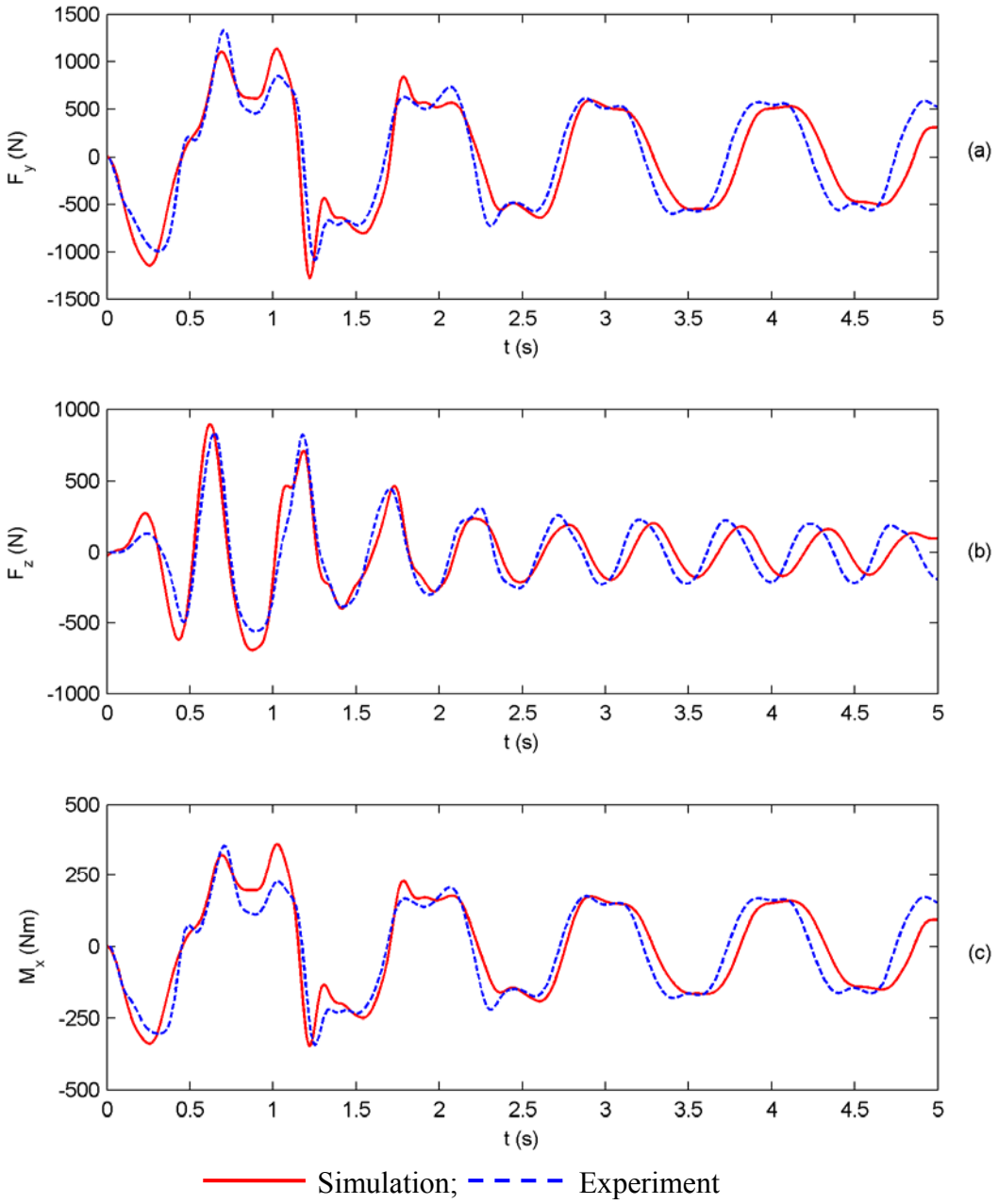

Fig. 5.12: Comparisons of transient slosh force and moment responses of simulation model with measured results (a) lateral force; (b) vertical force; (c) roll moment. (Tank – 'T2"; Fill volume – 50%; Excitation – single cycle sinusoid lateral acceleration of magnitude 4.34 m/s^2 at 1.5 Hz)

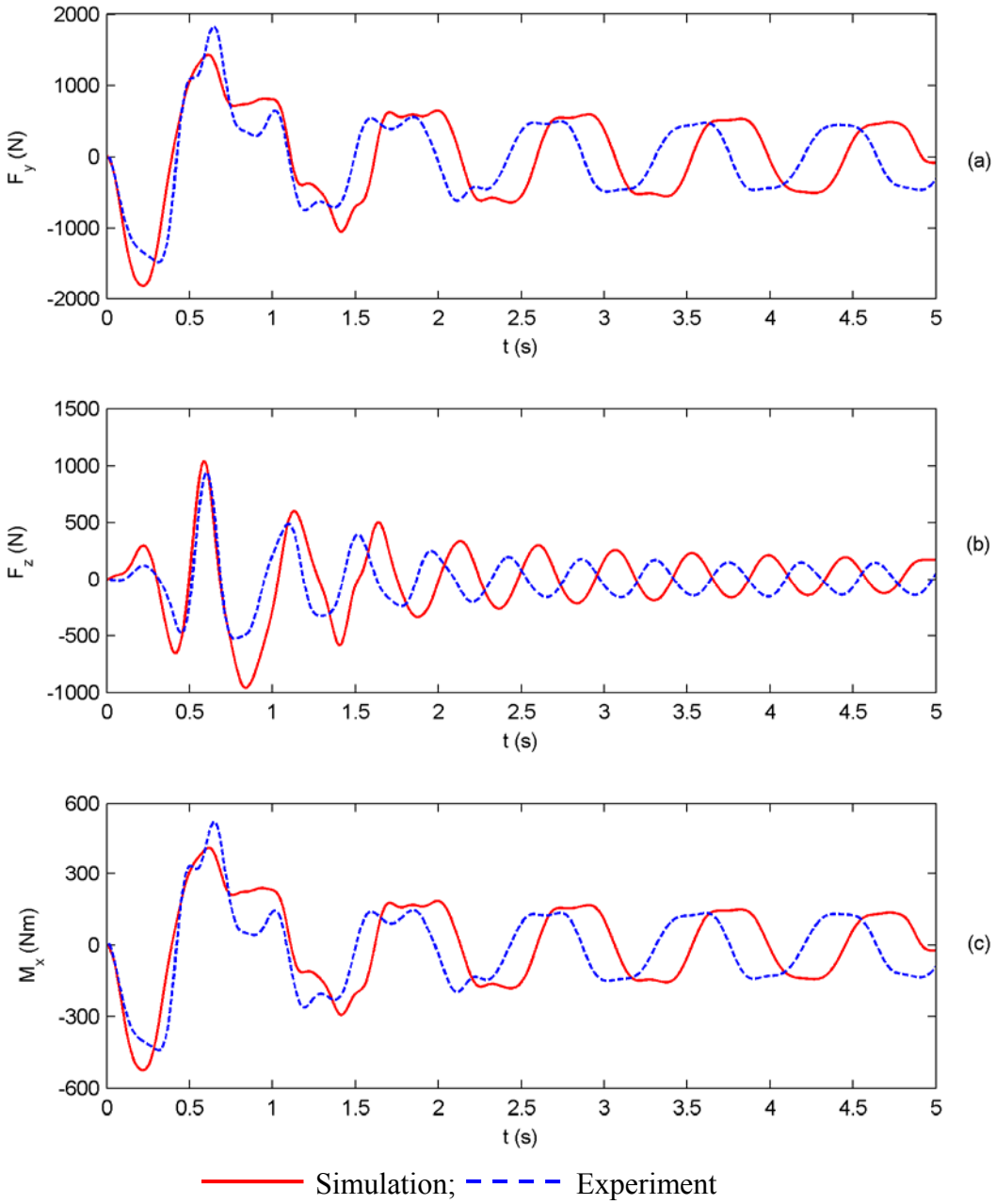

Fig. 5.13: Comparisons of transient slosh force and moment responses of simulation model with measured results (a) lateral force; (b) vertical force; (c) roll moment. (Tank – 'T2"; Fill volume – 70%; Excitation – single cycle sinusoid lateral acceleration of magnitude 4.34 m/s^2 at 1.5 Hz)

From the experiments, a three-dimensional fluid flow was consistently observed under single-axis harmonic excitations in the vicinity of the resonant frequency. This three-dimensional flow was observed in steady-state under both lateral as well as longitudinal harmonic excitations, and was not as notable under transient single-cycle sinusoidal excitation. This is evident in Fig. 5.7, which shows presence of a low frequency component and beat-like phenomenon, and is far more significant in tank with multiple-orifice baffles (configuration 'T3'), as shown in Figs. 5.14 and 5.15. The figures show time-histories of slosh forces and moments, respectively, measured for

tank 'T3' with 50% fill volume and subjected to lateral harmonic excitation of 1 m/s^2 in the vicinity of the resonance at 1 Hz. The figures clearly show beat-like behavior attributed to three-dimensional flow within the tank, even though the excitation is applied only along the lateral axis. This is mostly attributed to resonant slosh and in-part to higher flow resistance offered by multiple-orifice baffles. The results again show reasonable good agreements between the model and measured results.

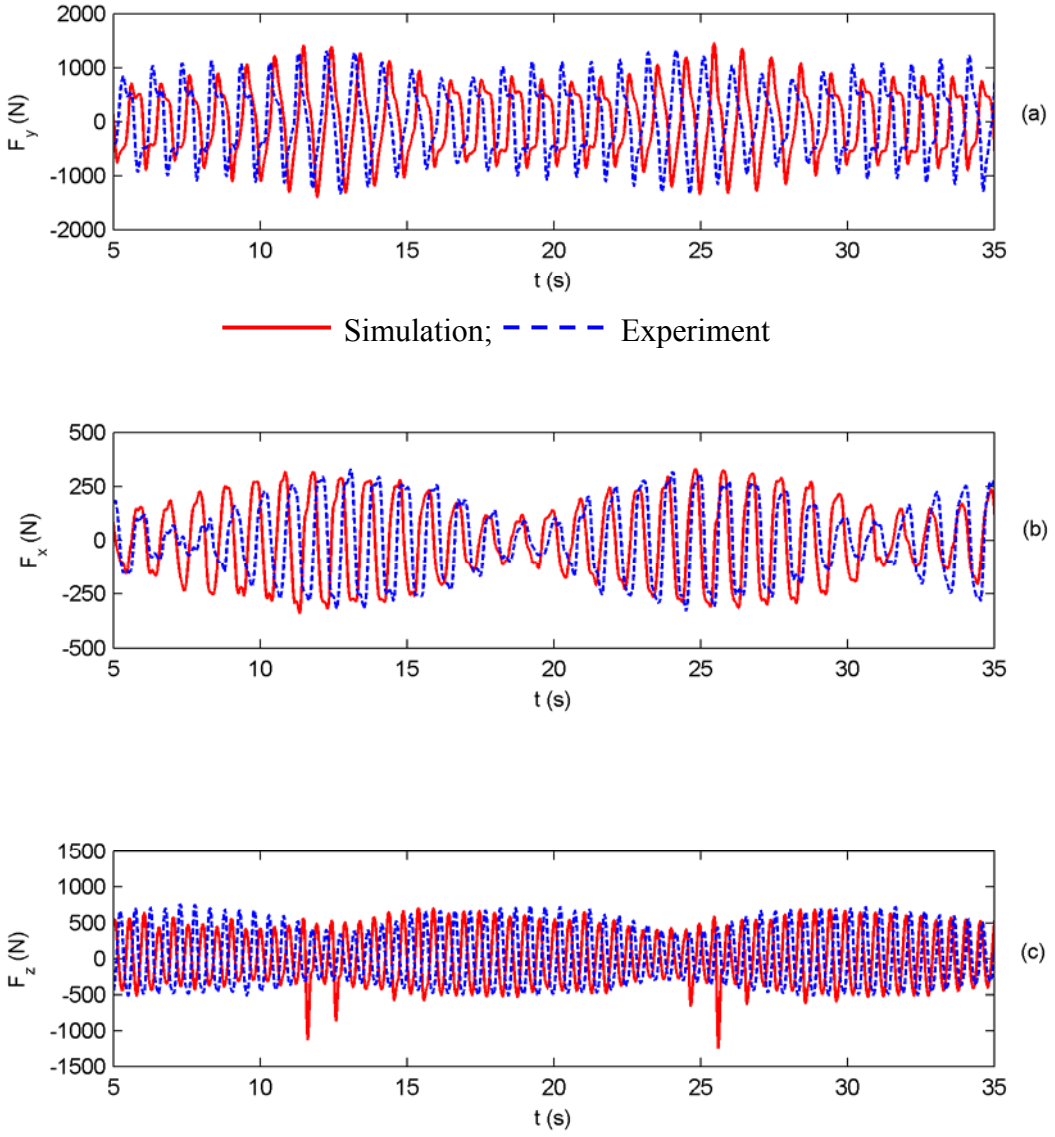

Fig. 5.14: Comparisons of steady-state slosh force responses of simulation model with measured results (a) F_X; (b) F_Y; (c) F_Z. (Tank – 'T3"; Fill volume – 50%; Excitation – harmonic lateral acceleration of magnitude 1 m/s^2 at 1 Hz)

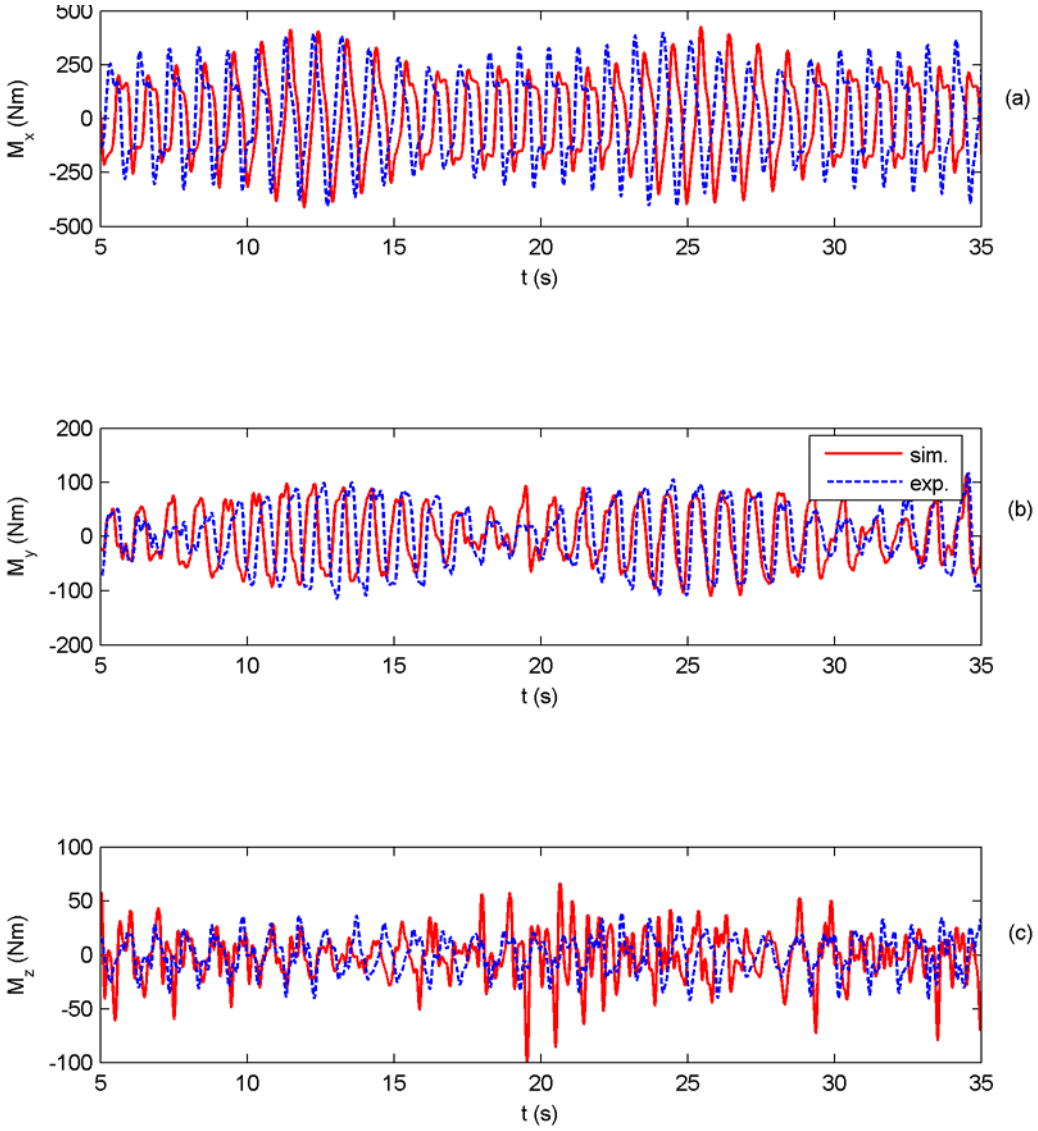

Fig. 5.15: Comparisons of steady-state slosh moment responses of simulation model with measured results (a) M_X; (b) M_Y; (c) M_Z. (Tank – 'T3"; Fill volume – 50%; Excitation – harmonic lateral acceleration of magnitude 1 m/s^2 at 1 Hz)

The magnitudes of slosh forces and moments tend to be quite significant when resonant slosh is encountered. This was clearly observed from the frequency response characteristics derived from the model and measured data. The peak slosh forces and moments developed at various excitation frequencies are evaluated from the model and the measured data. The results clearly showed excessive resonant magnitudes of slosh forces and moments. As an example, Figs. 5.16 and 5.17 illustrate comparisons of peak slosh forces and moments as a function of excitation frequency for cleanbore tank with 50% fill volume. The results are presented for two magnitudes of excitations: 1 and 2 m/s^2. From the results, it is apparent that magnitudes of lateral, longitudinal and vertical slosh forces tend to be excessive under excitation in the vicinity of lateral mode resonance (≈1 Hz). The peak lateral force tends to be twice that observed at a lower

frequency of 0.6 Hz. This trend is also evident in peak roll, pitch and yaw moments (Fig. 5.17). The figures further show reasonably good agreements between the model and measured results.

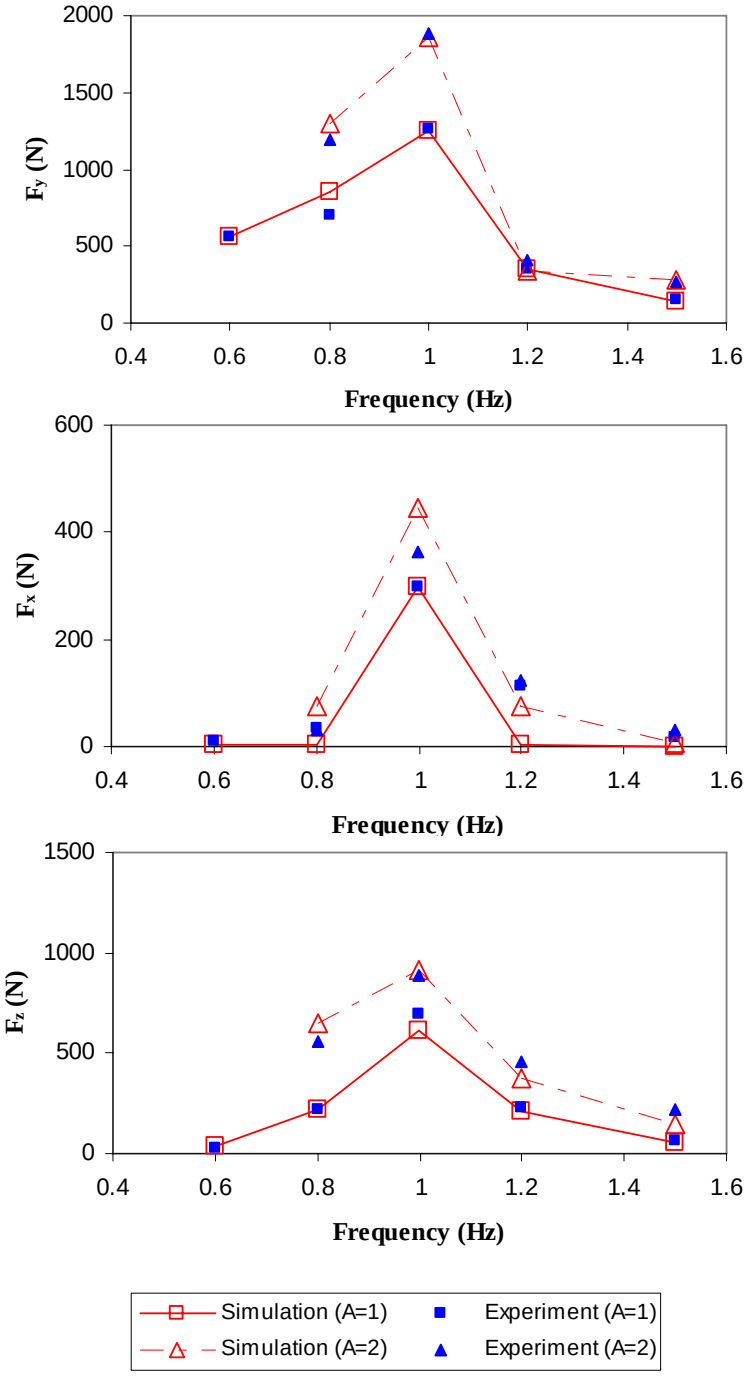

Fig. 5.16: Comparisons of peak slosh force responses of model with measured data as a function of magnitude and frequency of lateral excitation: (a) F_Y; (b) F_X; (c) F_Z. (Tank – 'T1"; Fill volume – 50%)

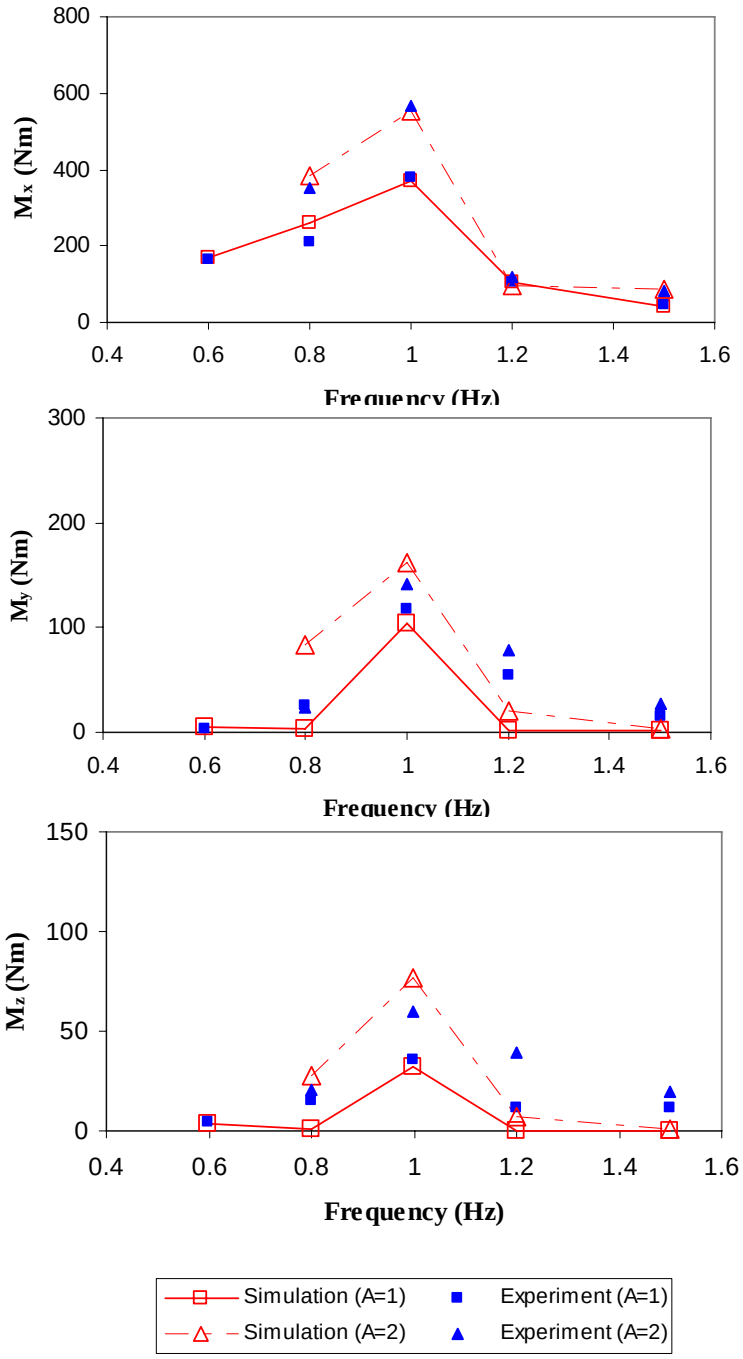

Fig. 5.17: Comparisons of peak slosh moment responses of model with measured data as a function of magnitude and frequency of lateral excitation: (a) M_X; (b) M_Y; (c) M_Z. (Tank – 'T1"; Fill volume – 50%)

5.4.2 Transient slosh forces and moments – Longitudinal acceleration excitation

The transient slosh forces and moments derived from the simulation model under 1 Hz ramp-step longitudinal acceleration, described in the previous chapter, are compared with the corresponding measured data to further demonstrate the model validity. The comparisons are

performed for un-baffled and baffled tanks under various fill volumes and excitation conditions. Comparisons of a few sample results, however, are presented to demonstrate the model validity. The results generally revealed considerably lower magnitudes of transient lateral force, and roll and yaw moments. The results thus show comparisons of lateral and vertical forces and pitch moment. Figures 5.18 to 5.20 illustrate comparisons of results attained for the cleanbore tank ('T1') corresponding to 30%, 50% and 70% fill volumes, respectively. Figures 5.21 and 5.22 illustrates comparisons of responses for single-orifice baffled tank ('T2') corresponding to 50% and 70% fill volumes, respectively. The results in general show good agreements between the measured and model results, irrespective of the tank configuration and fill volume.

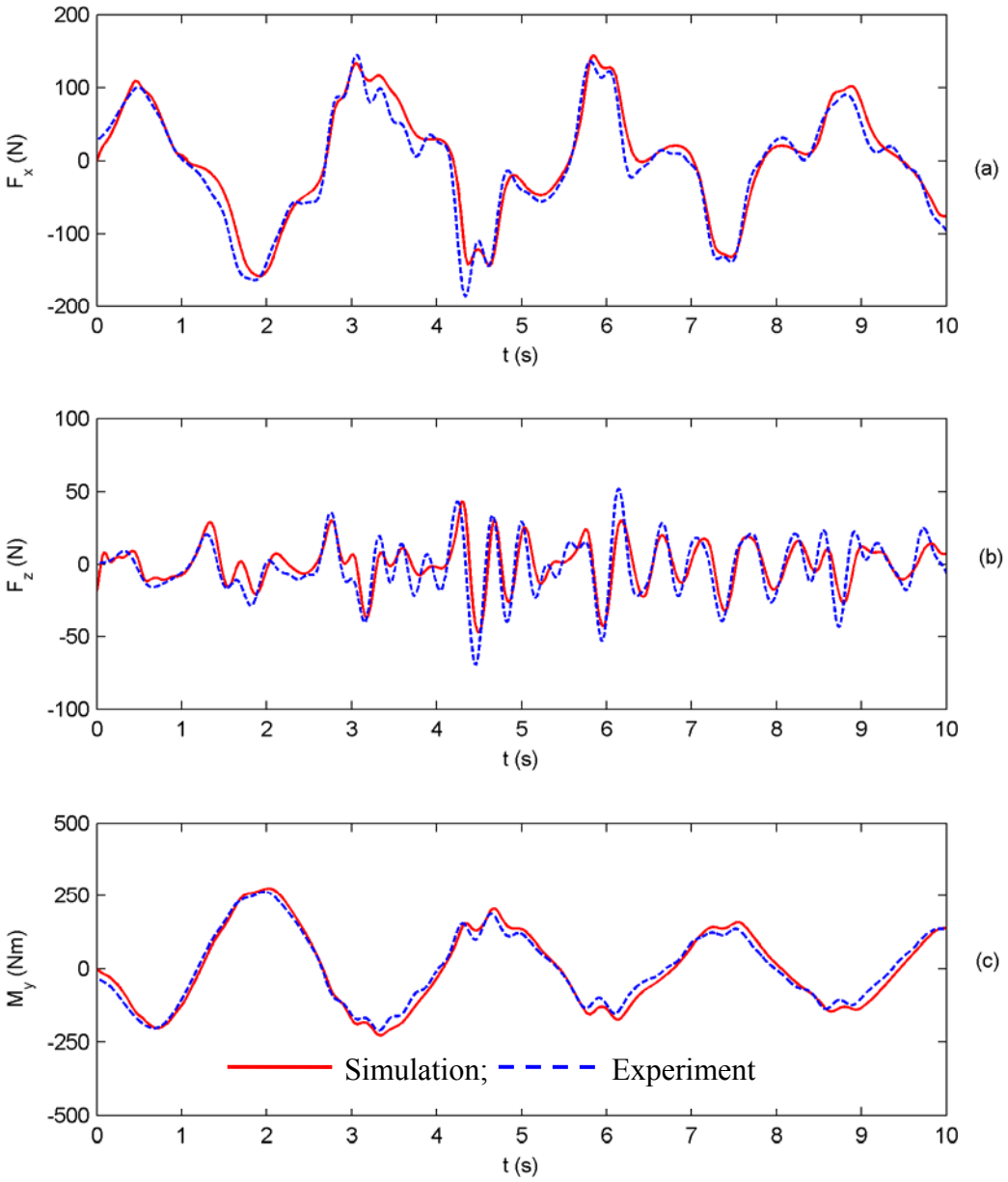

Fig. 5.18: Comparisons of transient slosh force and moment responses of simulation model with measured results (a) longitudinal force; (b) vertical force; (c) pitch moment. (Tank – 'T1"; Fill volume – 30%; Excitation – 1 Hz ramp-step longitudinal acceleration)

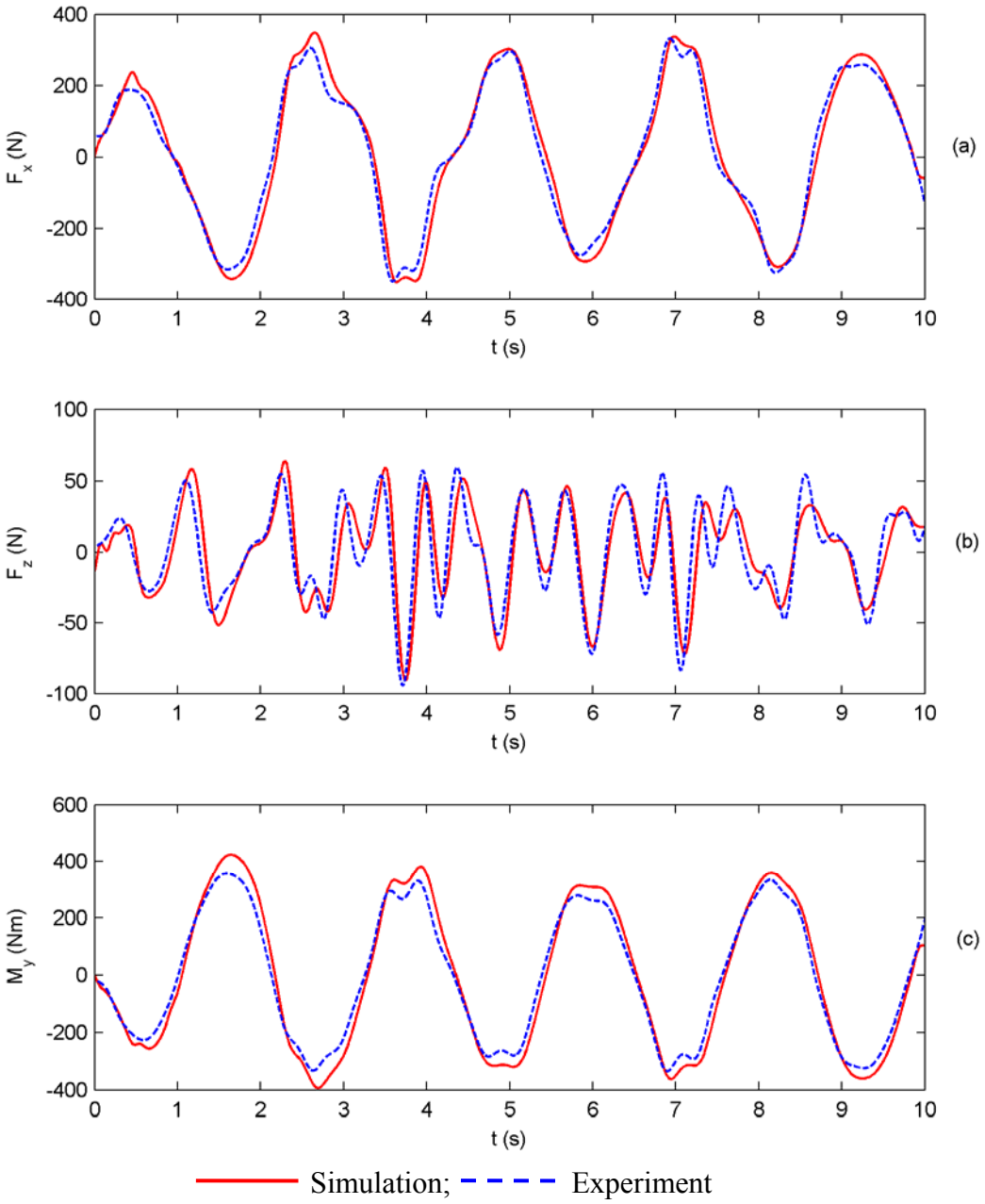

Fig. 5.19: Comparisons of transient slosh force and moment responses of simulation model with measured results (a) longitudinal force; (b) vertical force; (c) pitch moment. (Tank – 'T1"; Fill volume – 50%; Excitation – 1 Hz ramp-step longitudinal acceleration)

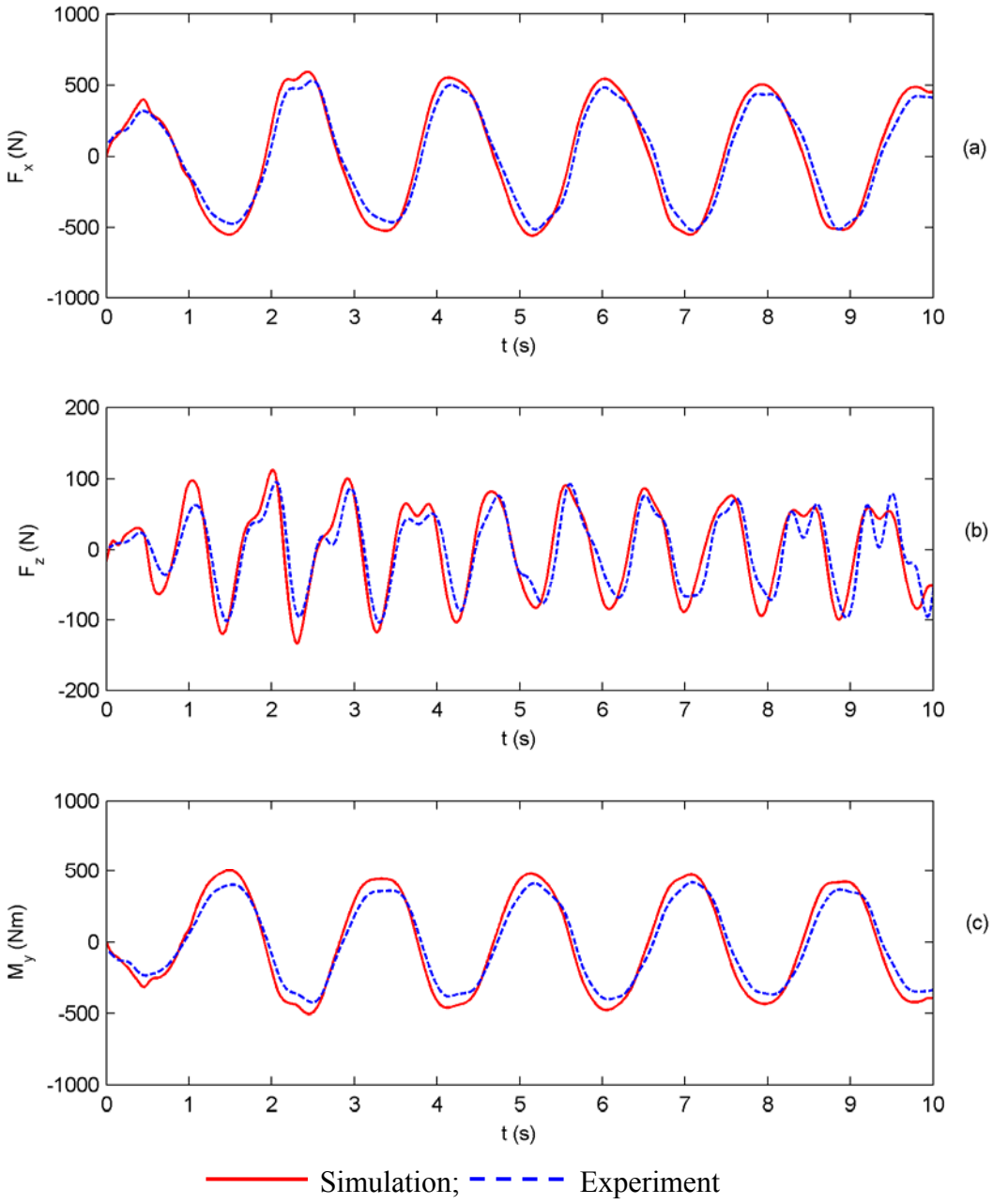

Fig. 5.20: Comparisons of transient slosh force and moment responses of simulation model with measured results (a) longitudinal force; (b) vertical force; (c) pitch moment. (Tank – 'T1"; Fill volume – 70%; Excitation - 1 Hz ramp-step longitudinal acceleration)

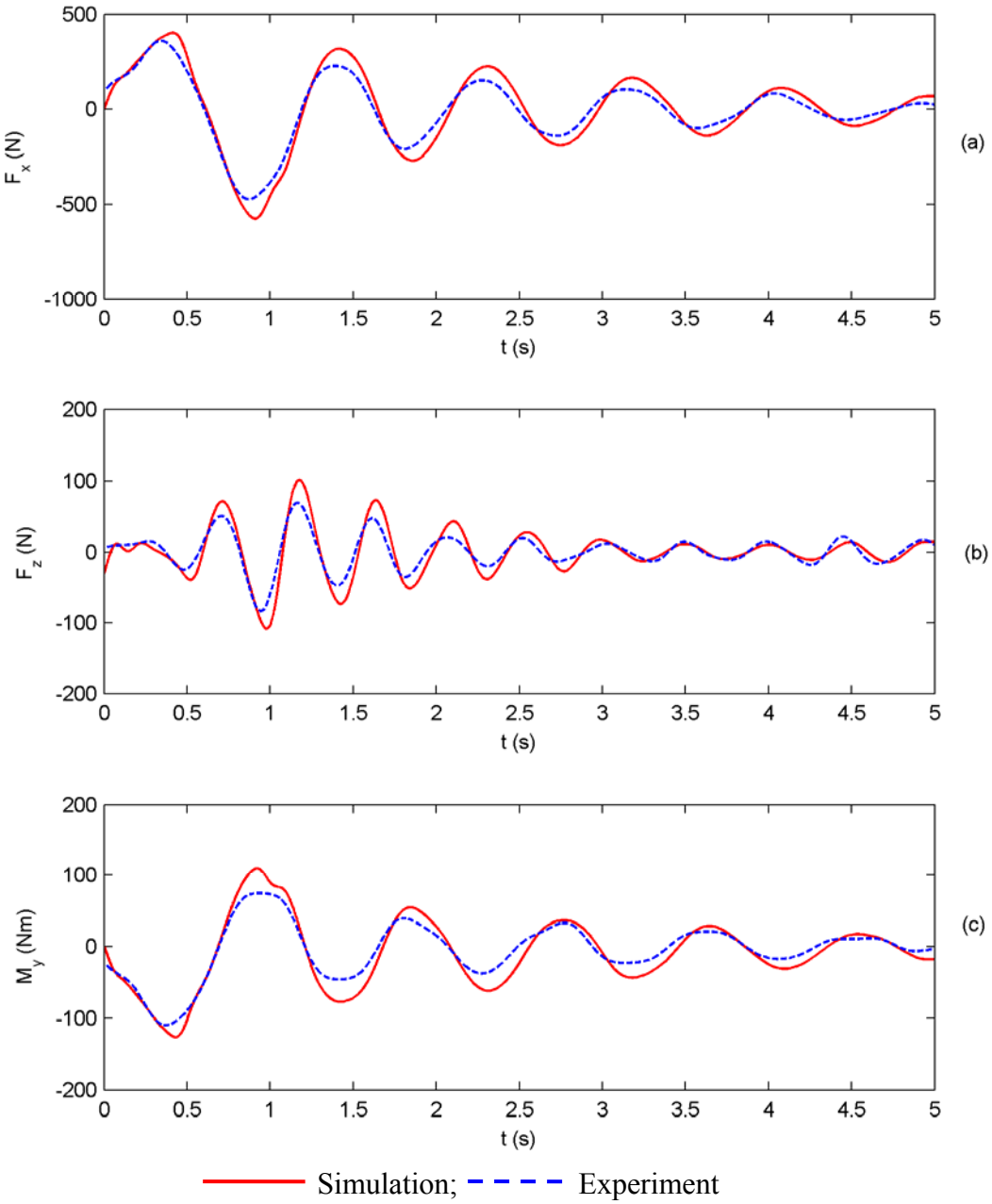

Fig. 5.21: Comparisons of transient slosh force and moment responses of baffled tank model with measured results (a) longitudinal force; (b) vertical force; (c) pitch moment. (Tank – 'T2"; Fill volume – 50%; Excitation – 1 Hz ramp-step longitudinal acceleration)

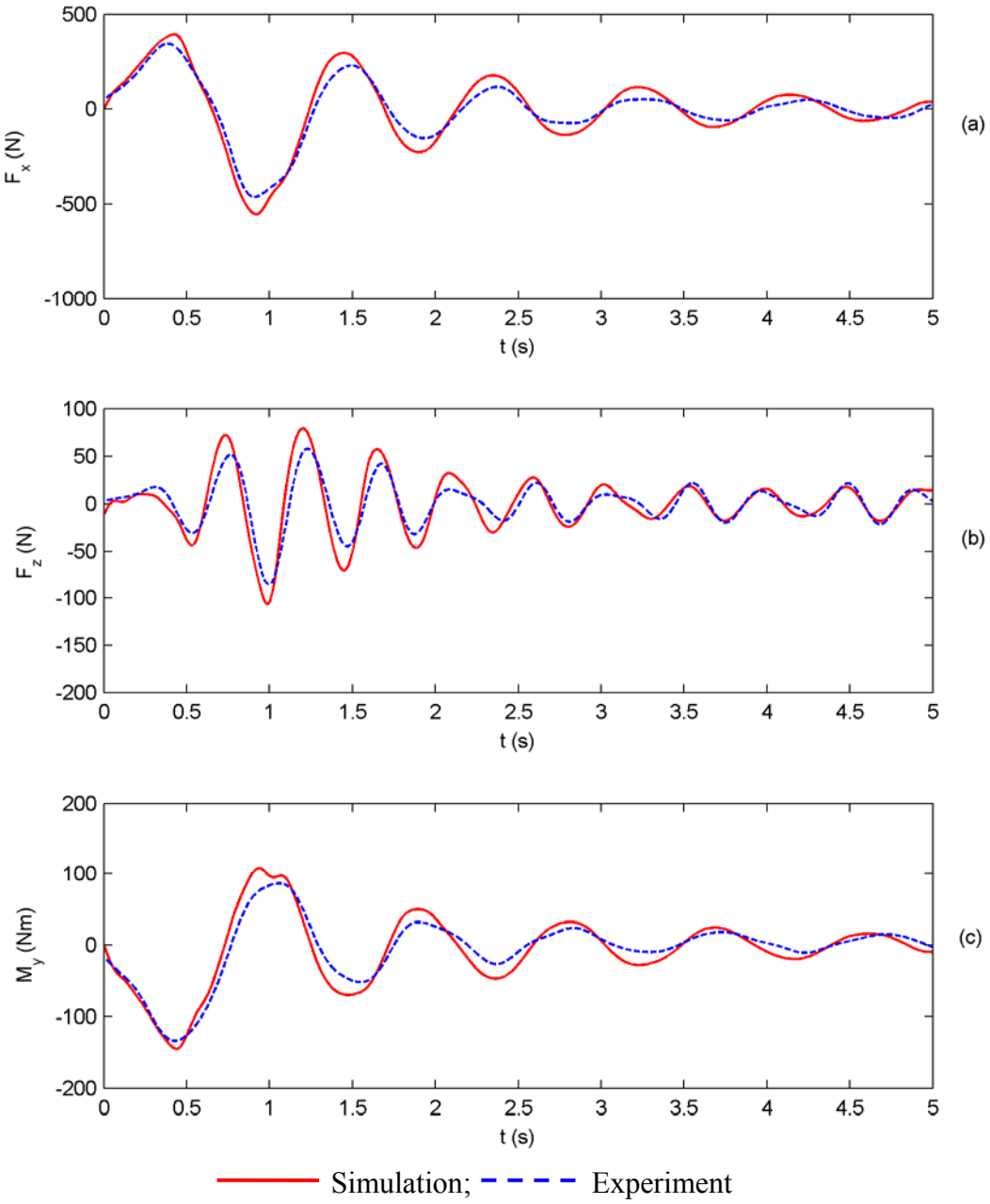

Fig. 5.22: Comparisons of transient slosh force and moment responses of baffled tank model with measured results (a) longitudinal force; (b) vertical force; (c) pitch moment. (Tank – 'T2"; Fill volume – 70%; Excitation – 1 Hz ramp-step longitudinal acceleration)

6. TRANSIENT SLOSH ANALYSIS AND ROLE OF BAFFLES

The vast majority of studies on fluid slosh within baffled tanks are either based on experiments with scale model tanks of arbitrary geometry or analyses of two-dimensional slosh. A tank vehicle is subject to three dimensional slosh loads encountered under directional maneuvers involving simultaneous applications of acceleration/braking and steering. An analysis of slosh forces and moments based upon three-dimensional slosh behaviour within cleanbore and baffled tanks is thus desirable to obtain better understanding of destabilizing forces.

The validated model of the partly-filled tank is applied to study the transient fluid slosh behaviour of a tank truck and role of baffles in controlling the magnitudes of transient as well as steady-state fluid slosh forces and moments. The three-dimensional fluid slosh model, described in the previous chapter, permits for analyses of transient as well as steady-state slosh forces and moments under lateral, longitudinal, and combined lateral and longitudinal accelerations. Moreover, the role of baffles in limiting the slosh forces could be effectively investigated. The model also allows for studies of various concepts in baffles designs. In this section, the model is applied to a full-scale tank model to study the dynamic slosh forces and moments caused by various directional maneuvers. Kineto-static modeling approach is applied and the solutions are compared with the dynamic responses to demonstrate the significance of dynamic slosh in cleanbore tanks.

6.1 Kineto-Static Analysis

The validity of the dynamic slosh forces and moments derived from three-dimensional fluid slosh model is further examined by comparing the steady-state solutions with corresponding quasi-static solutions obtained under identical fill and excitation conditions. Considering that the reported quasi-static models are not applicable for fluid load shift in tanks with unequalized baffles considered in this study, the comparisons are limited for the cleanbore tank alone. For the quasi-static motion of the fluid under application of lateral (a_y) and longitudinal (a_x) accelerations, the total pressure differential can be expressed as [4]:

$$dP = \frac{\partial P}{\partial x}dx + \frac{\partial P}{\partial y}dy + \frac{\partial P}{\partial z}dz \tag{6.1}$$

Upon application of force balance on a liquid element in steady state, the above pressure differential yields:

$$a_x = \frac{1}{\rho}\frac{\partial P}{\partial x};\ a_y = \frac{1}{\rho}\frac{\partial P}{\partial y};\ a_z = \frac{1}{\rho}\frac{\partial P}{\partial z} \tag{6.2}$$

The total pressure differential may thus be expressed as:

$$dP = \rho a_x dx + \rho a_y dy + \rho a_z dz \tag{6.3}$$

Considering that the pressure at the free surface vanishes or is uniformly distributed (dP=0), the equation of the liquid free surface under static condition is obtained as:

$$Y(x,z) = -G_x x - G_z z + c_o \text{ , } -R \le x \le R \text{ ; } -\frac{L}{2} \le z \le \frac{L}{2} \tag{6.4}$$

where $G_x = a_x/a_z$, $G_y = a_y/a_z$ and c_0 is a constant that is derived upon considering constant fluid volume.

The coordinates of the mass center of the fluid (x_{cg},y_{cg},z_{cg}) with respect to the origin are then derived from moment integration over the fluid domain, such that:

$$x_{cg} = \frac{1}{V_\ell}\iiint_v x d\upsilon; \;\; y_{cg} = \frac{1}{V_\ell}\iiint_v y d\upsilon; \;\; z_{cg} = \frac{1}{V_\ell}\iiint_v z d\upsilon \tag{6.5}$$

where V_ℓ is total fluid volume and υ defines the domain of integration. The moving fluid in the three-dimensional field may assume different locations and slopes and thus the domains of integration, depending upon the fill volume and the magnitudes of applied accelerations. The methodology for identifying the domains of integration for varying fill and excitation conditions has been well described in [4,15].

The pitch, roll and yaw moments caused by the liquid load shifts about a point located at the bottom of the tank directly beneath the origin (Fig. 3) are computed from the forces and the coordinates of the mass center, such that:

$$\overline{M}_y = (z_{cg} + R)\overline{F}_x - x_{cg}\overline{F}_z; \;\; \overline{M}_z = x_{cg}\overline{F}_y - y_{cg}\overline{F}_x; \;\; \overline{M}_x = y_{cg}\overline{F}_z - (z_{cg} + R)\overline{F}_y \tag{6.6}$$

where $\overline{M}_x, \overline{M}_y \; and \; \overline{M}_z$ are the pitch, yaw and roll moments, respectively, caused by kineto-static fluid motion within a circular cross-section tank of radius R. $\overline{F}_x = -ma_x$, $\overline{F}_y = -ma_y$, and $\overline{F}_z = ma_z$ are the lateral, vertical and longitudinal forces, respectively, due to quasi-static motion of fluid of mass m.

The mass moments of inertia of the liquid volume about the three orthogonal axes passing through the center of cylindrical tank that coincides with the origin of the coordinate system (Fig. 3) are obtained from the following moment integrals:

$$\bar{I}_{XX} = \rho\iiint_V (y^2 + z^2)dv \text{ , } \bar{I}_{YY} = \rho\iiint_V (x^2 + z^2)dv \text{ , } \bar{I}_{ZZ} = \rho\iiint_V (y^2 + x^2)dv \tag{6.7}$$

where $\bar{I}_{XX}, \bar{I}_{YY}$ and $\bar{I}_{ZZ}$ are the pitch, yaw and roll mass moments of inertia of the deflected liquid corresponding to quasi-static analyses.

6.2 Dynamic Fluid Slosh Analysis

The analyses are performed for a full size circular cross-section for various fill levels and magnitudes of lateral and longitudinal acceleration excitations. The fluid flow equations were formulated for a circular cross-section tank with three lateral baffles designed with a single nozzle of diameter equal to 30% of the tank diameter. The total volume of the tank considered in the study was 23.6 m^3, and the geometry of the tank and baffles is shown in Fig. 5.1. The analyses were performed assuming fuel oil as the base fluid and two-phase fluid domain was considered to account for partial fill condition. Physical properties of the fluid and air considered for the partly-filled tank are summarized in Table 6.1. The fill condition in the study was defined as the ratio of fill height to tank diameter, which is different from the fill volume ratio defined for test tanks. The 40% and 60% fill condition in this study correspond to fluid volumes of 8.74 and 14.73 m^3, respectively. It should be noted that the primary goal of this task was to study the significance of dynamic fluid slosh and role of baffles while considering a full size tank and validated dynamic slosh model.

Table 6.1: Physical properties of fuel oil and air

Parameter	Value	Unit
Fuel oil density	850	kg/m3
Fuel oil dynamic viscosity	0.0867	kg/m-s
Air density	1.225	kg/m3
Air dynamic viscosity	1.7894e-5	kg/m-s

It has been shown that the mean values of dynamic slosh forces and moments agree reasonably well with those derived from quasi-static solutions for fluid motion within cleanbore tanks [42] This finding is also assumed to hold true for the baffled tanks considered in this study. The peak deviations in dynamic response values from the corresponding steady solutions are quantified in the form of amplification factors defined, as the ratio of the peak value of dynamic response quantity to the corresponding mean response, such that:

$$M_{Rp} = \frac{Max(Rp)}{\overline{Rp}} \tag{6.8}$$

where Rp is the selected response parameter that may include slosh force or moment along a particular direction, and Max refers to its peak value. $\overline{Rp}$ is its mean value, which is comparable to that obtained from the static solution. M_{Rp} is the amplification factor, which defines the peak amplification of the response variable in the transient state with respect to the steady solution, and thus characterizes the transient nature of the oscillatory slosh forces and moments. This ratio describes the significance of transient fluid slosh within a partly-filled tank.

The mean value $\overline{Rp}$ is obtained by evaluating the time integral of the response Rp over a selected duration:

$$\overline{R}_p = \frac{1}{t_2 - t_1} \int_{t_1}^{t_2} R_p(t)\, dt\,, \qquad (t_2 - t_1) \rangle\rangle\, n\tau \tag{6.9}$$

Where t_2 and t_1 define the integration period which comprises n (>1) cycles of oscillations, and τ is the period of oscillation. For the simulation time considered in this study (40 s), the integration periods varied between 30 and 38 s. It should be noted that the frequency of fluid oscillation is a function of fill volume, acceleration level and geometry of the tank (baffled or cleanbore tank).

6.3 Results and Discussions

6.3.1 Dynamic slosh forces

The three-dimensional quasi-static and dynamic slosh models of fluid within a partly-filled cleanbore tank are initially solved under two different constant magnitudes of longitudinal deceleration (0.3 g and 0.6 g) alone and two different fill conditions (40% and 60%). The mean values of longitudinal slosh forces F_X are derived from the dynamic pressure distribution and compared with those derived from the quasi-static (QS) analysis for 0.3 *g* longitudinal acceleration in Fig. 6.1(a). The comparisons suggest very good agreements between the mean dynamic and quasi-static forces, for both fill levels within the cleanbore tank. The dynamic mean responses, however, tend to be 1-2% higher than the corresponding quasi-static values. This deviation is attributed to the slightly different fluid volume estimated from the mesh in the Fluent model. The similar degree of agreement was also observed for 0.6 *g* acceleration. A higher fill volume yields higher mean force due to higher mass, while an increase in magnitude of deceleration from 0.3 *g* to 0.6 *g*, causes significantly higher mean longitudinal force, as evident in Fig. 6.1(b). The results suggest that the mean longitudinal slosh force representing the steady state solution increases nearly linearly with the deceleration level and fill volume, which further agrees with the quasi-static formulation presented in the previous section.

The directional dynamic analyses of partly-filled tank vehicles have been invariably based upon mean forces and the corresponding moments, while the magnitudes of dynamics slosh forces and moments could be significantly higher. Figure 6.2 presents the amplification factors of longitudinal and vertical forces, as derived from the dynamic responses, for different levels of fill within a cleanbore tank and longitudinal acceleration. The results show the amplification in longitudinal slosh force could vary in the 1.67 to 1.96 range depending upon fill and excitation condition considered, as evident in Fig. 6.2(a). This suggests that the peak magnitudes of the longitudinal transient slosh force under a pure longitudinal deceleration are significantly higher than the corresponding mean values, and could further deteriorate the directional performance of the vehicle. An increase in the fill level reduces the response amplification, while the magnitude of corresponding peak force would be higher due to its higher mass. The peak longitudinal force corresponding to 40% fill and a_x=0.3 g approaches nearly two times its corresponding mean force, which could adversely affect braking performance of vehicle under a lower fill level. The relative difference between the peak and mean dynamic forces, however, are lower under higher fill condition, which is attributed to reduced slosh under constraints imposed by tank boundary. The vertical force amplification factors caused by fluid slosh under deceleration tend to be

somewhat lower when compared to the longitudinal forces, which attains a maximum value of near 1.12 under lower fill and higher deceleration magnitude.

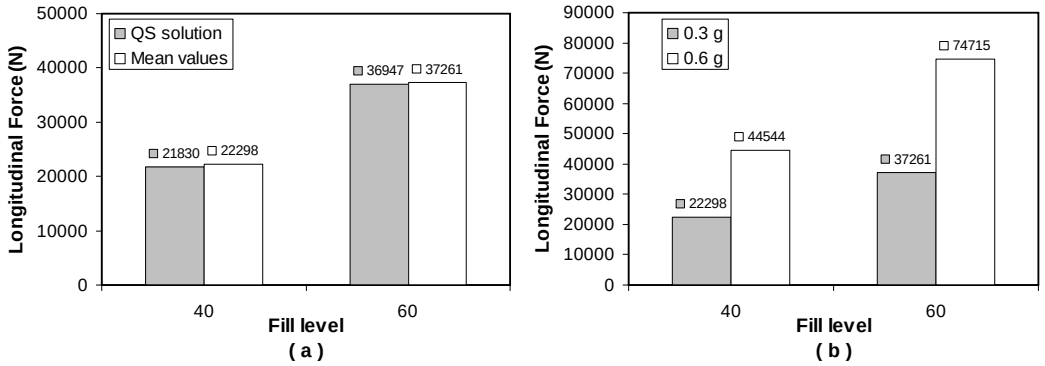

Fig. 6.1: Quasi-static and mean dynamic longitudinal forces developed due to fluid motion in a cleanbore tank subject to a_x = 0.3g: (a) comparsion of mean dynamic force with the quasi-static force; (b) influence of longitudinal acceleration magnitude**.**

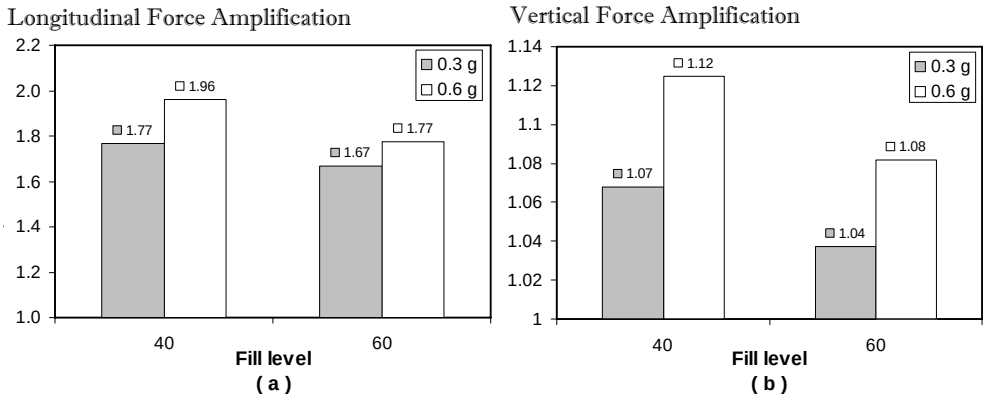

Fig. 6.2**:** Influence of fill level and magnitude of acceleration on: (a) longitudinal force amplification; and (b) vertical force amplification.

Figure 6.3 illustrates the effects of fill level and magnitude of longitudinal acceleration on longitudinal force due to fluid slosh within the tank with and without baffles. The results reveal that the baffles reduce the intensity of force amplification significantly from 1.77 that occurs in a cleanbore tank to nearly 1.32 for the 40% filled tank subject to a_x=0.3 g. The results also suggest that force amplification factor increases with an increase in acceleration, when a clean bore tank is considered. This trend, however, is reversed for a baffled tank, for the discrete acceleration levels considered in this study. This can be attributed to the reduced fluid slosh due to additional constraints imposed by the baffles.

It has been reported that the roll stability of a partly filled tank vehicle with a cleanbore tank is further reduced when subjected to simultaneous lateral and longitudinal accelerations [4], which has been attributed to relatively higher magnitudes of destabilizing roll moment as a function of the slosh force components and load shifts in the roll and pitch planes. The dynamic slosh forces

developed along the lateral axes are evaluated under simultaneous applications of a_y=0.25 g, and a_x=0.3 and 0.6 g, and responses are evaluated to derive mean lateral force caused by fluid slosh within baffled and cleanbore tanks for 40 and 60% fill conditions, as shown in Fig. 6.4. The results show negligible effects of baffles on the mean lateral force, irrespective of the fill level. This trend is supported by observations reported from field experiments, which concluded that the presence of lateral baffles does not affect the lateral stability limit of the vehicle. The effect of baffles, however, could be observed when transient lateral forces are considered. Figure 6.5 illustrates time histories of lateral slosh forces attained for 40%-filled cleanbore and baffled tanks subjected to 0.25g lateral and 0.3g longitudinal accelerations. The results suggest that fluid motion in a cleanbore tank yields higher magnitude of lateral force, when compared to that for the baffled tank. The slosh force for cleanbore tank, however, diminishes rapidly, while the response for the baffled tank shows continued oscillations of considerable magnitudes. This is attributed to constraints imposed by baffle walls on fluid motion. Visualization of liquid slosh within baffled tank showed a phase lag between liquid slosh in partitioned volumes within the tank. This may further explain the oscillatory behaviour of liquid slosh shown in Fig. 6.5.

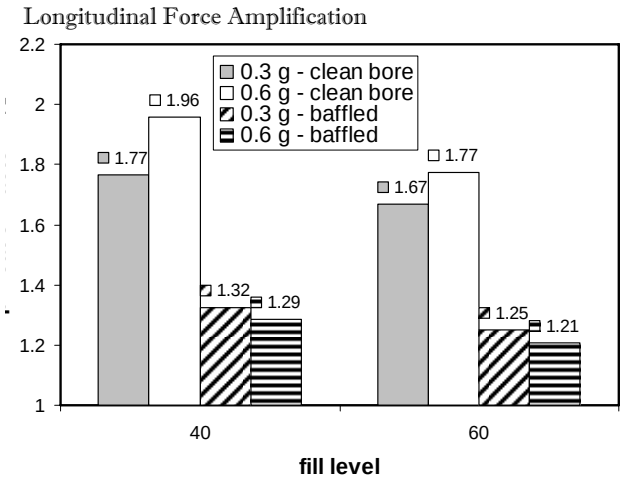

Fig. 6.3**:** Influence of baffles on the longitudinal force amplification.

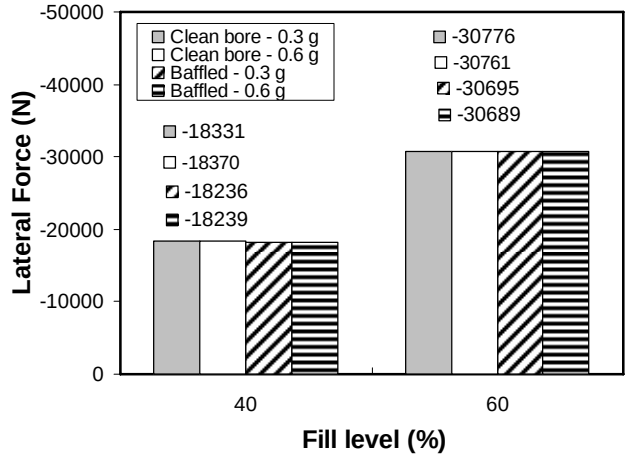

Fig. 6.4: Mean lateral slosh force acting on the partly-filled tank with and without baffles subject to simultaneous lateral and longitudinal accelerations under 40 and 60% fill conditions**.**

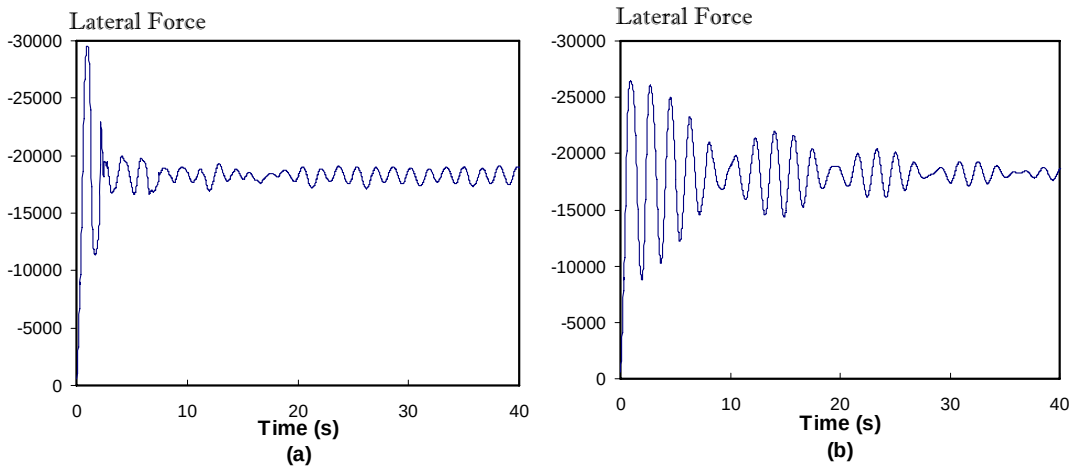

Fig. 6.5: Time histories of lateral slosh force developed for 40% fill, and simultaneous applications of a_y=0.25 g and a_x=0.3 g accelerations: (a) cleanbore; and (b) baffled tank.

The lateral force response for the baffled tank exhibits the presence of a lower beat frequency, which is believed to be caused by the coupling effects of fluid slosh in the roll and pitch planes, and resonant oscillations. The visualization of the free surface revealed coupled fluid motions in both the planes, which was also observed in the experiments. Results presented in Fig. 6.5(b) suggest predominant frequency of 0.55 Hz, which is close to the fundamental frequency of lateral slosh reported for 40% fill condition [11,17], and a beat frequency near 0.05 Hz attributed to the coupling between the lateral and longitudinal modes. The responses corresponding to the free oscillation of the liquid inside the tank were analyzed to compute frequencies of fluid slosh using FFT analysis. The analyses were performed using a total of 3000 samples and period of *75* s and a frequency resolution of *0.0133* Hz. The fundamental slosh frequencies in the pitch plane were obtained as 0.16, 0.19, 0.21 and 0.26 Hz under fill conditions of 40, 50, 60 and 80%, respectively, which showed good agreements with those reported by Abramson for a cylindrical tank with flat end caps [11] (0.16, 0.18, 0.21, 0.26 Hz). The flat ends yield constant length of the free surface, irrespective of the fill level. The fundamental slosh frequencies in the roll plane were also obtained for 40, 50, 60 and 80% fill levels as 0.56, 0.58, 0.61 and 0.74 Hz, respectively, which are again comparable to those reported by Budiansky [17] and Abramson [11] (0.56, 0.59, 0.62, 0.74). The results suggest that the curved end caps considered in this study have insignificant effect on slosh frequencies in the roll and pitch planes.

Figure 6.6 illustrates lateral force amplification factor for the 60% filled clean bore tank subject to pure lateral acceleration as well as simultaneous lateral and longitudinal accelerations. The figure also shows the influence of magnitude of longitudinal acceleration on the amplification factor. The results are presented for three types of excitations: **A** – 0.25 g lateral acceleration; **B**- 0.3g longitudinal and 0.25g lateral accelerations; and **C**- 0.6 g longitudinal and 0.25g lateral accelerations. The results show that the lateral force amplification for the cleanbore tank increases considerably with an increase in longitudinal acceleration, suggesting higher peak force under higher longitudinal acceleration. This trend is not evident from the results reported on the basis of the mean or quasi-static solutions [4], and can be entirely attributed to transient fluid slosh in the three-dimensional domain. The simultaneous applications of lateral and longitudinal accelerations would thus most likely deteriorate both the braking and turning performance of the

vehicle. The presence of baffles also tends to limit the peak lateral force amplification to considerably lower levels, while the effect of magnitude of longitudinal acceleration considered in the study is almost insignificant.

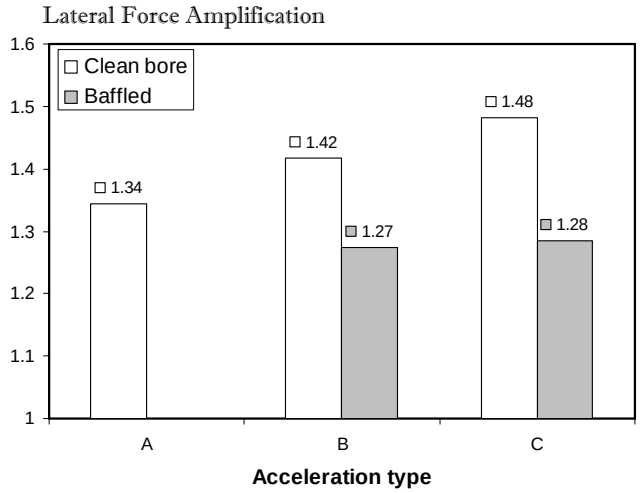

Fig. 6.6: Lateral force amplification factor for the 60% filled cleanbore and baffled tanks subject to: **A** – 0.25 g lateral acceleration, **B**- 0.3g longitudinal and 0.25g lateral accelerations, and **C**- 0.6 g longitudinal and 0.25g lateral accelerations

Figure 6.7 illustrates the influence of fill level on lateral force amplification factor due to fluid slosh in a cleanbore tank subject to longitudinal and lateral accelerations (a_y=0.25g; a_x=0.3 and 0.6g). The lateral force amplification factor approaches a value near 1.85 corresponding to lower fill condition of 40% and higher longitudinal acceleration of 0.6 g. A higher fill yields relatively lower amplification of lateral force due to reduced fluid slosh and constraints imposed by the boundaries. An increase in magnitude of longitudinal acceleration leads to increase in amplification factor, irrespective of the fill level, although the increase is relatively small under higher fill condition. Figure 6.8 illustrates corresponding vertical and longitudinal force amplification factors, as a function of fill level and magnitude of longitudinal acceleration, while the magnitude of lateral acceleration is held constant (0.25g). Both the vertical and longitudinal amplification factors show similar trends, namely, the amplification factors decrease with an increase in fill level and increase when the longitudinal acceleration magnitude is increased. The results suggest that amplification of longitudinal force increases significantly with magnitude of acceleration, while the dynamic vertical force deviation is not significant as observed earlier under pure longitudinal acceleration. The peak amplification factors for both responses occur under lower fill level and higher longitudinal acceleration. The presence of baffles helps in suppressing the peak longitudinal force and thus the amplification factor considerably, as shown in Fig. 6.8(b). The peak longitudinal force due to fluid slosh within the baffled tank tends to be relatively insensitive to both the fill level and magnitude of a_x. Furthermore, the peak values of longitudinal force in a baffled tank are considerably smaller than those derived for the cleanbore tank.

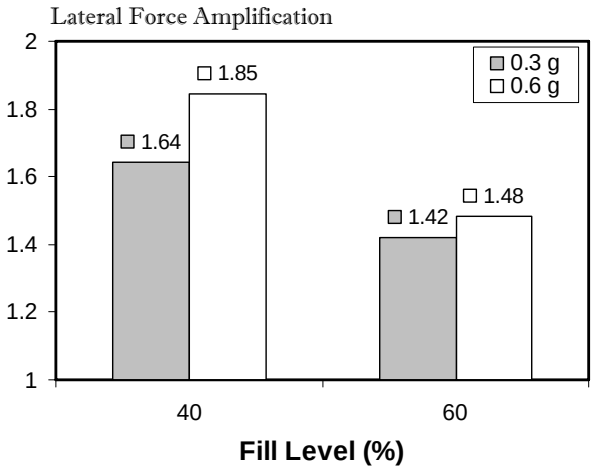

Fig. 6.7: Effect of fill level and magnitude of longitudinal acceleration on the lateral force amplification factor (a_y= 0.25g)

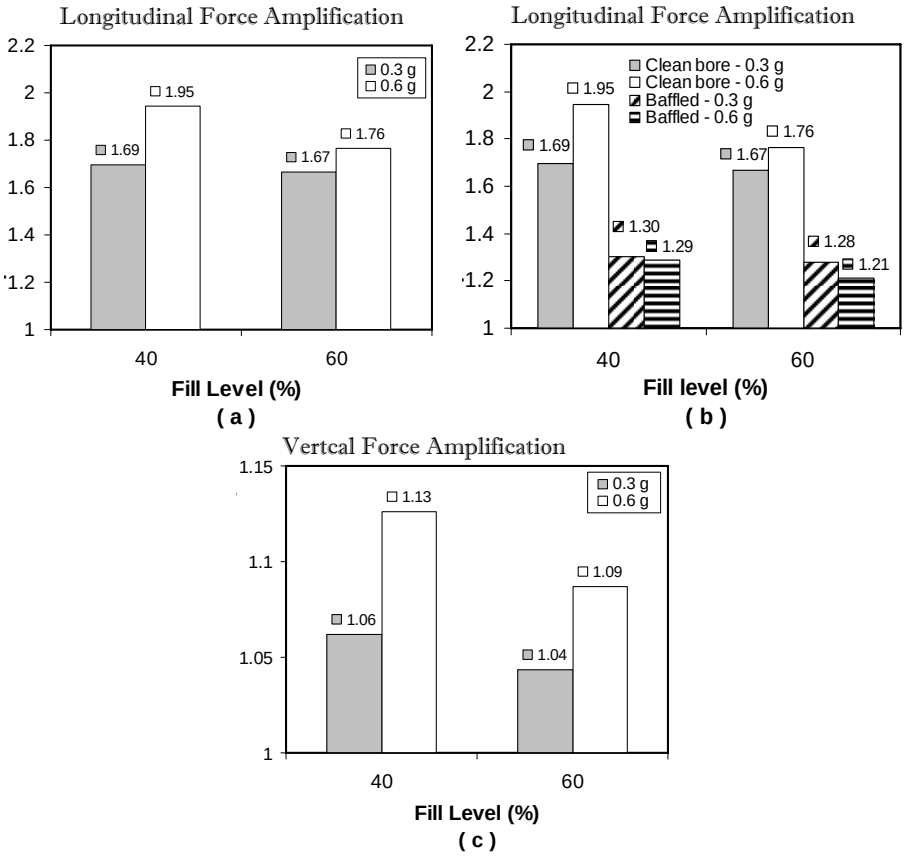

Fig. 6.8: Longitudinal and vertical forces amplification factors under simultaneous application of lateral and longitudinal accelerations: (a) M_{Fx} – cleanbore tank; (b) M_{Fx} – baffled tank; (c) M_{Fz} – cleanbore tank.

6.3.2 Dynamic slosh moments

The mean and peak values of moments caused by fluid slosh under lateral and longitudinal accelerations are computed for the cleanbore as well as baffled tanks, and the results are compared to study the role of baffles as functions of the fill condition and magnitudes of excitation. Figure 6.9 illustrates the pitch moment amplification factor due to dynamic slosh for the 40% and 60% filled cleanbore tank together with the mean values under longitudinal acceleration excitations alone. The influence of baffles on the pitch moment amplification factor is shown through comparison of peak moments normalized with respect to the mean values corresponding to a cleanbore tank, respectively. The results show that the peak value of the pitch moment amplification approaches nearly 1.25 times the corresponding mean value for 40% fill condition and $a_x = 0.3g$. The pitch moment amplification factor tends to decrease with increase in the fill volume, while the corresponding mean values increase, as observed for longitudinal slosh forces in Figs. 6.1 and 6.2. Unlike the longitudinal force amplification, pitch moment amplification factor decreases with increase in deceleration magnitude, although the mean moment tends to be higher under higher deceleration. Lower amplification ratio of pitch moment under higher deceleration is partly attributed to higher mean moment, and partly to contributions due to instantaneous coordinates of the mass center and opposing effect of the vertical force, as it is evident in Eq(6.6).

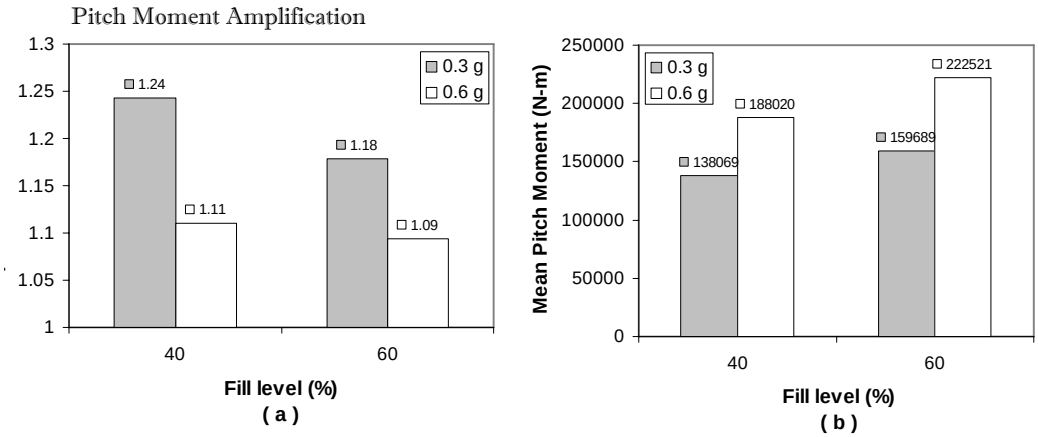

Fig. 6.9: Effect of fill level and magnitude of acceleration on (a) the pitch moment amplification factor and (b) mean pitch moment

Presence of baffles significantly diminishes the peak magnitudes of pitch moment, as illustrated in Fig. 6.10, for 40 and 60% filled tanks subject to $0.3g$ and $0.6g$ longitudinal acceleration fields. The results illustrate that amplification factor reduces to magnitudes less than unity for a baffled tank, irrespective of fill and acceleration level. This is attributed to volume of liquid entrapped within partitions discretized by baffles without an equalizer, which results in relatively smaller displacement of liquid *cg* in a baffled tank when compared to that for a cleanbore tank. The results further suggest that the amplification factor decreases with an increase in acceleration as well as fill level for a cleanbore tank, as shown in Fig. 6.10. This trend, however, is reversed for a baffled tank, which exhibits an increase in amplification factor under higher acceleration and fill level. This is attributed to accumulation of larger liquid volume in the leading section of the tank, caused by imposition of more sever acceleration field.

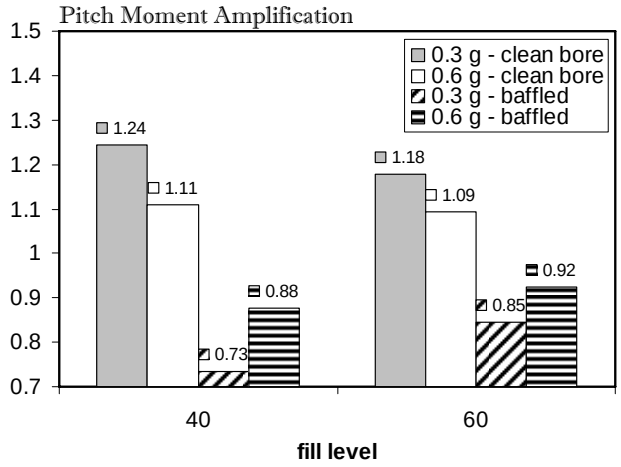

Fig. 6.10: The influence of baffles on pitch moment amplification factor for different fill levels and magnitudes of a_x

The influence of baffles on roll moment amplification (M_{Mx}) of 60% filled tank subject to lateral acceleration alone, and combined longitudinal and lateral accelerations is presented in Fig. 6.11. The results show that roll moment amplification due to fluid slosh in a clean bore tank increases with an increase in magnitude of longitudinal acceleration. Evidently the most significant response amplification is attributed to higher longitudinal acceleration (case C). The results further show that presence of baffles tends to limit the peak roll moment significantly, as observed for the lateral force in Fig. 6.6. The results also show that magnitude of peak roll moment varies only slightly for the baffled tank, when longitudinal acceleration is increased from 0.3 *g* to 0.6 *g*, while the corresponding increase for the cleanbore tank is considerable. A comparison with lateral force amplification suggests that ratio of roll moment amplification to lateral force amplification for the clean bore tank is equal to the tank radius (1.016 m), irrespective of fill level. This is in agreement with that derived from the quasi-static roll-plane formulation, which suggests identical ratio of roll moment to the lateral force, irrespective of fill level and magnitude of lateral acceleration.

The influences of fill condition and longitudinal acceleration magnitude on the roll moment are further shown in Fig. 6.12, for the clean bore tank. The results show that the roll moment amplification factor approaches nearly 1.85 for lower fill level and higher longitudinal acceleration. The higher fill level, however, causes the roll moment amplification factor to decrease, which tends to increase only slightly with increase in magnitude of a_x. This particular trend in roll moment amplification factor was also observed from the two-dimensional analysis under a lateral acceleration [16,25]. The pitch and yaw moment amplification responses due to fluid slosh in the cleanbore tank are shown in Fig. 6.13, as functions of fill level and magnitude of longitudinal acceleration, while a constant lateral acceleration (0.25 *g*) is also applied. The results shown are attained for clean bore tank with 40% and 60% fill levels. An increase in fill level or magnitude of longitudinal acceleration reduces the amplification factors of pitch and yaw moments, as it was observed from the pitch moment under a pure longitudinal acceleration. The yaw moment amplification corresponding to 60% fill, however, forms an exception to this trend, i.e. the moment amplification factor increases with increase in acceleration under higher fill level. The results further reveal that the peaks as well as the corresponding means of

moments increase with an increase in acceleration magnitude, irrespective of the fill level. The variations in these moments are strongly influenced by longitudinal coordinate of the liquid cargo c.g., which is further affected by the geometry of the tank as well as the magnitude of the longitudinal acceleration.

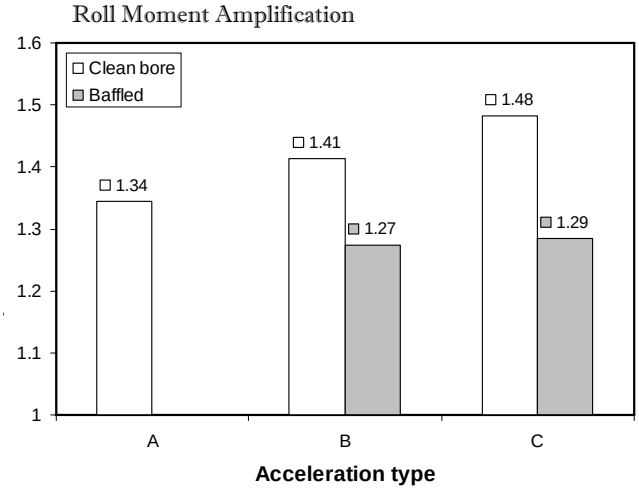

Fig. 6.11**:** The roll moment amplification due to fluid slosh in a cleanbore and baffled tanks: **A** – 0.25 g lateral acceleration, **B**- 0.3g longitudinal and 0.25g lateral acceleration, and **C**- 0.6 g longitudinal and 0.25g lateral acceleration

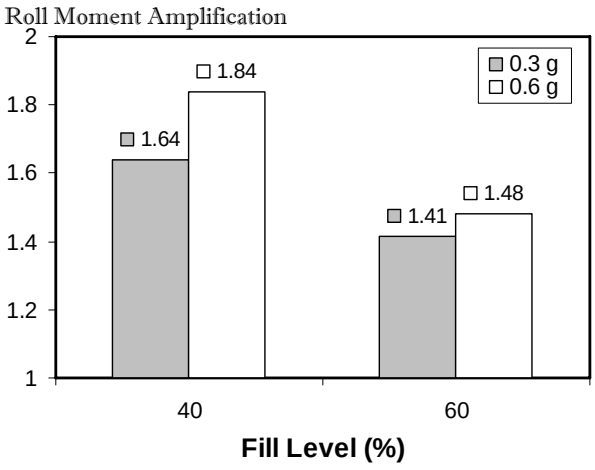

Fig. 6.12: Influence of fill level and longitudinal acceleration on the roll moment amplification (M_{Mx})

Addition of lateral baffles helps suppress peak pitch moment, as shown in Fig. 6.14, for the 60% filled baffled tank. The figure illustrates a comparison of time-history of pitch moment response of baffled tank subject to a_y=0.25g and a_x=0.6g, with the constant quasi-static value for the cleanbore tank. The results suggest that baffles diminish the peak moment and yield lower steady value of pitch moment. The lower steady-state value is attributed to lack of equalizers in baffles,

which causes portion of fluid to be trapped in lower section of tank between two consecutive baffles or between the baffle and end cap. Figure 6.15 illustrates the effectiveness of lateral baffles in suppressing peak pitch, yaw and roll moments under different fill and excitation conditions considered. The results show that an increase in fill level yields lower moment amplification factors for a cleanbore tank, as it was observed for the peak longitudinal force in Fig. 6.3. As evident in the figure, the roll moment amplification factor increases with an increase in acceleration level and decreases when the fill level is increased, for both cleanbore as well as baffled tanks although the baffles clearly help in suppressing the peak roll moment. The results further suggest that the moments invariably increase with an increase in fill or acceleration level for a baffled tank. The presence of baffles suppresses the pitch, yaw as well as the roll moment amplifications considerably. The settling times for moments caused by transient slosh within the baffled tank increases significantly, when compared to those for cleanbore tank, as observed for the lateral force in Fig. 6.5.

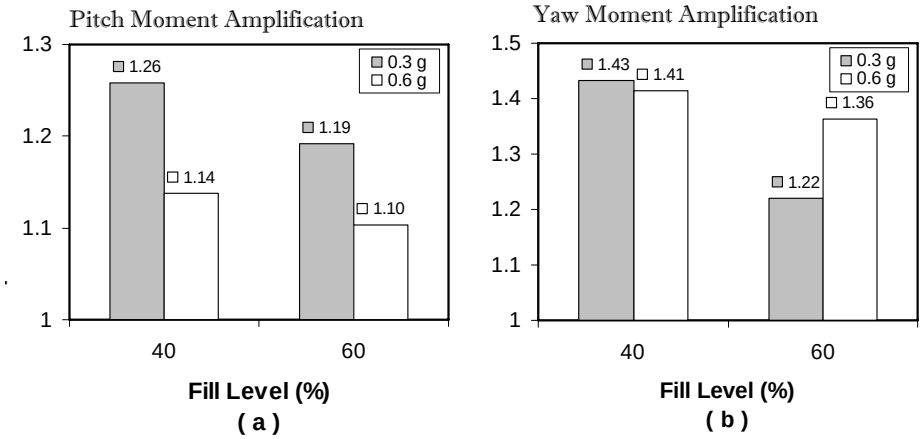

Fig. 6.13: Influence of fill level and deceleration magnitude on the (a) Pitch and (b) Yaw amplification factors in a clean bore tank subject to lateral and longitudinal accelerations

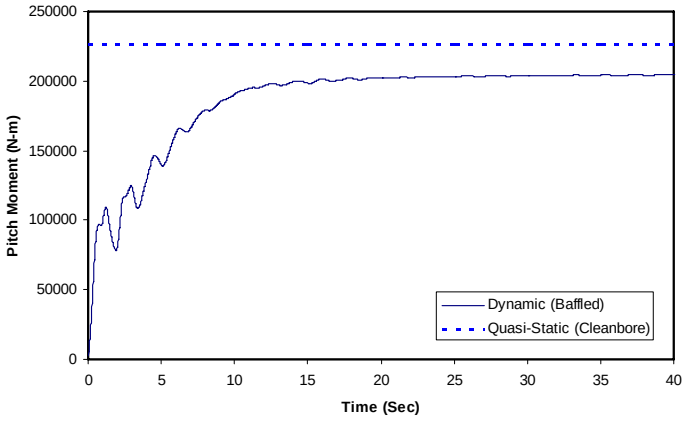

Fig. 6.14**:** Comparison of time histories of pitch moment derived from dynamic slosh and quasi-static solution. (fill -60%; a_y -0.25g and a_x -0.6g)

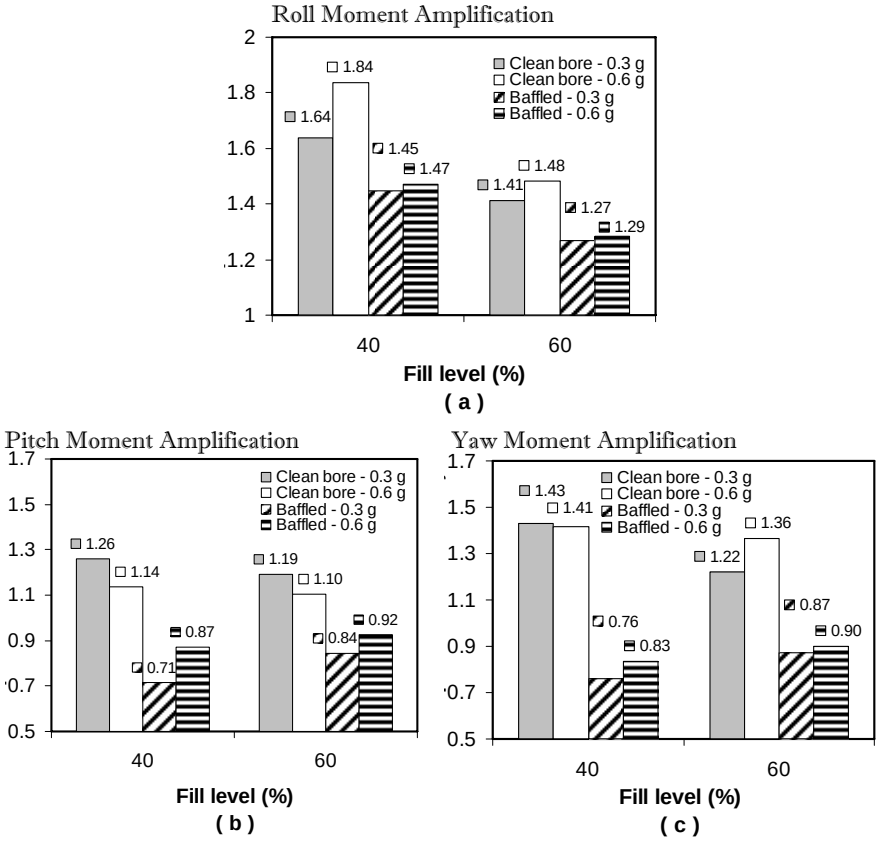

Fig. 6.15: The moment amplification factors due to transient fluid slosh in cleanbore and baffled tanks subject to a_y=0.25 g and two different levels of a_x (a) Roll moment; (b) Pitch moment; (c) Yaw moment

6.3.3 Variations in mass moments of inertia

The directional dynamic responses of a freight vehicle are also influenced by the mass moment of inertia of the cargo, which are time variants when slosh within a partly-filled tank is considered. The application of a pure longitudinal acceleration would not only alter the pitch mass moment of inertia, but also the roll and yaw mass moments of inertia. The mass moments of inertia of sloshing cargo are evaluated about the origin located at the geometric center of the tank, using Eq (5.8). The deviations in peak values in the transient state from the mean or static solutions are evaluated for cleanbore as well as baffled tanks under different fill and excitation conditions considered. The peak pitch mass moment of inertia of the liquid cargo within 40% and 60% filled tanks subjected to 0.3 g and 0.6 g longitudinal accelerations is also obtained as shown in Fig. 6.16. The figure 6.16(a) illustrates the mean values of the pitch mass moment of inertia of fluid within a cleanbore tank subject to two different levels of longitudinal acceleration for the 40% and 60% fill conditions. For the 40% fill condition, the mean value increases with increasing deceleration, but the trend is opposite for 60% fill condition, which may be attributed to increased clustering of fluid towards the leading section of the tank under higher deceleration. The ratio of peak to mean values, the amplification factor, approaches near 1.17 corresponding to 40% fill condition and 0.3 g acceleration, as shown in Fig. 6.16(b). The amplification factor

tends to vary in a nonlinear manner with increasing fill volume and longitudinal deceleration. The variations in amplification factors due to variations in acceleration magnitude are relatively small, particularly for 60% fill condition.

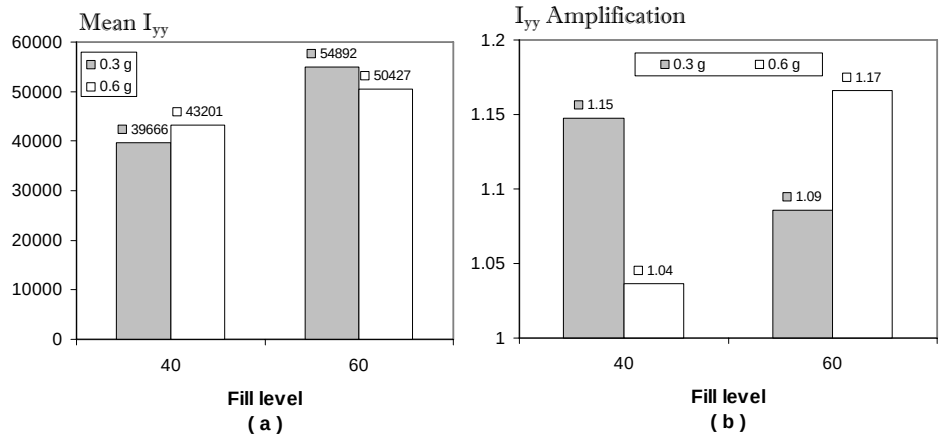

Fig. 6.16: Influence of fill level and magnitude of acceleration on (a) mean and (b) amplification factor of the pitch mass moment of inertia of the liquid cargo

The roll, pitch and yaw mass moments of inertia are further derived under simultaneous applications of lateral and longitudinal accelerations. The effects of fill level and magnitudes of longitudinal and combined longitudinal/lateral accelerations on the roll, pitch and yaw mass moments of inertia amplifications for a clean bore tank are shown in Fig. 6.17. The results obtained under longitudinal acceleration alone suggest that roll mass moment of inertia (I_{xx}) amplification increases slightly with increase in a_x for both fill conditions. Further application of a lateral acceleration (0.25g) tends to alter the amplification factors only slightly, irrespective of the fill condition and magnitude of a_x. The largest I_{xx} amplification in the order of 1.17 occurs for lower fill level under a_y=0.25g and a_x=0.6g. The amplification factors for the pitch and yaw mass moments of inertia under different fill levels and accelerations revealed similar trends. The pitch and yaw mass moments of inertia vary only slightly when a lateral acceleration (0.25g) is applied in addition to the longitudinal accelerations, as shown in Figs. 6.17(b) and (c). Furthermore, both the amplification factors tend to be lower under higher deceleration for the low fill level, but higher for the higher fill level.

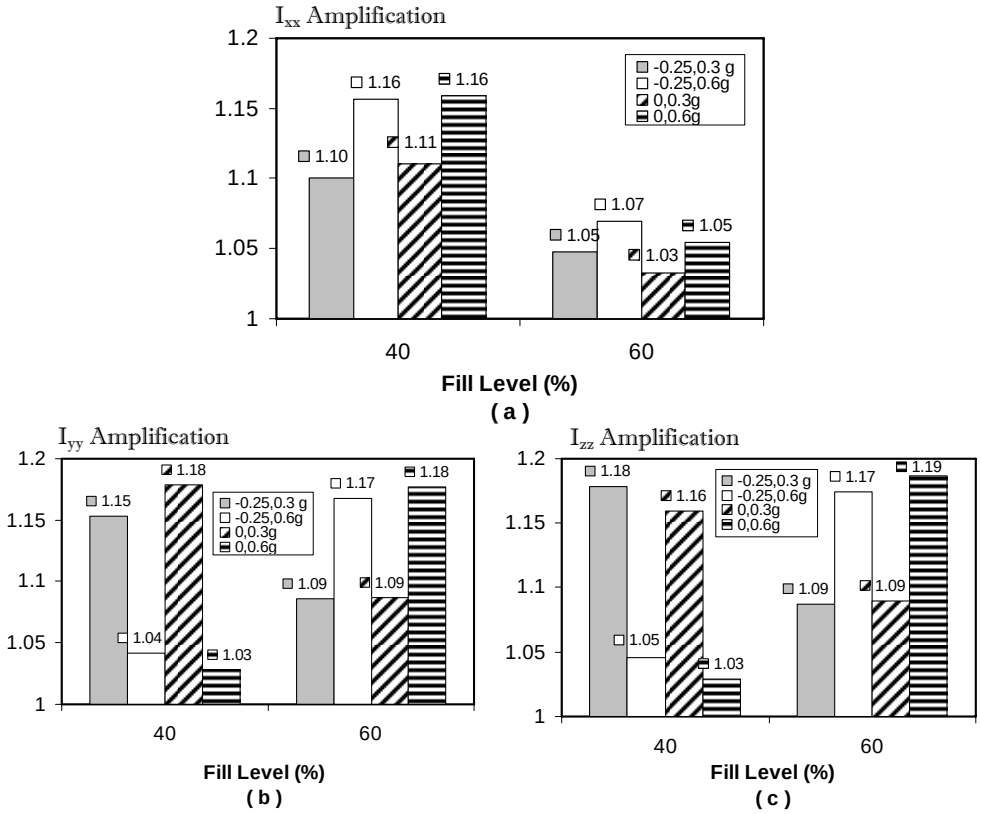

Fig. 6.17: Amplifications factors in mass moments of inertia of fluid in a clean bore tank under different fill levels and acceleration magnitudes: (a) I_{xx}; (b) I_{yy}; and (c) I_{zz}

7 Roll Stability Analysis of a Tank Vehicle

The dynamic fluid slosh can potentially lead to large magnitudes of load shifts, longitudinal and lateral forces, and roll, pitch and yaw moments, during different directional manoeuvres, such as breaking/accelerating, cornering and path changing. The effects of load shift and fluid motion within a partly-filled tank on the roll stability limits of the vehicle have thus far been limited to quasi-static or mean responses [4,19,42]. The results described in previous sections clearly show that magnitudes of dynamic slosh forces are significantly higher than those of the mean responses. Furthermore, the transient magnitudes of slosh forces and moments are considerable larger than the steady-state dynamic values. The roll stability of partly-filled tank vehicles may thus be expected to be lower than that predicted using quasi-static fluid slosh. Moreover, the experimental and simulation results obtained in this study show the presence of three-dimensional flows even under a single axis excitation. This suggests stronger coupling effects of slosh along the lateral and longitudinal directions. Only limited efforts, however, have been made to integrate the dynamic slosh model of a tank to that of a heavy vehicle, to study the impact of dynamic slosh forces on the directional responses of the tank vehicle [42]. This study considered two-dimensional slosh and an off-line coupling of the vehicle with a fluid slosh model.

The dynamic analysis of a partly-filled tank vehicle is a challenging task, since it involves complex coupling of the nonlinear dynamic slosh model of the tank with a three-dimensional model of the articulated vehicle combination. Extreme computational demands of the slosh models coupled with nonlinear vehicle system do not permit for direct analysis of the coupled vehicle-tank system. Furthermore, the magnitudes of slosh forces and moment are strongly dependent upon the tank geometry, fill volume and the severity of the manoeuvre, in a highly nonlinear manner. Considering that the roll stability of a vehicle is closely represented by its steady-turning rollover threshold acceleration, the task of coupling the two elaborate models could be simplified through consideration of roll moment equilibrium of the partly-filled vehicle, and transient slosh force and moment. The magnitudes of slosh force and moment, however, require considerations of the tank cross-section, fill volume and the nature of excitation. Circular cross-section tanks, in general, yield relatively high center of mass of the sprung mass (*cg*) but relatively smaller lateral movement of the *cg* under application of a lateral acceleration field, when compared to a modified oval cross-section tank [4].

In this study, the transient lateral slosh force and roll moment caused by a time-varying lateral acceleration, evaluated using the FLUENT software, are integrated into the roll moment equilibrium of an articulated vehicle to compute the roll stability limits of the partly-filled combination, as functions of fill volume and magnitude of the applied acceleration. The analyses are performed for two different tank geometries: circular and optimal cross-sections. The results attained are compared with those derived from the QS analyses to demonstrate the role of transient slosh loads on the roll stability limits.

7.1 Analyses of Transient Slosh Force and Moment

The validated dynamic slosh model was applied for both the circular and optimal cross-section tanks with various fill conditions. The resulting pressure distributions over the wetted wall were analyzed to compute transient responses in terms of lateral and vertical slosh forces, and roll moment. The instantaneous free surface curvature is used to estimate the coordinates of the cargo *cg*. To make the analysis comparable for both tanks, the cross-section areas of both tanks are set approximately equal to 3.3 m^2. The height and the maximum width of the optimal tank were set equal to 1.88 m and 2.2 m, respectively, and the diameter of the circular tank was set equal to 2.03 m. The domain for the numerical simulations was set equal to the cross-sectional area of the tank. The computational domain was discretized into 3490 cells of quadrilateral shape, for the optimal tank, and 3352 quadrilateral cells for the circular tank. The simulations were performed for 44%, 50% and 80% fill-volumes. For each fill-volume state, simulations were conducted for five different magnitudes of steady lateral accelerations (a_y = 0.1, 0.2, 0.3, 0.4, 0.5g). Two different fluids, water and sulphuric acid, were considered in these simulations. The 50% and 80% fill-volume simulations were conducted with water and 44% fill-volume simulations were carried out with sulphuric acid. It should be noted that cargo loads are approximately the same for 80% volume-filled water and 44% volume-filled sulphuric acid due to the difference in densities of the two fluids. The time steps in the simulation runs varied from 0.001 to 0.01 sec for different values of the lateral accelerations and the fill volume, in order to obtain accurate solutions within a reasonable computational time.

The simulation results were validated for both tanks, by comparing the mean values of the liquid *cg* position with those obtained from the QS model. Figure 7.1 illustrates comparisons of the mean values of vertical and lateral coordinates of the liquid load *cg* (derived from the dynamic fluid slosh), with $\overline{Y}_{cg}$ and $\overline{Z}_{cg}$ computed from the QS model. The results are presented for the optimal tank with 50% fill volume and subject to a_y = 0.1g to 0.5g. An excellent agreement is observed between the results obtained from the two approaches. The maximum difference between these results was observed to be less than 4%. The results attained for the circular tank also revealed similar degree of agreement. These results also provide validation of the mesh size used in the present study. The mean values of the responses obtained from the dynamic slosh model are therefore used to represent the quasi-static estimations for all simulation runs in the study.

7.2 Roll Stability Model of the Vehicle

The roll stability limit of the coupled partly-filled tank and vehicle combination under the influence of transient slosh can be conveniently evaluated by integrating the fluid slosh forces and roll moment, to the moment equilibrium equation for the vehicle. Such an approach would permit for the independent CFD analysis of the partly-filled tank under steady levels of lateral acceleration. The method has been applied to derive analytical solutions for the steady-turning rollover threshold of vehicles with partly-filled circular, modified-oval and elliptical tanks, while considering the QS slosh forces and roll moment [42]. The effect of transient slosh forces and roll moment on the steady-turning rollover threshold of the partly-filled tank vehicle can also be evaluated using the same approach, where the primary overturning moment would be based on the transient responses attained from the dynamic slosh analysis.

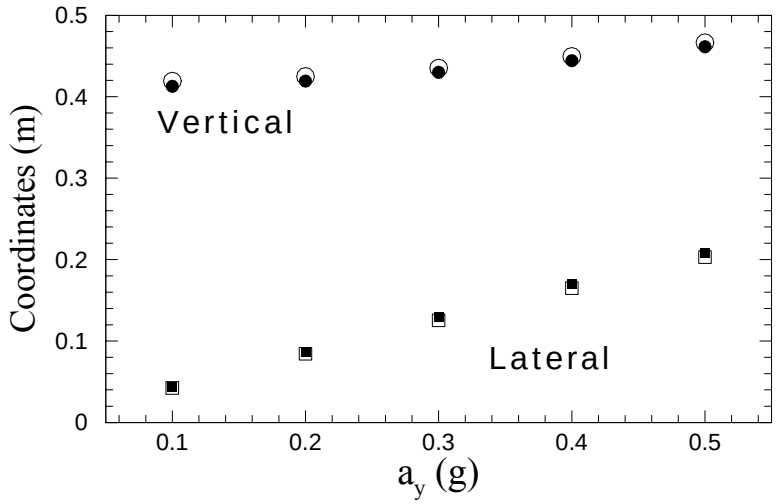

Figure 7.1: Comparisons of mean lateral and vertical *cg* coordinates derived from dynamic slosh model for the optimal tank under 50% fill volume and a_y=0.1g to 0.5g with those estimated from the quasi-static method (Lateral coordinate: ■-mean dynamic, □-QS; vertical coordinate: ●-mean dynamic, ○-QS)

A 6-axle tractor-semitrailer tank combination is considered for investigating the impact of transient slosh behaviour on its rollover threshold acceleration. The vehicle combination comprises a three-axle tank semi-trailer and a three-axle tractor, as shown in Fig. 7.2(a). The groups of semi-trailer and tractor drive axles are lumped together to represent each group by single equivalent axles, assuming similar properties of individual axles within the group. The combination is thus, considered as a three-axle articulated vehicle. The tractor sprung weight is modeled as two rigid masses supported by the front and composite drive axle, while the masses due to semi-trailer structure and liquid cargo are supported by the trailer composite axles, as described in [4]. Each of the sprung and composite unsprung weight is represented in the roll plane, as shown in Fig. 7.2(b).

It is known that the liquid sloshing and suspended tank structure interact in a very complex manner. Owing to the considerable complexities associated with the integration of the dynamic slosh model to the vehicle model, the analysis is simplified by assuming small roll angles and small unsprung weights relative to the sprung weights. The roll moment equilibrium is derived upon consideration of three components for each sprung weight in the roll plane, namely the primary overturning moment (M_{1i}) arising from the centrifugal acceleration, lateral displacement moment (M_{2i}) caused by lateral *cg* translation due to roll deflection of the sprung weight, and restoring moment (M_{3i}) due to the lateral transfer of vertical load from inner to outer tires. Figure 7.3 illustrates the moment equilibrium for a multi-axle articulated vehicle combination [56]. The maximum primary overturning moment arising from the lateral acceleration can be expressed as the sum of the overturning moments due to sprung weights supported by three composite axles. The overturning moment imposed on each composite sprung weight can be derived from:

$$M_{11} = W_1 h_1 a_y^{*}; \quad M_{12} = (W_{2T} h_{2T} + W_{2ST} h_{2ST} + C_{Fy} W_{2L} h_L) a_y^{*} + C_{Fz} W_{2L} Y_L \text{; and}$$

$$M_{13} = (W_{3ST} h_{3ST} + C_{Fy} W_{3L} h_L) a_y^{*} + C_{Fz} W_{3L} Y \tag{7.1}$$

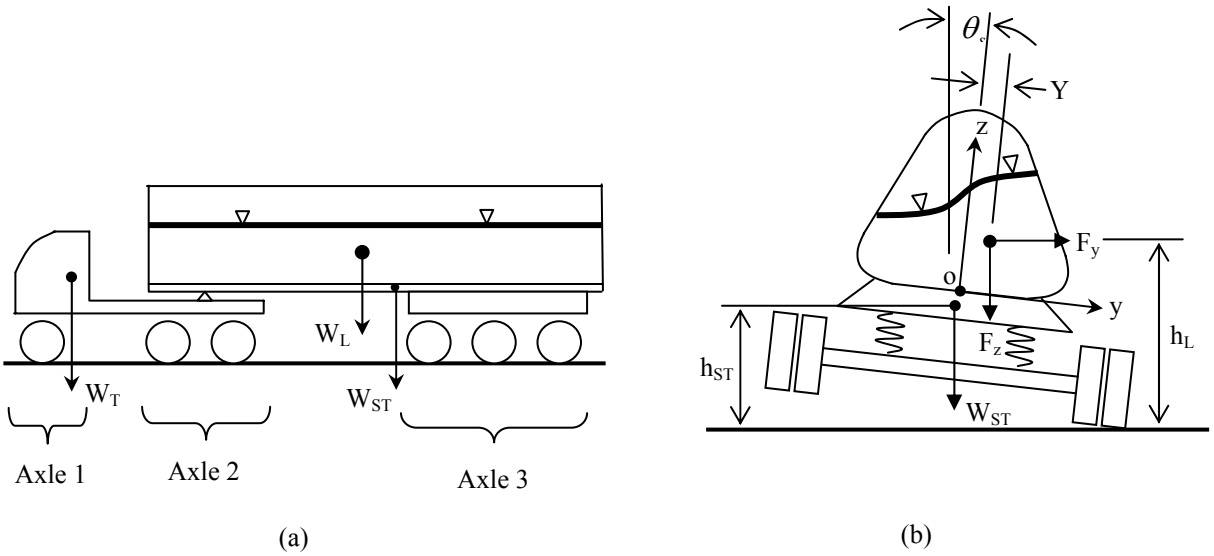

Figure 7.2: Pitch and roll plane representation of a partly filled six-axle tractor semitrailar tank vehicle: (a) pitch plane model; (b) roll plane model.

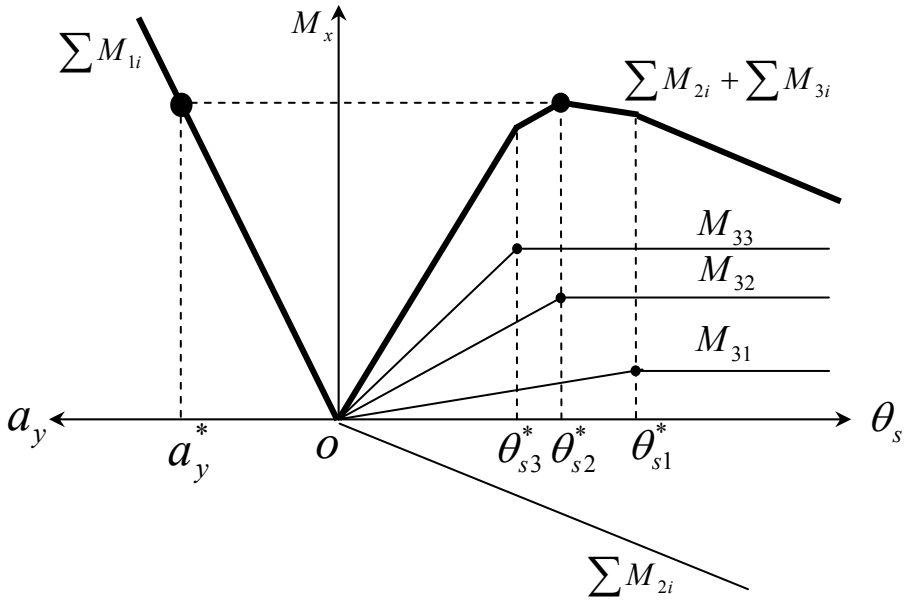

:

Figure 7.3: The roll moment diagram of the three composite axle tank vehicle model

where W_1, W_2 and W_3 are sprung weights supported on composite axles 1, 2 and 3, respectively. The sprung weight W_2 comprises tractor weight supported by the rear axle (W_{2T}), and portions of the rigid tank semitrailer structure weight (W_{2ST}) and the liquid cargo (W_{2L}). The sprung weight W_3 also comprises portions of weights due to tank semitrailer structure (W_{3ST}) and the liquid cargo (W_{3L}), such that $W_2 = W_{2L} + W_{2T} + W_{2ST}$, $W_3 = W_{3L} + W_{3ST}$, and $W_L = W_{2L} + W_{3L}$. The a_y^* is the lateral acceleration corresponding to the relative rollover condition, when primary overturning moment approaches the net restoring moment. h_1, h_{2T}, h_{2ST} and h_{3ST} are the *cg* heights of W_1, W_{2T}, W_{2ST} W_{3ST}, respectively, with respect to the ground. h_L is the vertical coordinate of the liquid cargo *cg*, corresponding to peak roll moment, as derived from Z_{cg} and Y_L is the corresponding lateral coordinate Y_{cg}. Coefficients C_{Fy} and C_{Fz} are used to account for transient lateral and vertical slosh forces, and defined as the ratios of the lateral and vertical sloshing forces at the instant of the maximum roll moment, to the corresponding mean values, respectively, which were referred to as amplification factors.

The roll moment caused by lateral translations of sprung weights (M_{2i}, i=1,2,3), corresponding to relative rollover condition, expressed by lift-off of tires of axles 2 and 3 at roll angles, θ_{s2}^* and θ_{s3}^*, are expressed as:

$$M_{21} = W_1 h_1 \theta_{s2}^*; \quad M_{22} = (W_{2T} h_{2T} + W_{2ST} h_{2ST} + C_{Fz} W_{2L} h_L)\theta_{s2}^*; \text{ and}$$

$$M_{23} = (W_{3ST} h_{3ST} + C_{Fz} W_{3L} h_L)\theta_{s2}^* \tag{7.2}$$

In the above equation, the relative rollover condition is considered to occur, when the tractor rear axle experiences lift off corresponding to angle θ_{s2}^*. At this moment, the restoring moments caused by the composite axle suspension 2 and 3 attain their maximum values of $W_2 T_2$ and $W_3 T_3$, respectively. The restoring moment due to axle 1, however, approaches $W_1 T_1 (\theta_{s2}^* / \theta_{s1}^*)$. The restoring moments (M_{3i}, *i*=1,2,3), may thus be expressed as:

$$M_{31} = -W_1 T_1 \frac{\theta_{s2}^*}{\theta_{s1}^*}; \qquad M_{32} = -W_2 T_2; \text{ and } M_{33} = -W_3 T_3 \tag{7.3}$$

where T_1, T_2, T_3 are the half tire tracks of the three axles, respectively.

The roll moment equilibrium for the combination corresponding to relative rollover condition may be expressed as:

$$\sum M_{1i} + \sum M_{2i} + \sum M_{3i} = 0 \tag{7.4}$$

Upon substituting for the moments from Eqs (7.1), (7.2) and (7.3), the moment equilibrium equation is obtained as:

$$M_t a_y^* + C_{Fz} W_L Y_L = W_3 T_3 + W_2 T_2 + W_1 T_1 \frac{\theta_{S2}^*}{\theta_{S1}^*} - M_t \theta_{s2}^* \tag{7.5}$$

where

$$M_t = W_T h_T + W_{ST} h_{ST} + C_{Fy} W_L h_L \tag{7.6}$$

In the above formulation, Y_L, h_L, C_{Fy} and C_{Fz} are functions of lateral acceleration a_y and fill volume, which are derived from the transient fluid slosh analysis. These functions are expressed as second-order polynomial regressions in a_y for two different fill volumes. Similar regression functions were also identified for 50%-volume filled with water (load = 202 kN), to study the roll stability limit under variable load condition. The roll angles corresponding to wheel lift-off in the above equations are determined from equivalent roll stiffness of tires and the suspension springs (Rakheja and Ranganathan, 1993):

$$\theta_{Si}^{\ *} = W_i T_i \left(\frac{1}{K_{Si}^{\ *}} + \frac{1}{K_{Ti}^{\ *}} \right) - \frac{W_i h_{rci}}{K_{Si}^{\ *}} a_y^{\ *}; \ (i = 1,2,3) \tag{7.7}$$

where $K_{Si}^{\ *}$ and $K_{Ti}^{\ *}$ are the equivalent roll stiffness of i^{th} axle suspension springs and tires, respectively; h_{rci} is the roll center height of the i^{th} axle. The equivalent torsional stiffness of the i^{th} axle suspension springs and tires can be computed, respectively, from:

$$K_{Si}^{\ *} = k_{si} S_i^{\ 2} + K_{\theta i}; \text{ and } K_{Ti}^{\ *} = k_{ti} T_i^{\ 2}, \quad (i = 1,2,3) \tag{7.8}$$

where k_{si} and k_{ti} are the constant vertical stiffness coefficients due to suspension springs and tires, respectively, and $K_{\theta i}$ is the auxiliary roll stiffness of the i^{th} axle, and S_i is half the suspension track. Equations (7.1) thru (7.8) are solved in an iterative manner until a convergent solution of rollover threshold a_y^* is obtained.

7.3 Results and Discussions

7.3.1 Load shift, slosh forces and roll moment

The fluid slosh within partly-filled circular and optimal cross-section tanks were analyzed using the FLUENT software, as described in the previous section. The amplitude of transient slosh can be characterized by the instantaneous values of *cg* coordinates, slosh forces and roll moment as evident from the dynamic responses presented in the previous section. Figure 7.4 illustrates time variation in the lateral and vertical coordinates of the liquid *cg* and the lateral and vertical slosh forces, as derived from the dynamic slosh model, respectively, for 50% volume-filled optimal tank subject to 0.3g lateral acceleration. The results show considerably large variations in the *cg* coordinates and slosh forces, while the oscillatory fluid slosh continues over a long duration with relatively small rate of decay. The figure further illustrates the mean values of the *cg* coordinates and the slosh forces, which are representatives of the results, obtained from the QS model. From the results, it is evident that the magnitudes of dynamic slosh forces are significantly larger than the mean or QS forces. Moreover, such large amplitude forces are imposed on the tank structure and vehicle, for a sustained duration, which could lead to roll instability at acceleration levels well below the rollover threshold limits that are estimated from the QS solution. The results further show that variations in lateral direction are significantly large as compared to those in the vertical direction, suggesting larger lateral load shift under steady acceleration. The dynamic fluid slosh yields nearly 70% higher deviation in the lateral *cg* coordinates, when compared to the QS solution. The corresponding peak-mean difference for the vertical coordinates is in the

order of 10%. The transient peak magnitude of the lateral slosh force approaches nearly 140% of the respective mean value for the 50% volume-filled condition and a_y = 0.3g. The corresponding magnification of the vertical force, however, is relatively small in the order of 106%.

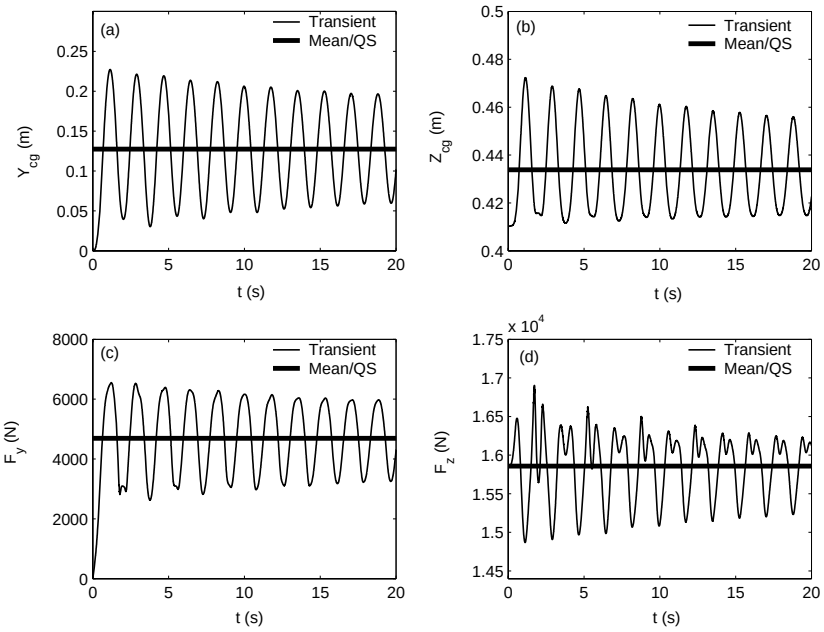

Figure 7.4: Time histories of *cg* coordinates, and lateral and vertical forces for 50% volume-filled optimal tank and a_y= 0.3g: (a) lateral *cg* position; (b) vertical *cg* position; (c) lateral slosh force; (d) vertical slosh force.

Figure 7.5 illustrates roll moment variations under same conditions as derived from dynamic slosh model. The results show large variations in roll moment and relatively small rate of decay of oscillations, as observed for the lateral slosh force response. The peak roll moment is nearly 1.4 times the mean/QS moment, which is sustained over a long period. From the results, it can be concluded that an analysis based on the steady-state (i.e. QS) values substantially undermines the impact of these parameters on the roll stability of the tank vehicles.

The variations in the coordinates of the cargo *cg* serve as the primary measure of slosh phenomenon. The transient deviations of the lateral *cg* coordinates directly relate to the transient lateral load shift, which is more closely related to the relative rollover condition for the heavy vehicles. The variations in *cg* coordinates are thus, considered to describe transient slosh phenomenon under different fill and lateral acceleration conditions. The analyses are performed for both tanks and fill volumes of 44% (sulphuric acid) and 80% (water), which provided comparable cargo loads of approximately 317 kN and 323 kN, respectively, for the circular and optimal tanks. Figures 7.6 and 7.7 present the mean and peak values of the lateral and vertical *cg* coordinates for the circular and optimal tanks. The results, as expected, show smaller amplitude of sloshing under higher fill volume or less severe lateral excitation. The circular tank is observed to exhibit larger *cg* translations than the optimal tank in almost all cases, except for lateral translations under smaller fill volume (44%). The lower mean and peak values of vertical

cg coordinate of optimal tank are attributed to its wider bottom design [4]. The lower values of the lateral coordinate under a higher fill volume are due to its narrower width in the upper half. The results clearly show that amplitude of fluid slosh can be considerably reduced by the optimal cross-section tank for fill volumes in excess of 50%. The amplitude or severity of transient fluid slosh can be further assessed in terms of the ratio of maximum to mean values of the coordinates. This ratio could reach as high as 1.83 for the lateral *cg* translation, and 1.25 for the vertical *cg* translation for the 44% sulphuric acid filled optimal tank. The highest values of this ratio for the circular tank in this situation are 1.88 and 1.18, respectively.

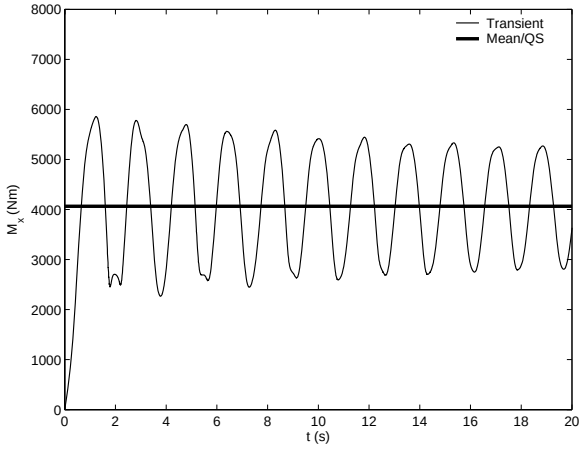

Fig. 7.5: The time history of the roll moment of the liquid cargo sloshing within the 50% volume-filled optimal tank under a_y= 0.3g

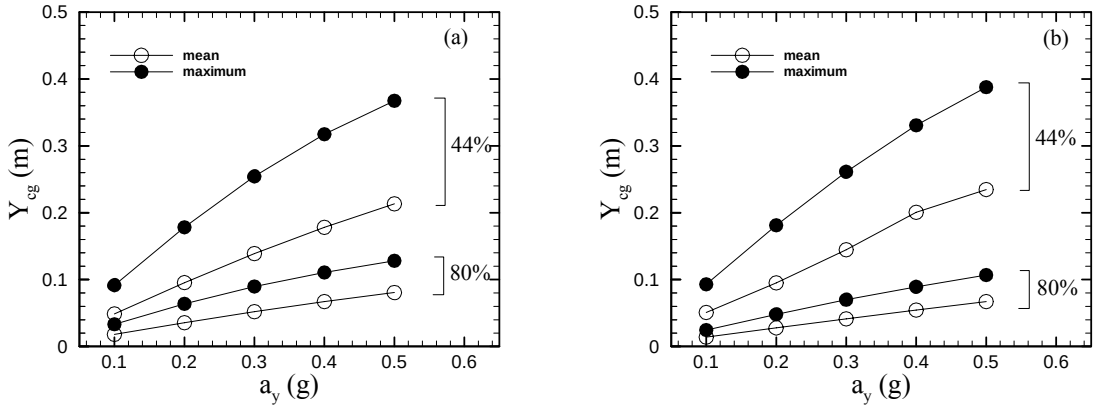

Fig. 7.6: Mean and maximum values of lateral *cg* coordinates of liquid cargo in partly filled optimal and circular tanks: (a) circular tank; (b) optimal tank

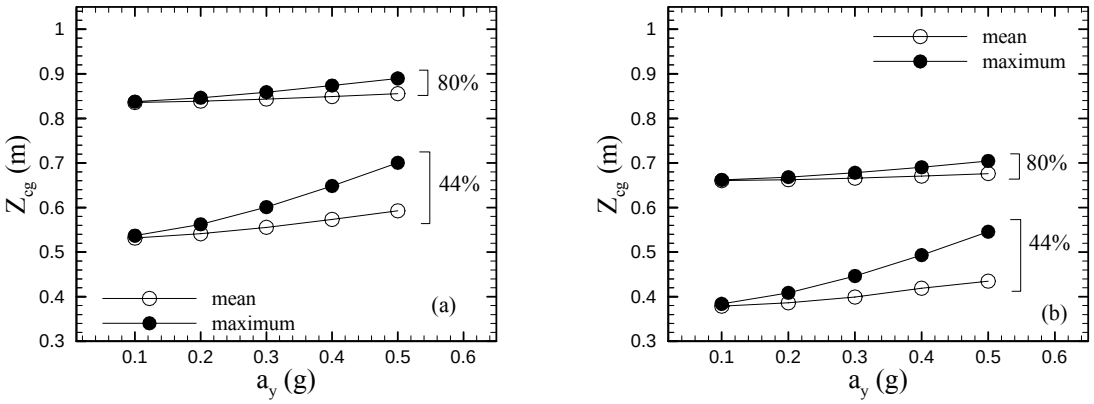

Fig. 7.7: Mean and maximum values of vertical *cg* coordinates of liquid cargo in partly filled optimal and circular tanks: (a) circular tank; (b) optimal tank

The sloshing phenomenon is also characterized by the unsteady lateral sloshing forces generated due to the impact of liquid motion on the tank walls. The magnitudes of slosh forces depend on lateral acceleration, fill volume and tank shape. Figure 7.8 shows the dependence of lateral sloshing force (F_y) on lateral acceleration, fill volume and tank shape. For the circular tank, the mean lateral force does not vary with fill volume, but increases linearly with magnitude of lateral acceleration. The mean/QS lateral slosh force under 44% fill, however, tends to be slightly higher for the optimal tank. The amplification of lateral force increases with decrease in the fill volume, suggesting that the uncertainty associated with the QS model increases as the fill volume decreases. The level of this uncertainty for the circular tank tends to be higher for acceleration levels less than or equal to 0.4g, except for 44% fill volume and the maximum acceleration. The peak lateral force exhibits a rapid change as a_y increases from 0.4g to 0.5g for optimal tank, which may be caused by the occurrence of free-surface separation.

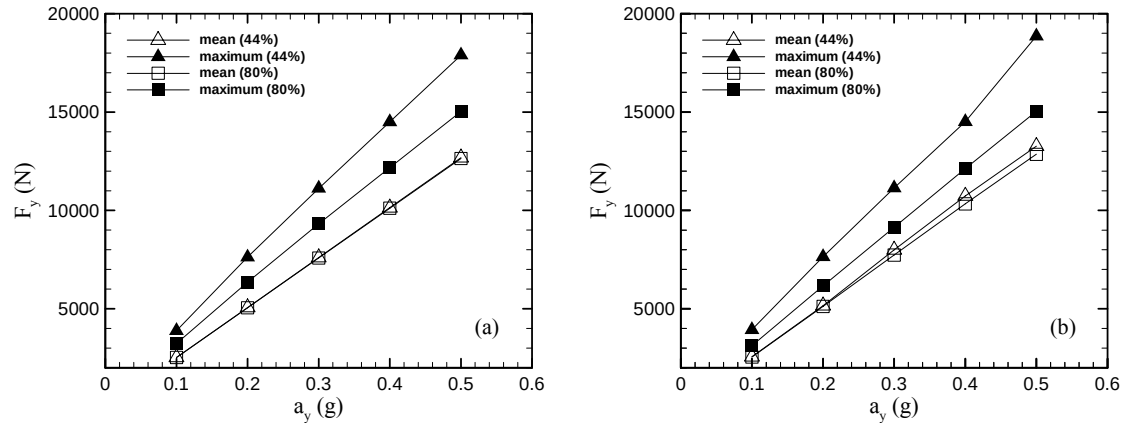

Fig. 7.8: The mean and maximum lateral slosh force as a function of lateral acceleration and fill volume: (a) circular tank; (b) optimal tank

The corresponding peak and mean magnitudes of vertical slosh forces for both tanks are illustrated in Fig. 7.9. The magnitudes of peak as well as mean vertical slosh forces are considerably lower for the circular tank, irrespective of the fill condition and lateral acceleration. The peak magnitudes increase with increase in the acceleration level, while the rate of increase is significantly higher for the optimal tank. It should be noted that the payload for the optimal tank considered is 1.9% higher than the circular tank. Consequently, the mean vertical force for the optimal tank tends to be slightly higher for the 80% fill volume, as evident in Figure 7.9(b). The results further show slight difference, in the order of 2.2%, between the mean vertical forces corresponding to 44% and 80% fill volumes. This difference is attributed to relatively coarse meshing used in the wider bottom relative to the narrow top, and the treatment of partly-filled cells and round-off errors within the Fluent platform.

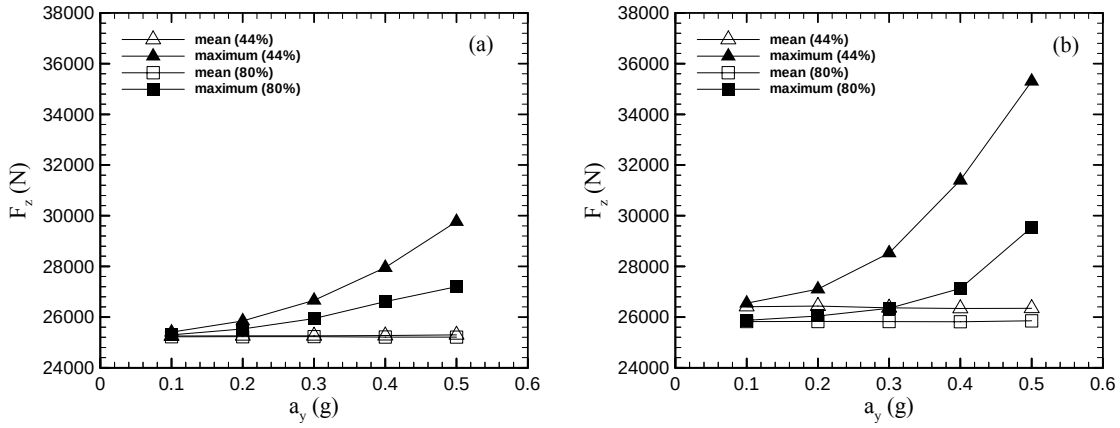

Fig. 7.9: The mean and maximum vertical slosh force as a function of lateral acceleration and fill volume: (a) circular tank; (b) optimal tank

Roll moment is the most significant measure that directly determines the roll stability. It reflects the combined effects of slosh forces, *cg* translation, and tank shape on roll stability. Figure 7.10 illustrates the maximum transient and mean/QS values of the roll moment for both tanks under same fill conditions and lateral acceleration levels. The figure shows that the slosh forces within the partly-filled circular tank generate higher mean as well as peak roll moment than the optimal tank. For the constant cargo load considered in the study, a lower fill volume yields significantly higher peak roll moment, while the optimal tank yields considerably lower roll moment than the circular tank. The circular tank yields identical roll moment for both fill conditions, while the optimal tank causes higher mean roll moment for lower fill (44%). The magnitudes of mean roll moment of the optimal tank, however, remain below those of the circular tank for the entire range of lateral acceleration considered.

7.3.1 Roll stability limits

The influence of transient slosh forces on vehicle roll stability was investigated by solving the moment equilibrium Equation (7.5), which incorporates the regression function in coordinates of liquid mass centre, and amplification factors of vertical and lateral slosh forces, derived from the

dynamic slosh analyses. Considering the phase differences between slosh forces, and the lateral and vertical coordinates of cargo *cg*, the peak values of these variables are not considered in the analysis. The results obtained from the fluid slosh analysis are evaluated to identify the instance of peak roll moment corresponding to each tank, fill volume and lateral acceleration combination. The coordinates of the cargo, vertical and lateral slosh force amplification factors, corresponding to the same instance are then integrated into the moment equilibrium equation to compute the rollover threshold acceleration under the influence of transient fluid slosh. The analyses are performed for two loading conditions: (i) approximately constant payload but varying fill volume (44% volume of sulphuric acid and 80% volume of water), which resulted in payloads of 323 kN and 317 kN for the optimal and circular tanks, respectively; (ii) variable cargo load (50% and 80% volume filled with water), where the 50% fill condition resulted in payload of 202 kN. The analyses are also performed on the basis of QS analysis of the fluid, and rigid cargo with identical load and cg height. The results are compared to demonstrate the effect of transient fluid slosh. The vehicle parameters used in the analyses are summarized in Table 7.1.

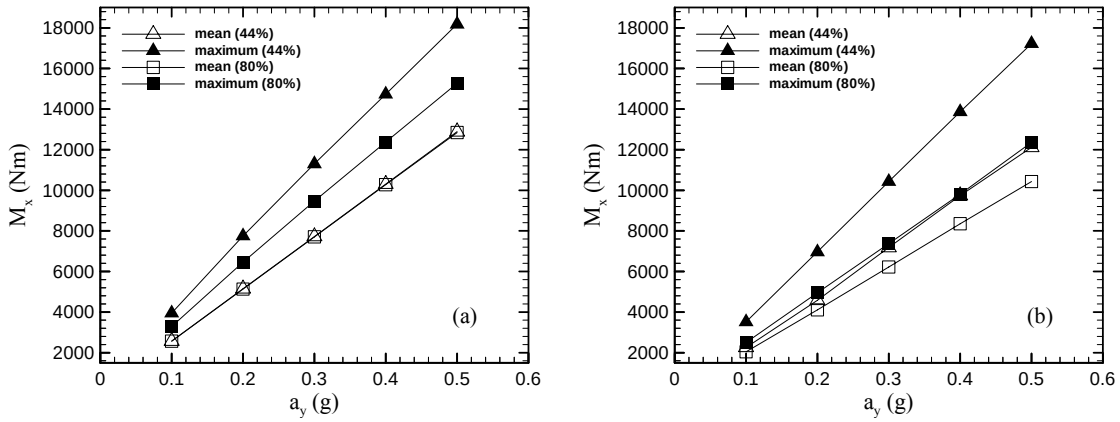

Fig. 7.10: The mean and maximum roll moment about the tank base as a function of lateral acceleration and fill volume: (a) circular tank; (b) optimal tank

Table 7.1: Simulation parameters

Tractor (three axles)		**Semitrailer (tri-axle)**	
Tractor weight (kN)	85.4	Trailer and tare tank weight (kN)	80.1
Wheelbase (m)	6.20	Wheelbase (m)	9.8
Front axle suspension stiffness (kN/m)	289.5	Tank length (m)	12.5
Rear axle suspension stiffness (kN/m)	700.7	Tanks cross-section area (m^2)	3.30
Auxiliary roll stiffness- rear axle (kNm/rad)	514.5	Auxiliary roll stiffness (kNm/rad)	514.5
Tire vertical stiffness (kN/m)	948.3	Suspension stiffness (each axle, kN/m)	70.1

The sloshing effects on roll instability were investigated in two aspects: same cargo liquid (variable fill level) but different cargo loads; and same cargo load but different cargo liquids (constant fill level). The first case was simulated by 50% and 80% tank volume filled with water, and the second case was realized by loading the tanks with 44% and 80% fill volumes of sulphuric acid and water, respectively. The rollover threshold, a_y^* was computed for both cases, considering different tank shapes (circular and optimal), and different liquid states, i.e. the transient maximum (based on the transient maximum roll moment), the average (based on the average value of the liquid cargo *cg* variations, which is equivalent to the steady-state behaviour in the quasi-static model), and additionally, considering the liquid cargo to be rigid.

Table 7.2 summarizes the rollover threshold acceleration for both tanks and loading conditions corresponding to equivalent rigid cargos, and liquid cargoes using mean/QS and peak transient slosh forces. For the same fill-volume, cargo load and tank shape, the rollover threshold is highest for the rigid cargo (as expected), which is followed by the limits attained from mean/QS analysis, while the consideration of peak transient forces yields lowest values of lateral acceleration threshold, irrespective of the tank geometry. These results clearly indicate that the quasi-static model underestimates the rollover threshold, when transient slosh forces are considered. This is mainly attributed to the lack of consideration of transient forces that are significantly large especially during the first few seconds of a maneuver. As shown previously in Fig. 7.5, the transient roll moment could be up to 40% larger than the mean roll moment under a maneuver-induced steady acceleration of 0.3g. Therefore, the rollover threshold based on the mean or quasi-static condition could be considered as an underestimate of the rollover risk, especially during the first few seconds of the maneuver. The results show that differences between the rollover thresholds predicted from QS and transient slosh approach as large as 30% and 24%, respectively, for circular and optimal tanks, when both tanks contain 44% fill-volume of sulphuric acid. These differences reduce to 15% and 19%, respectively, for the 80% fill volume. This indicates that the underestimation of the roll stability limit by the QS model is larger when the sloshing amplitude is larger. Comparisons of results attained for transient slosh and rigid cargo cases suggests that the rollover threshold under transient slosh could be as low as 55% of the equivalent rigid cargo vehicle under medium fill volume (44%), and 78% under larger fill volume (80%).

Table 7.2:Rollover threshold accelerations of the 6-axle tractor-semitrailer tank vehicle with circular and optimal tanks carrying different liquid cargos with different fill volumes

Cargo	Density (kg/m^3)	Fill level (%)	Cargo load (kN)	Tank	Rollover Threshold acceleration		
					Rigid load	Liquid Load	
						Mean/QS	Transient
Sulphuric acid	1826	44	323	Optimal	0.44	0.35	0.24
				Circular	0.40	0.32	0.25
Water	980	50	202	Optimal	0.46	0.39	0.29
				Circular	0.43	0.37	0.27
		80	323	Optimal	0.37	0.35	0.29
				Circular	0.34	0.31	0.25

The results further show that the optimal tank yields higher rollover threshold values under all fill conditions. The gain however is greater for higher fill condition of 80% in the order of 13%, when steady-state load shift is considered, and 16% when transient slosh is considered. The corresponding gains corresponding to 50% fill are in the order of 55 and 7%. The optimal tank could thus yield greater improvement in lateral stability under higher fill volumes. Lower fill volumes in an optimal tank, however, could yield greater transient slosh forces due to its wider bottom, as it is evident for the 44% fill volume of sulphuric acid, when compared to those of the circular tank. This is also in agreement with the results reported in [4]. Although the optimal tank yields larger lateral cargo *cg* shift and higher vertical slosh force under lower fill volume (44%), these adverse factors do not lead to any disadvantage in terms of the rollover threshold as compared to that for the circular tank. This is attributed to the lower *cg* height of the wide bottom optimal tank and smaller lateral slosh force due to its narrower top. The results attained under variable loading condition (50% and 80% volume of water) show similar trends with respect to the effect of transient slosh forces, although the effect is far more pronounced for the 50% volume condition, despite the lower associated load. Under the influence of peak transient slosh, the rollover threshold of the 50% volume filled optimal tank is 10% higher than that of the circular tank. The results that this particular fill condition yields considerable higher threshold values for both tanks are attributed to relatively smaller load. This gain in rollover threshold, however, is not evident, when transient fluid slosh is considered; suggesting that the fluid slosh would be the major contributory factor. The results also show that a lower fill volume (44% sulphuric acid) yields lower threshold values than the 80% fill volume of water, when transient slosh is considered. This trend, however, is not evident from the results attained from the mean/QS slosh. This is attributed to more severe sloshing under 44% fill volume, as illustrated in Figs. 7.6 to 7.10. Analysis of peak slosh forces developed in circular and optimal tanks also revealed similar trends. The amplification factors in lateral and longitudinal forces under combined lateral and longitudinal accelerations were observed to be lower for the optimal tank than the circular tank for higher fill volumes (above 60%). Lower fill volumes, however, resulted in relatively small gains for the optimal tank. For the 40% fill condition, both the tanks resulted in comparable amplification factors.

8. CONCLUSIONS

The reported studies have clearly established that magnitudes of transient as well as steady-state forces and moments associated with fluid slosh within partly-filled tanks are significantly higher than those reported for tank vehicles on the basis of quasi-static formulations. Moreover, the fundamental slosh frequency tends to decrease with lower fill volumes and may approach the steering frequencies. On the basis of review of reported studies, it was concluded that far more efforts are desirable in study of fluid slosh within partly-filled tanks, particularly on the analyses of three-dimensional flows, relative significance of transient and steady-state slosh forces, and roles of baffles. Moreover, relatively larger sizes of laboratory tanks of representative geometry were considered vital for such studies and for validations of computational fluid dynamics models. In this study, test tanks with circular and optimal cross-sections were designed with different baffles to investigate the dynamic slosh behaviors under partial fill conditions and various excitations. The tank simulator designed in the laboratory permitted for measurements of transient slosh forces and moments and synthesis of transient as well as steady-state excitations. The experiments performed with the simulator revealed complex flow and vibration phenomena associated with fluid slosh. The measured forces and moments revealed presence of a number of frequency contents, apart from the excitation and primary resonant frequencies. It featured the beating phenomenon and swirling motion of free surface when external excitation occurred in the vicinity of resonance. The resulting dynamic slosh motion could yield large amplifications in forces and moments imposed on the tank structure and the vehicle. These results further suggested that the directional control and stability limits of partly-filled tank vehicles could be lower than those predicted from the currently used quasi-static slosh formulations. The presence of baffles showed an effective control of this amplification of forces and moments.

A number of conclusions could be drawn from the analyses of measured data coupled with flow visualizations, which are summarized below:

- Fundamental natural frequency of fluid slosh is dependent on fill level, tank geometry, tank configuration (baffled or un-baffled) and magnitude of excitation. This frequency, in both lateral and longitudinal modes, increases with fill level. The addition of transverse baffles yields considerably higher slosh frequencies, distant from the expected steering frequency. Further studies are needed to examine the fundamental frequencies of baffled tanks that may lie in the vicinity of roll mode frequency of the vehicle.

- The measured slosh frequencies and moments clearly showed a beating phenomenon as excitation frequency approached the natural frequency of slosh. The results revealed presence of extremely low frequency component in slosh forces and magnitudes, suggesting that dynamic load shift caused by fluid slosh could be far greater.

- The steady-state fluid slosh under harmonic excitations revealed several spectral components. The lateral and longitudinal fluid slosh occurred primarily near the excitation frequency, while the variations in vertical frequency occurred at a frequency twice the excitation frequency. This is attributed to the wave effect, and would impose greater variations in the suspension and tire loads of the vehicle, which has not yet been identified in published studies.

- The measured data showed high significance of transient slosh forces and moments, observed in terms of amplification factors, the ratio of peak force or moment with respect to the mean value. The amplification factors decreased with higher fill volume and excitation due to boundary effects. The significance of transient slosh was far more evident in moments than the contributing forces. The amplification factors in lateral force and roll moment could approach as high as 2 under certain fill conditions, suggesting potentially lower roll stability limits when transient fluid slosh is considered.

- The fluid slosh under excitations in the vicinity of resonance revealed a strong three-dimensional motion of the free surface for both the baffled and un-baffled tank configurations, suggesting stronger coupling between the lateral and longitudinal forces.

- The transverse single- and multiple-orifice baffles play very effective role in damping of the fluid slosh and thus the resulting longitudinal force and pitch moment. The coupling between the lateral and longitudinal modes can also lead to beneficial effect of baffles on the roll moment.

From the experimental results, it was further concluded that further efforts in exploring alternate designs of baffles and anti-slosh devices are extremely vital for enhancing the stability limits of partly-filled tank trucks. The simulator designed in this study could serve as an effective tool for assessing effectiveness of alternate design concepts in baffles and anti-slosh mechanisms, and tank geometry.

From analysis of the slosh dynamic model of a partly-filled tank, it was established that volume of fluid (VOF) slosh model is capable of predicting the two- and three-dimensional slosh in the un-baffled and baffled tanks subject to excitations along lateral, longitudinal, and lateral and longitudinal axes. The tank equipped with multiple-orifice baffles, however, would require a much finer mesh. Both wedge and hexahedral grid cells would be adequate for analyses of dynamic slosh under transient as well as steady-state excitations. The results obtained for the optimal cross-section test tank under various excitations and fill volumes were compared with the measured data to demonstrate the validity of the models. The model validity under different excitations was particularly emphasized due to nonlinear nature of slosh and lack of such results in published studies. The results were also analyzed to derive fundamental slosh frequencies, which were further compared with those estimated from experimental data. The model results in-general showed very good agreements with the measured data for all the fill conditions and excitations considered. From the results it was thus concluded that the three-dimensional dynamic fluid slosh model developed in this study could be effectively applied to study the role of baffles and significance of transient slosh on the vehicle behavior.

The dynamic forces and moments caused by fluid slosh within a full-size horizontal tank subject to lateral, longitudinal and combined lateral/longitudinal accelerations were investigated using the validated nonlinear three-dimensional model. The results confirmed that the dynamic fluid slosh yields significantly higher magnitudes of transient forces and moments, when compared to those derived from the quasi-static or steady-state analyses, and could thus cause substantially poor directional performance. The mean values of dynamic forces and moments attained for the cleanbore tanks, however, correlated well with those derived from quasi-static solutions. It was thus concluded that tank-vehicle analyses, invariably based upon the kineto-static formulations,

could be considered valid only for steady-state conditions. Moreover, kineto-static formulations could not be applied for analyses of baffled tanks.

The results attained from the dynamic slosh analyses suggested that peak longitudinal slosh force for the cleanbore tank could approach nearly 2 times the quasi-static force for low fill condition (40%) and longitudinal acceleration of 0.6*g*. The addition of lateral baffles tended to limit this peak force amplification to 1.3 compared to 1.96 for a cleanbore tank under same conditions. The results further suggested that the pitch moment amplification is reduced to about 0.7 for the baffled tank, compared to 1.24 for a cleanbore tank. Simultaneous application of lateral and longitudinal accelerations resulted in higher peak forces and moments, which may further degrade the roll stability and braking characteristics of a partly-filled tank vehicle. The roll moment amplification factor approached 1.85, which was larger than that attained under a lateral acceleration alone (1.6). The addition of lateral baffles also resulted in reduced roll moment amplification to 1.47, suggesting that baffles can also help improve the roll stability of the vehicle apart from limiting the longitudinal slosh under a braking maneuver. The relatively large tank length generally results in considerably lower frequency of slosh in the pitch plane of a clean bore tank, in the order of 0.23 Hz. This would also yield large magnitude of longitudinal force amplification of nearly 2, for 40% filled cleanbore tank under a higher longitudinal acceleration. The peak longitudinal slosh force, and pitch and roll moments could be considerably suppressed through addition of lateral baffles, while the fundamental slosh frequency in the pitch and roll plane is considerably increased. The amplification factors of mass moments of inertia of liquid were also influenced by the magnitude of longitudinal acceleration, especially when both lateral and longitudinal accelerations are applied simultaneously. However, the deviations in the mass moments of inertia with respect to the corresponding mean values were generally small for the conditions considered.

Sloshing phenomenon induced inside a partially loaded tank subject to a steady lateral acceleration was also characterized by variable *cg* translation of the cargo and unsteady slosh forces, and consequently the variable roll moment by considering the partly-filled optimal tank with a six-axle tractor-semitrailer vehicle. The results revealed a considerably high ratio of transient maximum to mean values of lateral cargo *cg* shift and lateral sloshing force. Comparisons of results with those derived from the quasi-static method revealed that quasi-sttaic approach could be considered acceptable for cases involving high fill volume and low lateral excitation, where the magnitude of transient fluid slosh is relatively small. Owing to relatively small influence of fluid viscosity, the transient fluid slosh forces were observed to occur over a sustained period of time, thereby, the effect cannot be neglected for roll stability analysis of a partially filled tank truck subject to moderate or high lateral acceleration during steady turning. The simulation results revealed that the optimal tank exhibits smaller vertical *cg* translation and lateral slosh force, when compared to the circular tank. In terms of lateral *cg* translation and vertical slosh force, however, the former was found to be slightly inferior to the latter. The roll dynamic response of a partly-filled tank truck, however, relies more on roll moment caused by fluid slosh. The analyses of roll moment showed that the optimal tank is more superior to the circular one, and thus, yields higher rollover threshold, under the influence of transient slosh forces, although the results were comparable for both under 44% fill condition.

The results of the integrated slosh model and roll-plane vehicle model confirmed that partially filled liquid cargo tank trucks have much lower rollover threshold than rigid cargo trucks. The stability limits were generally lower than those established from quasi-static slosh, when transient slosh effect was considered. Under identical cargo load, a lower fill volume, despite its lower *cg* height, resulted in lower threshold acceleration, which suggested that the fluid slosh is a major contributory factor in view of roll stability of partly-filled tank trucks. This trend was not as evident when quasi-static analysis was considered. Under variable load conditions, a lower fill volume resulted in threshold limits comparable with those attained for higher fill volume. Considering that the *cg* height and cargo load associated with low fill volume are considerably lower, the results further attest to high significance of transient fluid slosh effects on the roll stability of vehicles.

The results gained from this study suggest that far more efforts are desirable in enhancing our knowledge on dynamic fluid slosh forces and moments, which would help realize more effective designs of baffles and anti-slosh devices. The tank simulator developed in this study could serve as a vital tool for assessment of fluid slosh within tanks of different geometry and effectiveness of various designs of baffles.

A few studies have suggested the use of longitudinal baffles to limit the lateral slosh forces. Such baffles, however, cannot be considered feasible due to the added excessive weight and material cost of the long baffles. Alternatively, different concepts in inclined or conical baffles need to be investigated to attain resistance to both lateral and longitudinal fluid slosh under barking and turning maneuvers. Moreover, partial baffle concepts should also be investigated to reduce the weight and thus the cost of the tank. Such baffles may provide adequate performance, particularly when the fill level is in the order of 50% or more, since the violent free surface slosh would occur mostly in the upper half of the tank cross-section. Some of these baffle concepts are illustrated in Annexe C.

It should also be emphasized that the proposed optimal configuration yields considerable lower cg height and would thus yield considerable gains in enhancing the vehicle stability in the yaw and roll planes, irrespective of the fill condition. From the previous study, it was shown that ‘OPT2’ design yields cg height of 0.84 m under 100% fill condition, which is considerably lower than 1.015 m for the circular tank of identical capacity. This cg height is comparable to that of a modified oval tank of identical capacity, while the wider design of modified-oval cross-section (2.44 m) yields significantly larger lateral load shift compared to that of the ‘OPT2’ design (maximum width = 2.14 m) under most of the fill conditions. It was thus shown that ‘OPT2’ design could lead to considerable greater roll stability under fill volumes larger than 70%, while the ‘OPT1’ design was considered more suitable for fills up to 60%.

The optimal design comprises 8 circular arcs similar to the modified-oval design, although the optimal design is asymmetric about the lateral axis, as it was deduced from the earlier project. Preliminary discussions held with potential manufacturers, in the course of the earlier study, suggested that the optima design would be feasible in view of manufacturing. A detailed stress analysis of the tank, however, would be vital to ensure the containability of the tank. It is thus suggested that a thorough stress analysis of the tank design be undertaken prior to further explorations in manufacturing feasibility.

REFERENCES

1. Ervin, R. D., *The Dependence of Truck Roll Stability on Size and Weight Variables*, Int. J. of Vehicle Design, Special Issue on Vehicle Safety, pp. 192-208, 1986.

2. Heglund, R. E., *Truck Safety - An Agenda for the Future*, SAE Publication No. P-181, pp. 154-159, 1986.

3. Mayenburg, M., Rossow, G. and Patterson, C., *Truck Safety Technology for the 21st Century*, SAE Paper No. 952260, 1995.

4. Rakheja, S. et al., *Évaluation de la problématique reliée à l'instabilité en roulement des véhicules routiers de type citerne, transportant des produits liquides*, Final Report, NATEQ/MTQ, August 2003.

5. Department of Transportation (DOT), *Cargo Tank Incident Report*, Hazardous Material Incident Report, 1983.

6. Sampson, D J M and Cebon, D., *Achievable roll stability of heavy road vehicles*, Proc. of the Inst. of Mechanical Engineers, Part D: Journal of Automobile Engineering, 217(4), pp 269-287, 2003.

7. Bauer, H. F., *Dynamic Behavior of an Elastic Separating Wall in Vehicle Containers: Part 1*, Int. J. Vehicle Design, Vol.2, No. 1, pp. 45-77, 1981.

8. Rakheja, S., Stiharu, I., Kang, X. and Romero, J.A., *Influence of road friction and tank cross-section on directional response of a prtly-filled tank truck under braking-in-a-turn*, Int. J. of Heavy Vehicle Systems, 9(3), 2002:223-240.

9. Goldman,R.W., El-Gindy, M. and Kulakowski, B.T., *Rollover dynamics of road vehicles: literature survey*, Int. J. of Heavy Vehicle Systems, 8(2), 2001:103-141.

10. Aliabadi, Shahrouz, Johnson, Andrew and Abedi, Jalal, *Comparison of finite element and pendulum models for simulation of sloshing*, Computers and Fluids, 32(4), 2003: 535-545.

11. Abramson, H. N., *The Dynamic Behavior of Liquids in Moving Containers*, NASA SP-106, 1966.

12. Sheu,T. W. H. and Lee, S. M., *Large-amplitude sloshing in an oil tanker with baffle-plate / drilled holes*, Int. J. of Computational Fluid Dynamics, 1998,vol. 10: 45-60.

13. Komatsu, K., *Non-linear Sloshing Analysis of Liquid in Tanks with Arbitrary Geometry*, Int. Journal of Non-Linear Mechanics, Vol.22, pp. 193-207, 1987.

14. Ziarani, M., Richard, M.J. and Rakheja, S., *Optimization of Liquid Tank Geometry for Enhancement of Static Roll Stability of Partially-Filled Tank Vehicles*, *Int. J. of Heavy Vehicle Systems*, 11(2), 2004, pp155-173.

15. Kang, X., Rakheja, S. and Stiharu, I., *Tank Shape Optimization for Enhancement of Roll Stability of Partially-filled Tank Vehicles in Steady Turning*, presented at ASME IMECE-2000, Orlando, Florida, Nov. 2000.

16. Popov, G. et al., *Dynamics of liquid sloshing in baffled and compartmented road containers*, J. of Fluids and Structure, vol. 7, 1993,, pp 803-821.

17. Budiansky, B., *Sloshing of Liquids in Circular Canals and Spherical Tanks*, J. of Aerospace Science, Vol. 27, No. 3, 1960.

18. Ervin, R.D., Barnes, M. and Wolfe, A., *Liquid Cargo Shifting and the Stability of Cargo Tank Trucks*, Final Technical Report, Volume II", 1985, UMTRI.

19. Strandberg, L., *Lateral Stability of Road Containers*, VTI (The Swedish National Road and Traffic Research Institute) Report No. 138A, Sweden, 1978.

20. Isermann, H., *Overturning Limits of Articulated Vehicle with Solid and Liquid Loads*, Motor Industry Research Assoc., Translation No. 22/76, 1976.

21. Ranganathan, R. and Yang, Y.S., *Impact of liquid load shift on the braking characteristics of partially filled tank vehicles*, Vehicle System Dynamics, vol. 26, 1996, pp 223-240.

22. Salem M.I., Mucino V.H., Saunders E. and Gautam M., *Parameters of Trammel Pendulums to Simulate Lateral Sloshing in Partially Filled Elliptical Tankers*, West Virginia University Report, 2001.

23. Mantriota, G., *Directional stability of articulated tank vehicles: A simplified model*, Int. J. of Hevay Vehicle Systems, 10(1-2), 2003, pp 144-165.

24. Rakheja, S., Ranganathan, R. and Sankar, S., *Field Testing and Validation of Directional Dynamics Model of a Tank Truck*, Int. J. of Vehicle Design, Vol. 13, No. 3, pp. 251-275, 1992.

25. Bauer H. F., *On the Destabilizing Effect of Liquids in Various Vehicles*, Vehicle System Dynamics, Vol. 1, pp. 227, 1972.

26. National Aeronautics and Space Administration, *Propellant Slosh Loads*, 1968, NASA SP-8009.

27. Bauer, F., *Fluid oscillations in the containers of a space vehicle and their influence upon stability*, NASA, NASA TR R-187, 1964.

28. Schlee K. et al., *Modeling and parameter estimation of spacecraft fuel slosh mode*", Proc. of the 2005 Winter Simulation Conference, 2005.

29. Nichkawde, C., Harish, P.M. and Ananthkrishnan, N., *Stability analysis of a multibody system model for coupled slosh–vehicle dynamics*", Journal of Sound and Vibration, Vol. 275, 2004, pp 1069–1083.

30. Park, S., *Simulation and Experiment of Nonlinear Dynamics of Liquid-Filled Shell Structure Subjected to Low Speed Impulsive Loading*, Ph.D. Dissertation, The Pennsylvania State University, 1996.

31. Cooper, R. M., *Dynamics of Liquids in Moving Containers*, J. of American Rocket Society, Vol. 30, pp. 725-729, Aug. 1960.

32. Demirbilek, Z., *A Linear Theory of Viscous Liquid Sloshing*, Ph.D. Thesis, Texas A&M University, 1982.

33. Armenio, V. and Rocca, M. L., *On the Analysis of Sloshing of Water in Rectangular Containers: Numerical Study and Experimental Validation*, Ocean Engineering, Vol. 23, No. 8, pp. 705-739, 1996

34. Solaas, F. and Faltinsen., O. M, *Combined Numerical and Analytical Solution for Sloshing in Two-dimensional Tanks of General Shape*, J. of Ship Research, Vol. 41, No. 2, pp. 118-129, 1997

35. Wu, G. X., Ma, Q. W. and Taylor, R. E., *Numerical Simulation of Sloshing Waves in a 3D Tank Based on a Finite Element Method*, Applied Ocean Research, Vol. 20, pp. 337-355, 1998

36. Ortiz, J. L. and Barhorst, A. A., *Closed-Form Modeling of Fluid-Structure Interaction with Nonlinear Sloshing: Potential Flow*, AIAA Journal, Vol. 35, No. 9, 1997

37. Ma, J. and Usman, Mohammad, *Modeling of Fuel Sloshing Phenomena Considering Fluid-Structure Interaction*, 8th International LS-DYNA Users Conference, 2005.

38. Grundelius, M., *Control of Liquid Slosh in an Industrial Packaging Machine*, Proc. of the 1999 IEEE, international Conference on Conlrol Applications, 1999.

39. Papaspyrou, S., Valougeorgis, D. and Karamanos, S.A., *Sloshing Effects in Half-Full Horizontal Cylindrical Vessels Under Longitudinal Excitation*, Journal of Applied Mechanics, Vol. 71(2), 2004, pp. 255-265.

40. Su, T. C. et al., *A nonlinear analysis of liquid sloshing in rigid containers*, Final Report, Contract DOT RC-92037, Rept. No. DOT/RSPA/DMA-50/82/1, 1982.

41. Wang, Zhanqi and Rakheja, S., *Influence of partition location on the braking performance of a partially-filled tank truck*, Proc. of the SAE Int. Truck and Bus Meeting, 1995.

42. Ranganathan, R., *Stability and Directional Response Characteristics of Heavy Vehicles Carrying Liquid Cargo*, Ph.D. Thesis, Concordia University, 1990.

43. Romero, J.A., Hildebrand, R., Martinez, M., Ramirez, O. and Fortanell, J.M., *Natural sloshing frequencies of liquid cargo in road tankers*," Int. J. of Heavy Vehicle System, 12(2), 2005, pp.121-138.

44. Modaressi-Tehrani, K. and Rakheja, S., *Role of Transverse Baffle Designs on Transient Three-Dimensional Liquid Slosh in a Partly-Filled Circular Tank*, SAE Commercial Vehicle Engineering Conference, November 2005, Rosemont, IL, USA, Publication no. SP-1984.

45. Mucino, V., *Analysis of fluid slosh different arrangements of partial and full baffles in the longitudinal plane of an elliptical tank*, personal communication, 2004, West Virginia University, USA.

46. Lamb, S. H., *Hydrodynamics*, 6th ed., Dover Publications, New York, 1945.

47. Kobayashi, N., Mieda, T., Shibata, H. and Shinozaki, Y., *A study of the liquid slosh response in horizontal cylindrical tanks*, Transactions of the ASME, Journal of Pressure Vessel Technology, vol.111, 1989,pp.32-38.

48. Leonard, H.W. and Walton,W.C. Jr., *An investigation of the natural frequencies and mode shapes of liquids in oblate spheroidal tanks*, NASA, Technical Note, TN D-904, 1961.

49. Ranganathan, R., *Stability analysis and directional response characteristics of heavy vehicles carrying liquid cargo*, Ph.D. Dissertation, Concordia University, Montreal, Canada, 1990.

50. Modaressi-Tehrani, K., *Analysis of transient liquid slosh inside a partly filled tank subjected to lateral and longitudinal acceleration fields*, M. A. Sc. Dissertation, Concordia University, Canada, 2004.

51. FLUENT 6.2.16, *User's Guide–Chapter 26*, http://202.41.85.84/doc/fluent6.2/ help/ index.htm, 2005.

52. Hirt, C.W. and Nichols, B. D., *Volume of fluid (VOF) method for the dynamics of free boundaries*, Journal of Computational Physics, 1981, vol. 39, pp 201-225.

53. GAMBIT 2.2.30, *Modeling Guide-Chapter 3*, http://www.me.mtu.edu/help/ computing/docs/fluent/manuals/gambit/help/users_guide/ugtoc.htm, 2005.

54. Modaressi-Tehrani, K., Rakheja, S. and Stiharu, I., *Three-dimensional analysis of transient slosh within a partly-filled tank equipped with baffles*, Vehicle Systems Dynamics, 2006, in-press.

55. Modaressi-Tehrani, K., Rakheja, S., Sedaghati, R. and Bussiere, M., *Influence of transient fluid slosh on the overturning moment of partly-filled moving container*, Proc. of the Canadian Multidisciplinary Road Safety Conference, Ottawa, Canada, 2004.

56. Ervin, R.D., *The influence of size and weight variables on the roll stability of heavy duty trucks*, *SAE paper* No. 831163, 1983.

Annex – A: Optimal and circular cross-section tank designs

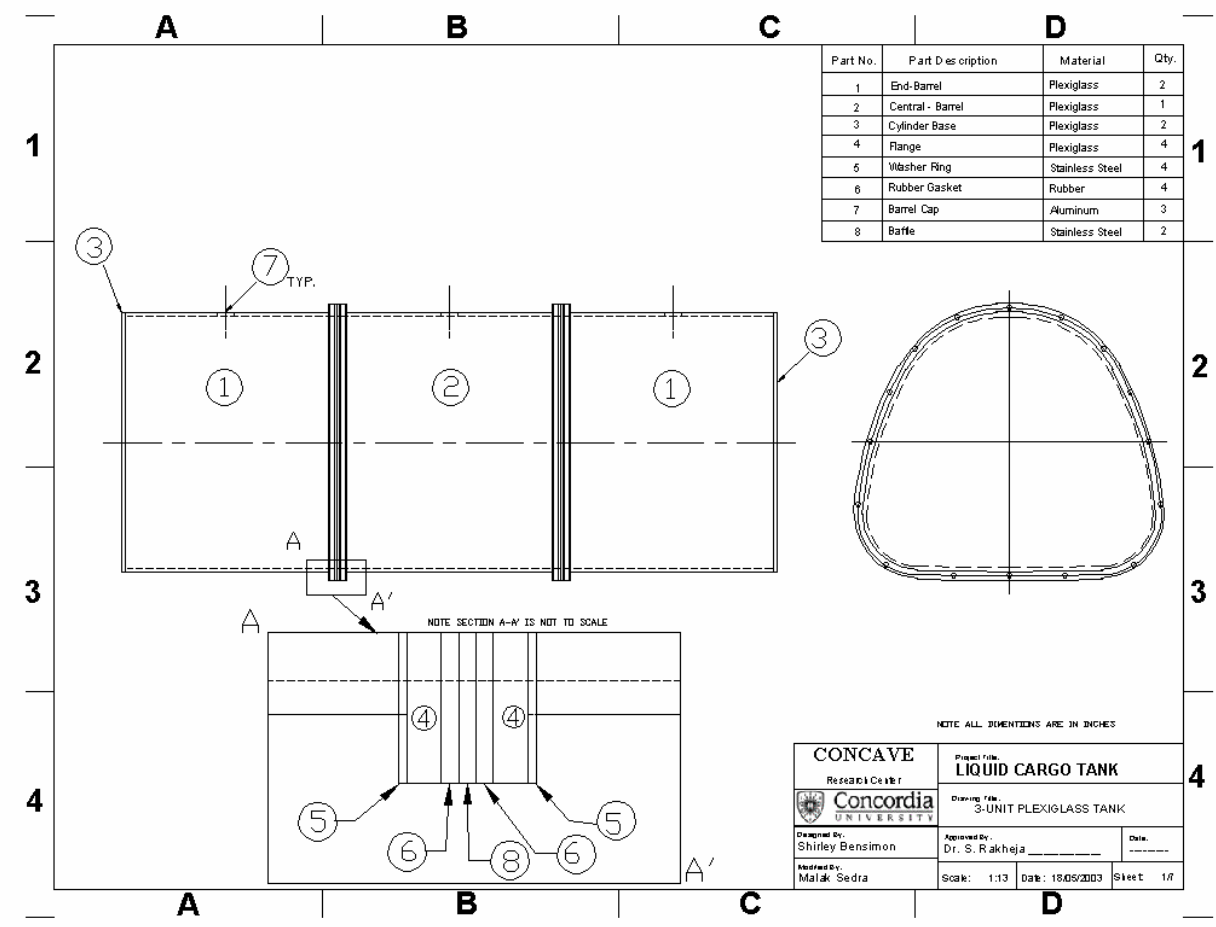

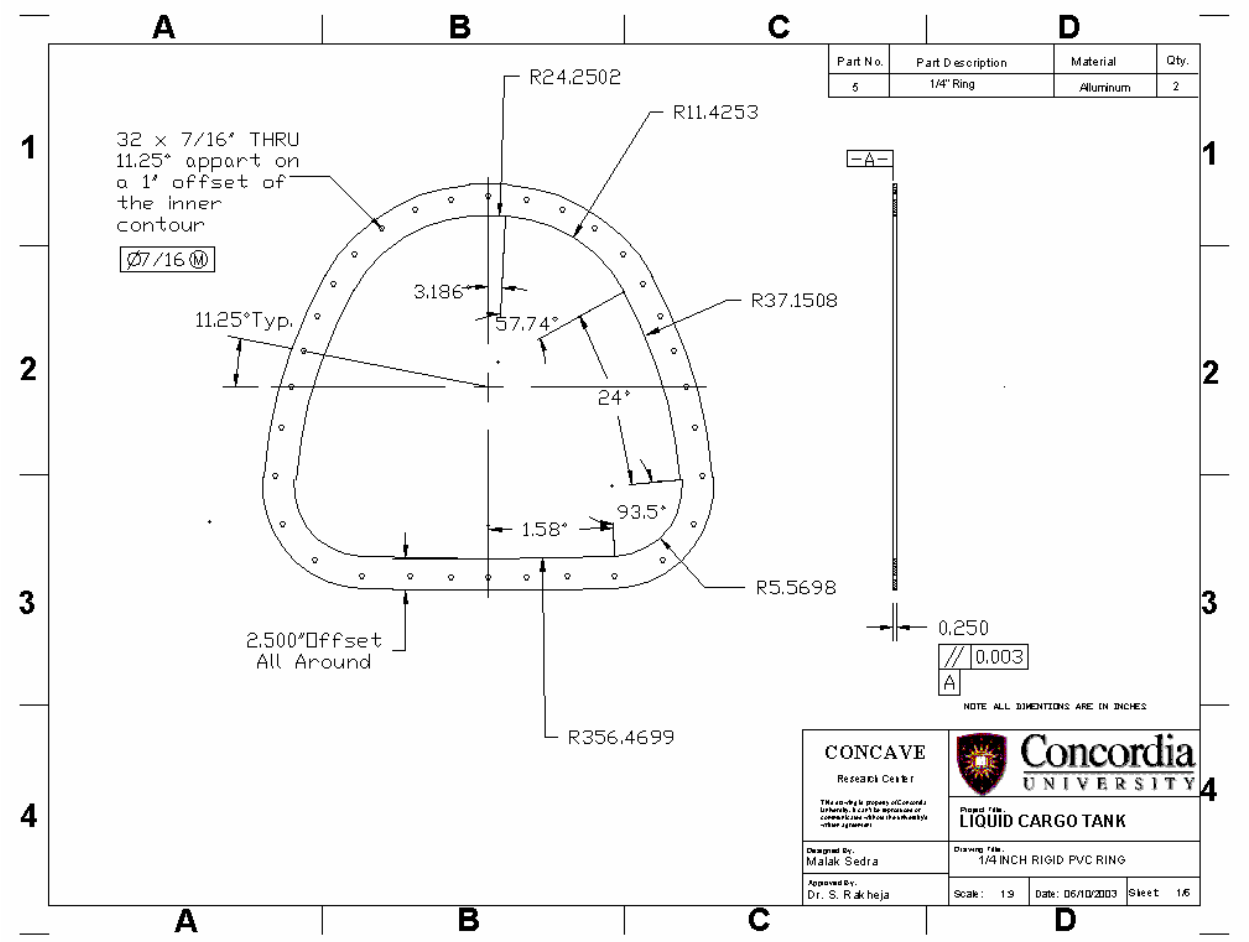
A
B
C
D
1
2
3
4
Part No. | Part Description | Material | Qty.
5 | 1/4" Ring | Aluminum | 2
R24.2502
R11.4253
32 x 7/16" THRU
11.25° apart on
a 1" offset of
the inner
contour
Ø7/16 M
3.186
57.74°
R37.1508
11.25°Typ.
24°
93.5°
1.58°
R5.5698
2.500"Offset
All Around
R356.4699
-A-
0.250
// 0.003
A
NOTE ALL DIMENTIONS ARE IN INCHES
CONCAVE
Research Center
Concordia
UNIVERSITY
Project Title:
LIQUID CARGO TANK
Designed By:
Malak Sedra
Drawing Title:
1/4 INCH RIGID PVC RING
Approved By:
Dr. S. Rakheja
Scale: 1:1
Date: 06/10/2003
Sheet 1/5

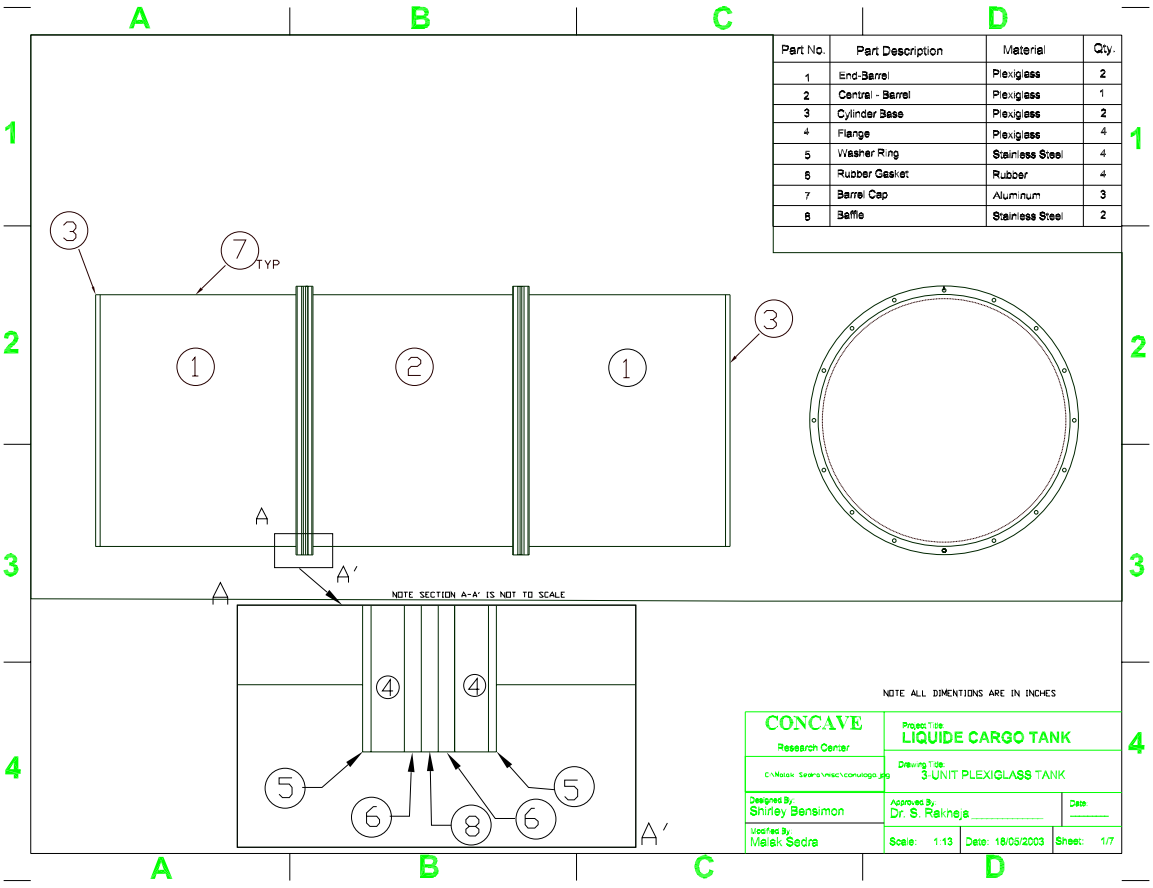
A
B
C
D
1
2
3
4
Part No. | Part Description | Material | Qty.
1 | End-Barrel | Plexiglass | 2
2 | Central - Barrel | Plexiglass | 1
3 | Cylinder Base | Plexiglass | 2
4 | Flange | Plexiglass | 4
5 | Washer Ring | Stainless Steel | 4
6 | Rubber Gasket | Rubber | 4
7 | Barrel Cap | Aluminum | 3
8 | Baffle | Stainless Steel | 2
TYP
NOTE SECTION A-A' IS NOT TO SCALE
NOTE ALL DIMENTIONS ARE IN INCHES
CONCAVE
Research Center
Project Title:
LIQUIDE CARGO TANK
Drawing Title:
3-UNIT PLEXIGLASS TANK
Designed By:
Shirley Bensimon
Approved By:
Dr. S. Raknejs
Date
Modified By:
Malek Sedra
Scale: 1:13
Date: 18/05/2003
Sheet: 1/7

Annex – B: Flow visualizations from experimens with different tank configurations

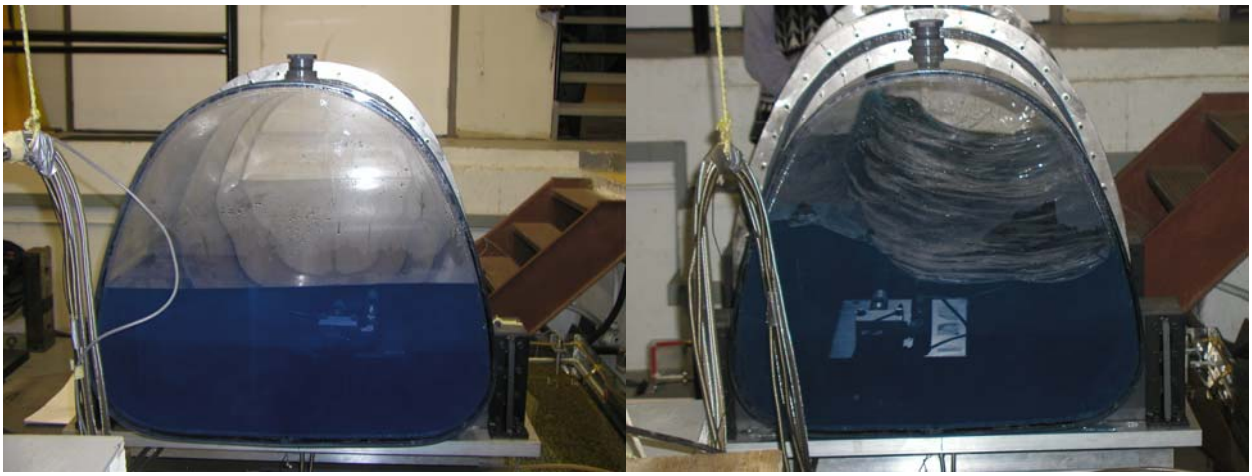

Configuration – ‘T0’; harmonic lateral acceleration excitation

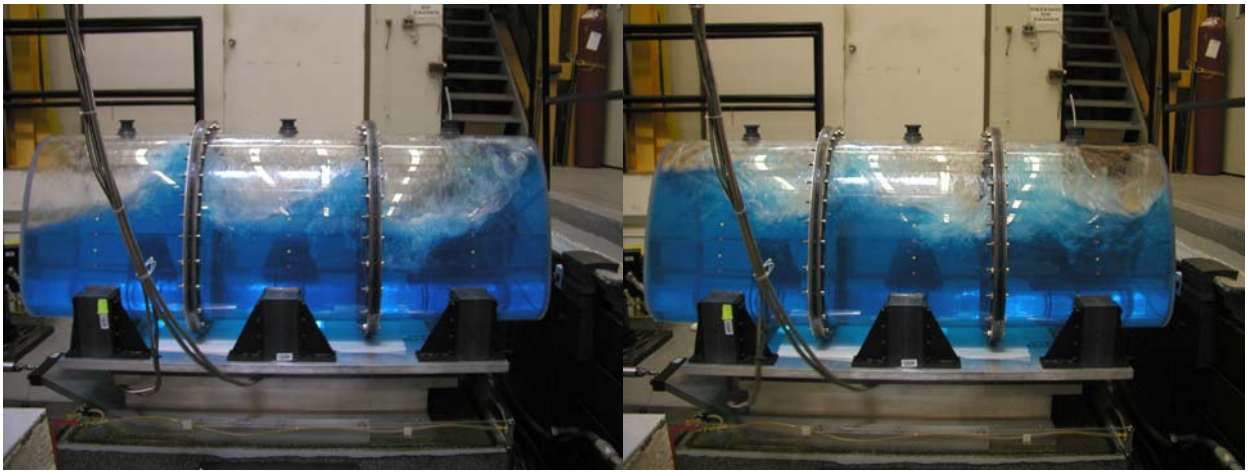

Configuration – ‘T3’; Harmonic longitudinal acceleration excitation

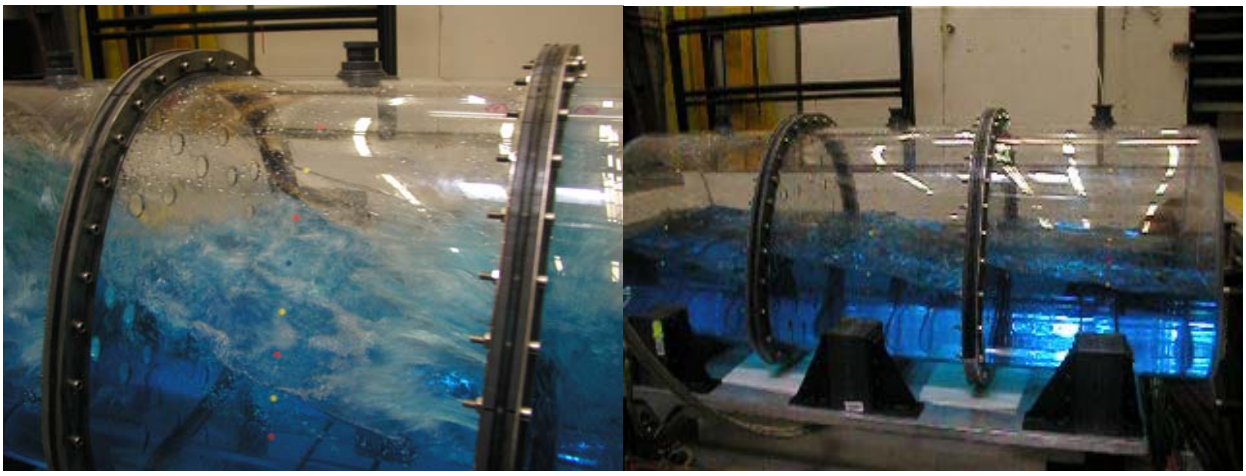

Configuration – ‘T3’; Harmonic longitudinal acceleration excitation

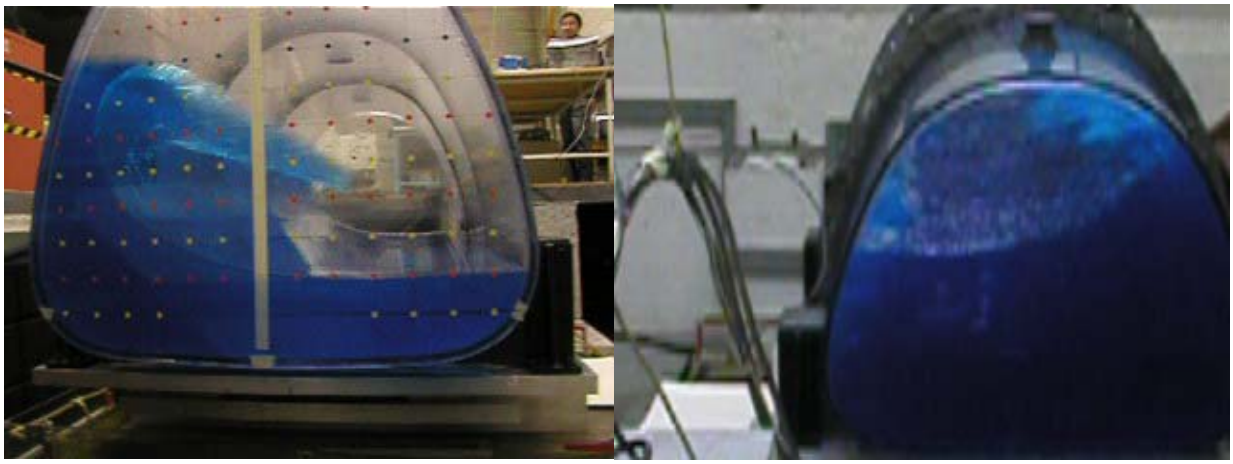

Configuration – ‘T0’; Transient lateral acceleration excitation

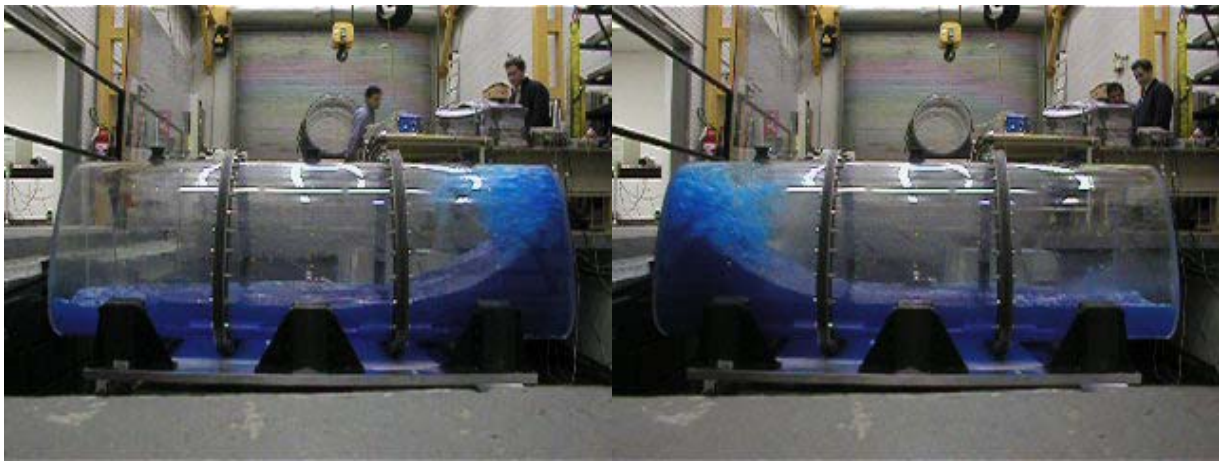

Configuration – ‘T0’; Transient longitudinal acceleration excitation

Annex – C: Selected Proposed Concepts in Baffles Design

- Partial baffles (reduced weight)

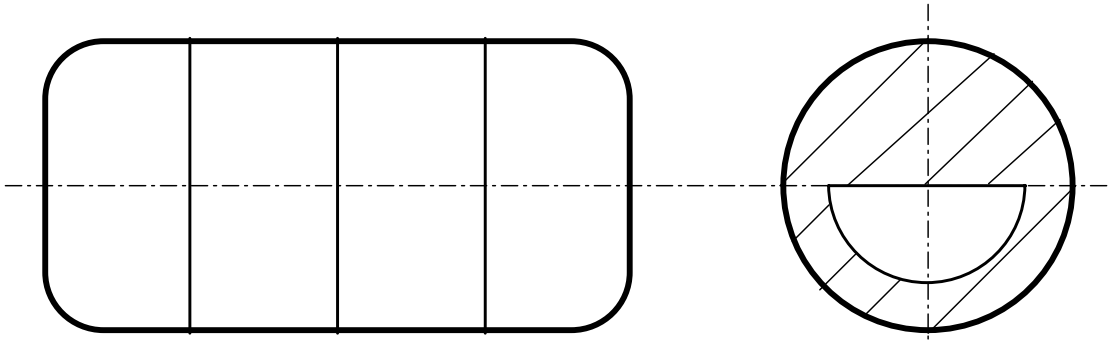

(a) (b)

- Conical full or partial baffles (expected to yield enhanced control of lateral slosh)

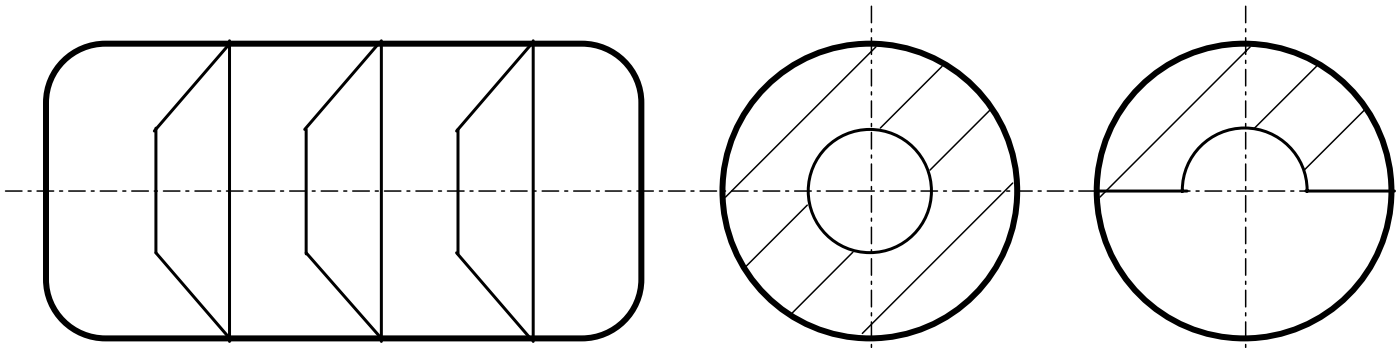

(a) (b) (c)

- Inclined full or partial baffles (expected to yield enhanced control of lateral slosh)

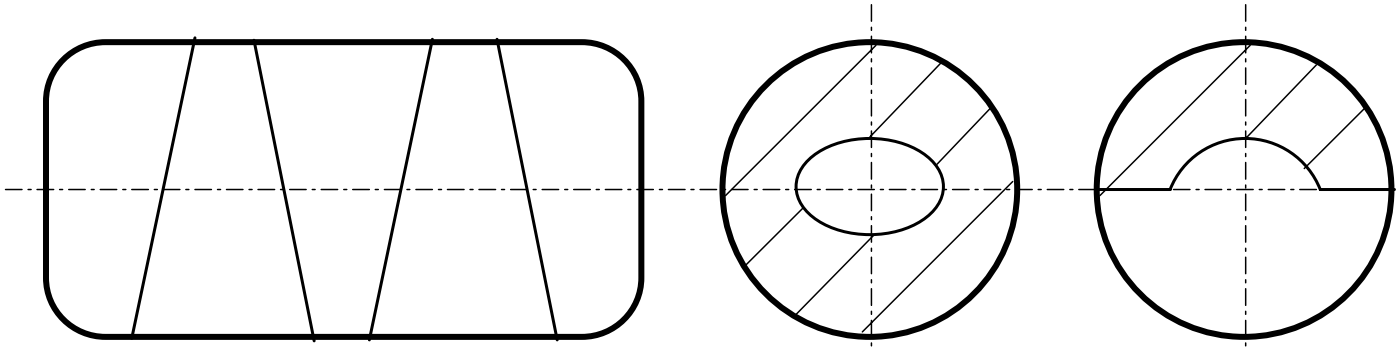

(a) (b) (c)